

Author Comments: Response to reviewers' comments

Title: Evaluation on the effect of regional joint control measures in changing photochemical transformation: A comprehensive study of the optimization scenario analysis

Reviewer #1:

This manuscript investigated the effects of joint local and regional regulations on air pollution during the 2nd World Internet Conference held in Jiaxing, Zhejiang. Both modeling and measurements were used for the evaluation. The authors performed careful case studies by controlling the meteorological conditions, air mass back trajectory, etc. Different emission reduction plans were proposed based on different scenarios. In particular, it is recommended to implement regulation along the transport channel to the receptor-site. This is an important study to develop effective control strategies to mitigate air pollution in China. Overall, the manuscript is well-written and the analysis is solid. I recommend publication after minor revision.

Thanks to the reviewer for the comments. We have carefully revised the manuscript accordingly.

Comments:

1. Line 202. Please show the equations to calculate the metrics. Also, “Index of Agreement” should be as “IOA”.

Revised. The equations have been added to the manuscript, as follows. The “I” has been revised to IOA.

Changes in manuscript:

The equations to calculate these statistical indexes are as follows:

$$NMB = \frac{\sum(P_j - O_j)}{\sum O_j} \times 100\% \quad (1)$$

$$NME = \frac{\sum |P_j - O_j|}{\sum O_j} \times 100\% \quad (2)$$

$$IOA = 1 - \frac{\sum (P_j - O_j)^2}{\sum (|P_j - \bar{O}| + |O_j - \bar{O}|)^2} \quad (3)$$

where P_j and O_j are predicted and observed hourly concentrations, respectively. \bar{O} is the average value of observations. IOA ranges from 0 to 1, with 1 indicating perfect agreement between model and observation.

2. Figure 2. Please include NMB, NME, and IOA (Table 2) in the figure.

Revised accordingly.

Changes in manuscript:

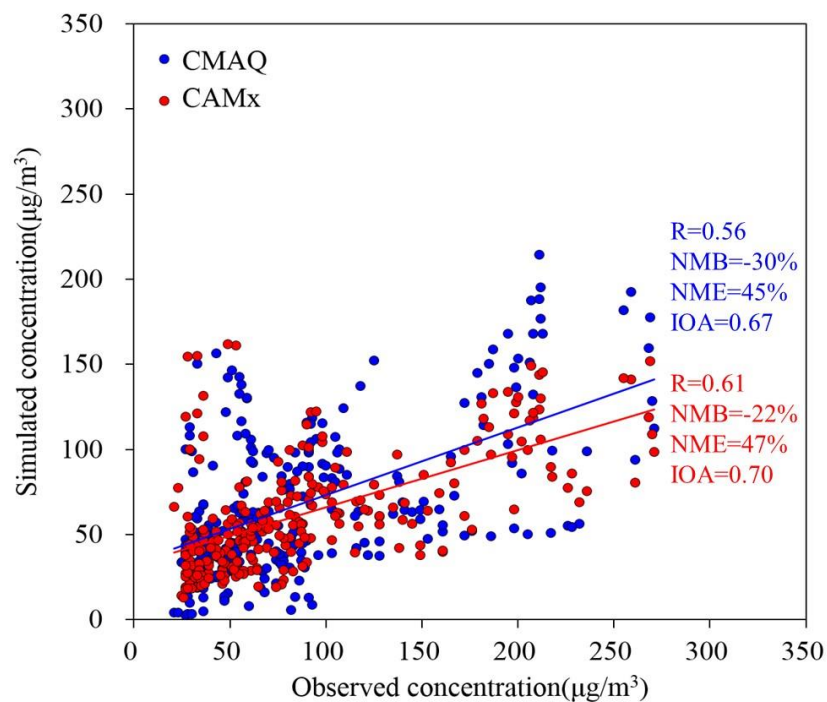


Fig. 3 Scatter plot of the simulated and observed $PM_{2.5}$ at the Shanxi supersite

3. Line 241-244. This sentence has grammatical error.

Revised.

Original sentence: For each of these processes, this study has comprehensively in the integrated emission-measurement-modeling method considered the backward air flow

trajectory, potential contribution source areas, meteorological conditions and the variation of PM_{2.5} concentration to analyse the evolution of the observed air quality.”

Changes in manuscript:

For each of these processes, this study utilized the integrated emission-measurement-modeling method to analyze the evolution of air quality from several aspects, including the backward air flow trajectory, potential source contribution areas, meteorological conditions and the variation of PM_{2.5} concentration.

4. Figure 3-7. In panel (d), please specific if the PM_{2.5} time series is from modeling or measurement.

It is from measurement. The original sentences “(d) PM_{2.5} time series for selected sites during ... ” have been revised to “(d) Observed PM_{2.5} time series for selected sites during ...” in Fig.3-7 (Fig.4-8 in the revised manuscript).

5. Figure 8 and Figure 9. These two figures are really intriguing. Why is “[SO₂] after control” is similar to “[SO₂ during control]”, but “[SO₄] after control” is much higher than “[SO₄ during control]”? The opposite trend is observed for [NO₂] and [NO₃]. Please make similar figure for the [SO₂]+[SO₄] and [NO₂]+[NO₃], which should better represent the effect of regulation. Another potential plot is the partitioning of SO_x and NO_x (e.g., SO₂/(SO₂+SO₄)). Interesting chemistry may be inferred from these analyses. Also, can the model reproduce these observations? Last comment, please consider to change the x-axis label from dates to “before/during/after regulation”.

It is a very good question and suggestion!

As is shown from the figure, the SO₂ concentration after control is a little bit higher than during control (+5.9%). However, the SO₄²⁻ after control is much higher than during control (+25.8%). This is probably due to two reasons: firstly, SO₂ emissions and primary sulfate emissions increased after the control measures were terminated; secondly,

previous studies have reported that increased NO_2 emissions could accelerate the formation of secondary sulfate (Cheng et al., 2016). This can be clearly seen from the SOR. A different trend is observed for NO_2 and NO_3^- , with the NO_2 concentrations after control being much higher than during control (+9.4%), while the increase of NO_3^- (+9.45%) is about the same. Sulfate originates from both primary emissions and secondary formation, but nitrate is mostly secondary. The NOR during and after regulation is about the same and most of the N is in the gas phase as indicated by $\text{NO}_x/(\text{NO}_x+\text{NO}_3^-)$ (0.87). Therefore, the increase of NO_3^- is smaller than SO_4^{2-} . The $\text{PM}_{2.5}$ concentration after control sharply rebounded by 31.8%, indicating that both primary emissions and secondary formation are activated.

To better illustrate emissions and chemistry before, during and after control measures, we revised the previous figures and added another two indicators for partitioning of SO_x/NO_x , and SOR/NOR.

Changes in manuscript:

The chemistry also changes if we compare during and after the regulation. As is shown from figure 10, the SO_2 concentrations after control is a little bit higher than during control (+5.9%). However, the SO_4^{2-} after control is much higher than during control (25.8%). This is probably due to two reasons: firstly, SO_2 emissions and primary sulfate emissions increased after the control measures were terminated; secondly, previous studies have reported that increased NO_2 emissions could accelerate the formation of secondary sulfate (Cheng et al., 2016). This can be clearly seen from the SOR. A different trend is observed for NO_2 and NO_3^- , with the NO_2 concentrations after control being much higher than during control (+9.4%), while the increase of NO_3^- (+9.45%) is about the same. Sulfate originates from both primary emissions and secondary formation, but nitrate is mostly secondary. The NOR during and after regulation is about the same and most of the N is in the gas phase as indicated by $\text{NO}_x/(\text{NO}_x+\text{NO}_3^-)$ (0.87). Therefore, the increase of NO_3^- is smaller than SO_4^{2-} . The $\text{PM}_{2.5}$ concentration after control sharply rebounded by 31.8%, indicating that both primary emissions and secondary formation are activated.

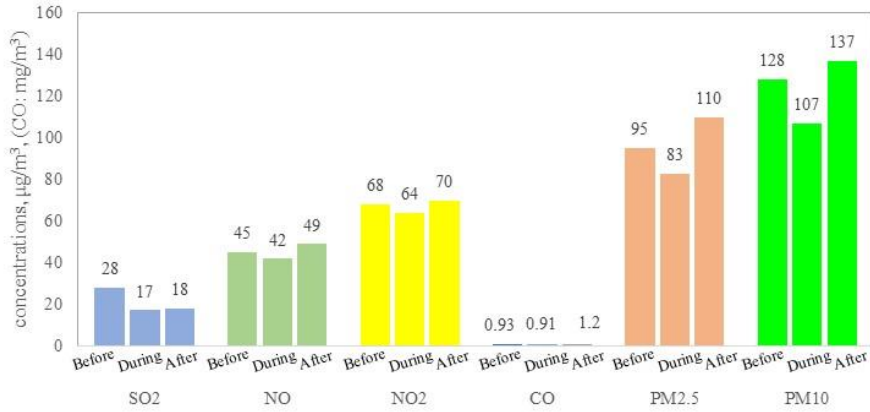


Fig. 9 Comparison between air pollutant concentrations at Shanxi station before, during, and after the campaign under stagnant meteorological conditions

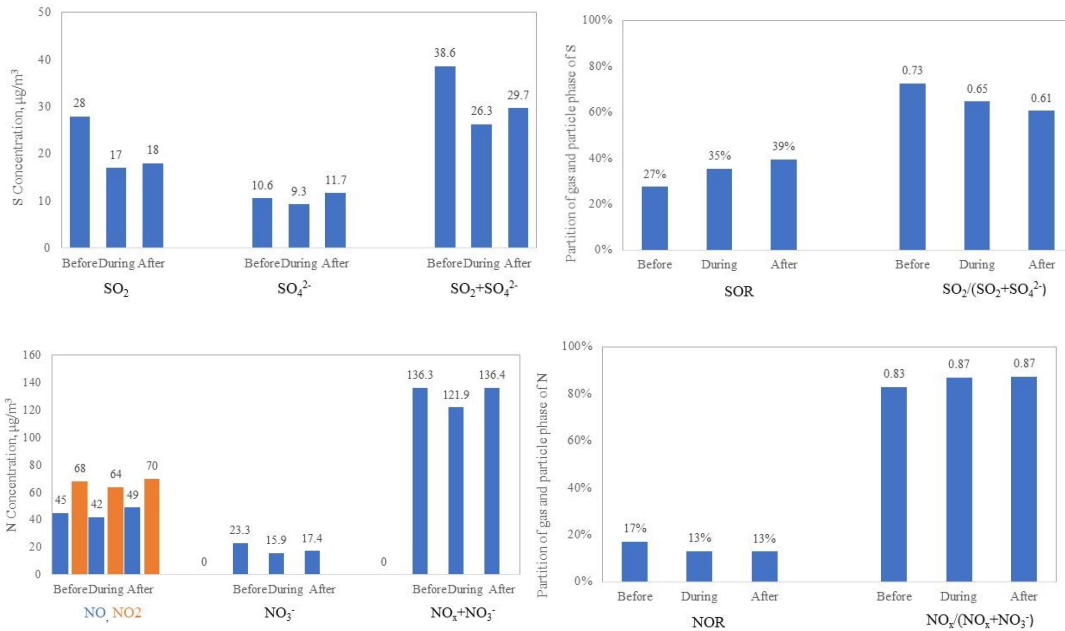


Fig. 10 Comparison between PM_{2.5} chemical components at Shanxi station before and after the campaign under static meteorological conditions

6. Line 511. “reduction in PM_{2.5} concentrations” is not accurate. It should be “PM_{2.5} decline ratio”.

Revised accordingly.

Changes in manuscript:

It can be seen that the PM_{2.5} decline ratio in Jiaxing varies with time. The PM_{2.5} decline ratio was the most significant on December 8-9 with a maximum reduction of 56%. The percentage reduction in hourly PM_{2.5} during the conference (December

16-18) ranged between 2%-24%, while the average decrease in PM_{2.5} concentration was 5.8 µg/m³ with an average improvement of about 12.9%.

7. Figure 14. It is surprising to see that the decline ratio is typically ~10% after such strict regulation policies. What are the sources of the residual PM? From transport?

The decline ratio changes with meteorological conditions even under the same emissions reduction situation, because meteorological conditions affect dispersion of primary emissions, secondary formation and regional transport. If we look at the decline ratio of hourly concentrations, we can find that the decline ratio was most significant on December 8-9 with a maximum reduction of 56%. The percentage reduction of hourly PM_{2.5} during the conference (December 16-18) ranged between 2%-24%. If we look at the PM_{2.5} decline ratio of daily average, we can see the improvement in PM_{2.5} before the conference (December 8 and 9) was relatively significant, with a daily average decline of 31% -35%, which corresponds to a decrease of around 17 µg/m³. The reduction in PM_{2.5} on December 14-15, two of the days with some of the highest observed PM_{2.5}, was relatively small at around 6%, while daily average PM_{2.5} concentrations on those days decreased by around 10.0 µg/m³. The magnitude of emission reductions during those two time periods was basically the same, so it is possible that the observed difference in PM_{2.5} levels was the result of meteorological differences. Overall, the residual PM may come from three aspects: (1) although stringent control measures have been implemented, there are still some precursor emissions in the city, which accumulated and formed secondary particles under favorable meteorological conditions; (2) enhanced transport under specific meteorological conditions, especially upwind emissions; (3) in view of the uncertainties of model performance (underestimation of PM_{2.5}, especially underestimation of SOA) described in previous sections, we should keep in mind that the secondary formation may probably be underestimated, causing modeled decline ratio lower than observed.

Changes in manuscript:

The decline ratio changes with meteorological conditions even under the same emissions reduction situation, because meteorological conditions influence dispersion from primary

emissions, regional transport and secondary formation. The magnitude of emission reductions during those two time periods was basically the same, so it is possible that the observed difference in $PM_{2.5}$ levels was the result of meteorological differences. Overall, the residual $PM_{2.5}$ may come from three aspects: (1) although stringent control measures have been implemented, there are still some precursor emissions in the city, which accumulated and formed secondary particles under favorable meteorological conditions; (2) enhanced transport under specific meteorological conditions, especially upwind emissions; (3) in view of the uncertainties of model performance (underestimation of $PM_{2.5}$, especially underestimation of SOA) described in previous sections, it should be noted that the secondary formation may probably be underestimated, causing modeled decline ratio lower than observed.

8. Effect of local emission reductions in Jiaying and Figure 18. Regional control only has slight extra benefit over local control. Does it suggest that less strict regulation should be implemented in nearby cities?

Figure 18 shows the decline ratio of daily average $PM_{2.5}$ concentrations under the regional emission reduction scenario, the Jiaying local emission reduction scenario and the transport channel emission reduction scenario (24 hrs in advance and 48 hrs in advance). Air quality improvement due to regional emission reductions was slightly larger than that of local emission reductions in Jiaying, and smaller than that of channel emission reductions. This suggests that emissions reduction in downwind cities does not have much effect on Jiaying's air quality. In contrast, emissions reduction based on predicted transport pathway in advance are more effective than local emissions reduction.

Changes in manuscript:

In this study, the main transport channel involved is the northwest transport channel in control areas, which basically represents the typical winter transport channel in the region. Air quality improvement due to regional emission reductions was slightly larger than that of local emission reductions in Jiaying, and smaller than that of channel emission reductions. This suggests that emissions reduction in the downwind cities does not have

much effect on Jiaxing's air quality. In contrast, emissions reduction based on predicted transport pathway in advance are much more effective than local emissions reduction as well as regional emission reductions. Therefore, a well-designed management plan for the main transport channel is necessary to ensure optimized air quality improvement in autumn and winter, in addition to reducing local emissions.

Author Comments: Response to reviewers' comments

Title: Evaluation on the effect of regional joint control measures in changing photochemical transformation: A comprehensive study of the optimization scenario analysis

Reviewer #2:

Review for “Evaluation on the effect of regional joint control measures in changing photochemical transformation: A comprehensive study of the optimization scenario analysis”

This paper investigates the effect of regional control during the 2nd World Internet Conference from December 16 to December 18, 2015. They analyzed the meteorology condition, observed air pollutant concentration, and quantified the effect of air pollution control using numerical models. They found the local emission reduction plays an important role in air quality improvement and suggest that a 48-hr advance pollution channel control before the event. Overall, this paper is well-organized and fits into the scope of Atmospheric Chemistry and Physics on the advance understanding of atmospheric chemistry process. I suggest this paper gets accepted with the following minor revisions.

Thanks to the reviewer for the comments, we have carefully revised the manuscript accordingly.

Minor comments:

1. In the model performance section, the author mentioned about the underestimation of the simulated $PM_{2.5}$ concentration compared to the observation. Where are the uncertainties possibly coming from? Knowing this uncertainty in the model, how do we interpret the results (possible uncertainty and limitation in the result)?

We agree with the reviewer. The predicted $PM_{2.5}$ is relatively lower than the observed data (NMB values are all negative), as described in the model performance section. These

underestimations may be due to three reasons. Firstly, winter underestimation of PM_{2.5} (especially SOA) is a common issue with CMAQ or CAMx simulations over China (Hu et al., 2017; Li et al., 2016), which can be explained by a lack of model calculated oxidants or missing reactions (Kasibhatla et al., 1997) of SOA formation pathways (Appel et al., 2008; Foley et al., 2010; Chen et al., 2017). Secondly, uncertainty still exists in the regional emissions inventory, including the basic emissions inventory and the control scenarios as well. Thirdly, the wind speed is slightly overestimated over the region, with NMB and NME of 28% and 33%, causing fast dispersion of air pollutants and lower prediction of ambient PM_{2.5} concentrations.

In view of these uncertainties, we mainly use observational data to interpret the photochemical change, while in Section 3.4, we should keep in mind that the secondary formation may probably be underestimated, causing the decline ratio lower than observed values.

Changes in manuscript:

Text has been added to interpret the model performance and the predicted results in the model performance section 2.3.2 and section 3.4.1.

Section 2.3.2

Figure 3 compares the simulated and observed PM_{2.5} concentrations at the Shanxi supersite. In general, model predicted data are lower than the observed data with the NMB value of -22% to -30%, the NME value of 45% to 47% and the IOA value of 0.67 to 0.70 (Table 2). These underestimations may be due to three reasons: Firstly, winter underestimation of PM_{2.5} (especially SOA) is a common issue with CMAQ or CAMx simulations over China (Hu et al., 2017; Li et al., 2016), which can be explained by a lack of model calculated oxidants or missing reactions (Kasibhatla et al., 1997) of SOA formation pathways (Appel et al., 2008; Foley et al., 2010). Secondly, uncertainty still exists in the regional emission inventory, including the basic emissions inventory and the control scenarios. Thirdly, the wind speed is slightly overestimated over the region, with

NMB and NME of 28% and 33%, causing fast dispersion of air pollutants. Overall, these statistics for both the meteorological parameters and simulated PM_{2.5} are generally consistent with the results in other published modelling studies(Zheng et al., 2015;Wang et al., 2014;Zhang et al., 2011;Fu et al., 2016;Li et al., 2015b;Li et al., 2015a), which suggests that the simulation performance is acceptable.

Section 3.4.1

In view of the uncertainties of model performance (underestimation of PM_{2.5}, especially underestimation of SOA) described in previous sections, it is noted that the secondary formation may be underestimated, causing the decline ratio lower than reactivity.

Added references:

Appel, K.W., Bhave, P.V., Gilliland, A.B., Sarwar, G., Roselle, S.J., 2008. Evaluation of the community multiscale air quality (CMAQ) model version 4.5: sensitivities impacting model performance; part II particulate matter. *Atmos. Environ.* 42, 6057-6066.

Chen, Q., Fu, T. M., Hu, J., Ying, Q., & Zhang, L. (2017). Modelling secondary organic aerosols in China. *National Science Review*, 4(6), 806-809.

Foley, K.M., Roselle, S.J., Appel, K.W., Bhave, P.V., Pleim, J.E., Otte, T.L., Mathur, R., Sarwar, G., Young, J.O., Gilliam, R.C., Nolte, C.G., Kelly, J.T., Gilliland, A.B., Bash, J.O., 2010. Incremental testing of the community multiscale air quality (CMAQ) modeling system version, 4.7. *Geosci. Model Dev.* 3, 205-226.

Kasibhatla, P., Chameides, W.L., Jonn, J.S., 1997. A three dimensional global model investigation of seasonal variations in the atmospheric burden of anthropogenic sulphate aerosols. *J. Geophys. Res.* 102, 3737-3759.

Li, J. L., ZHANG, M. G., GAO, Y., & CHEN, L. (2016). Model analysis of secondary organic aerosol over China with a regional air quality modeling system (RAMS-CMAQ). *Atmospheric and Oceanic Science Letters*, 9(6), 443-450.

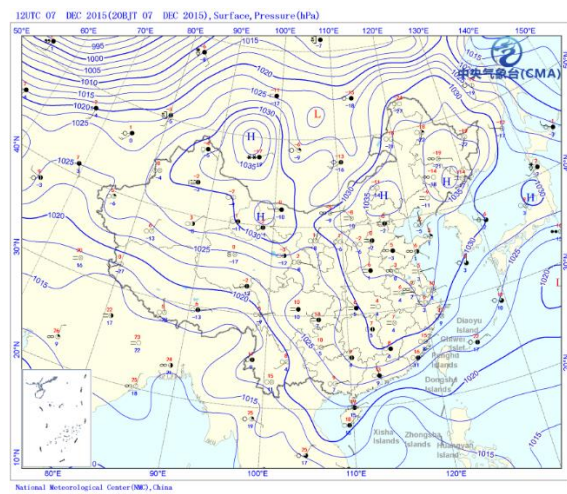
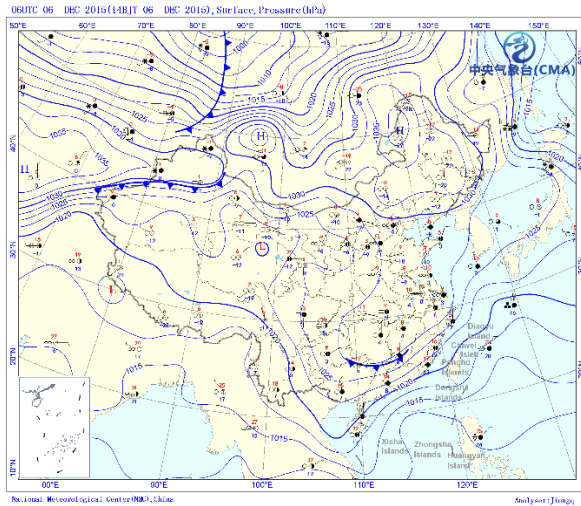
Hu, J., Wang, P., Ying, Q., Zhang, H., Chen, J., Ge, X., ... & Zhao, Y. (2017). Modeling biogenic and anthropogenic secondary organic aerosol in China. *Atmospheric Chemistry and Physics*, 17(1),

77-92.

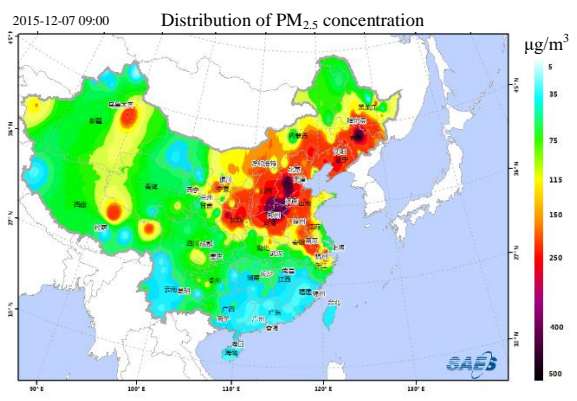
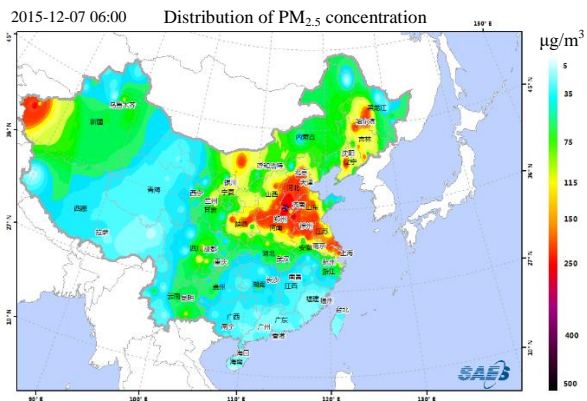
2. Some of the figure (Figure 3-7) contents are hard to read, for example, the values on the color bar on the panel (b) and contours on the synoptic maps (a). Moreover, the graph resolution is not consistent in these Figures, especially figure (c). What is the color scale in (c)?

We have revised these figures for better visualization (Figure 4-8 in the revised manuscript). We also added the color scale to figures (c).

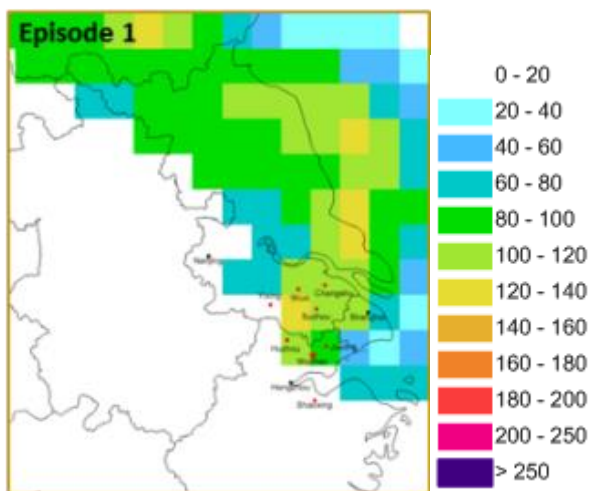
Changes in manuscript:



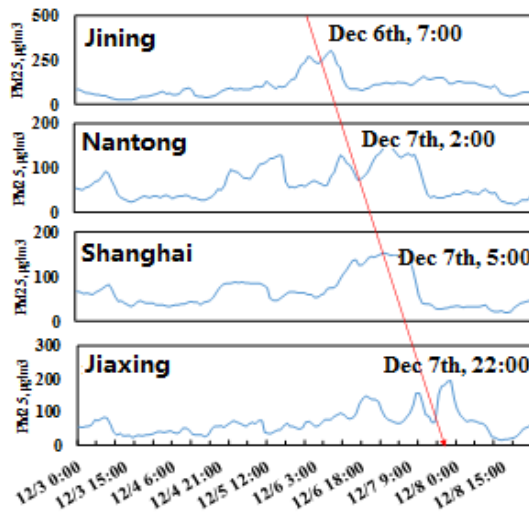
(a)



(b)

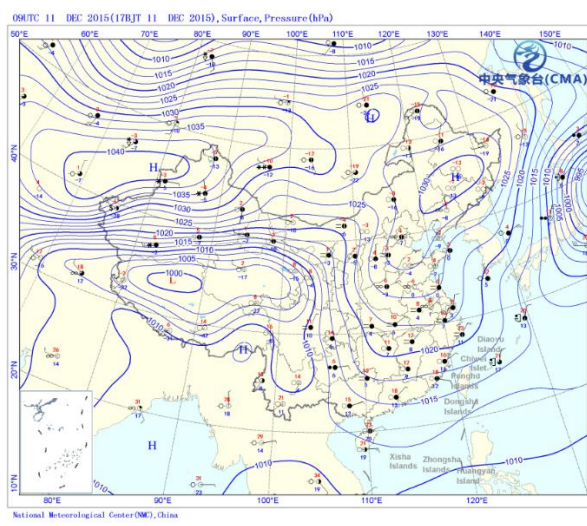
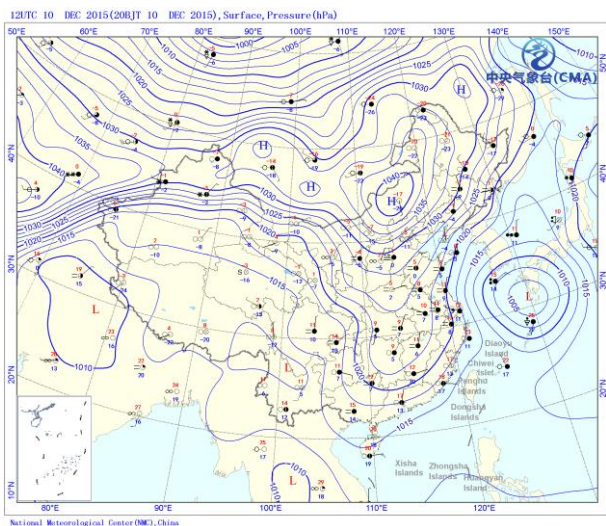


(c)

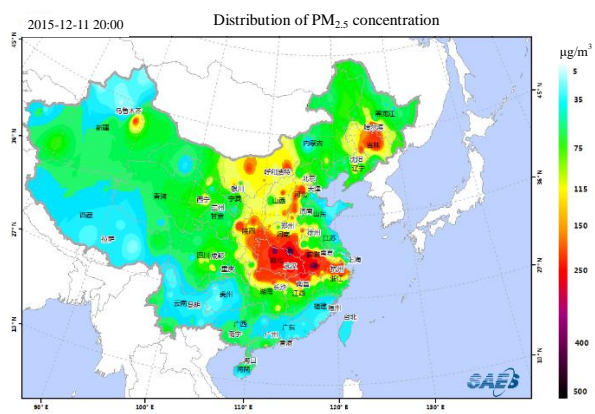
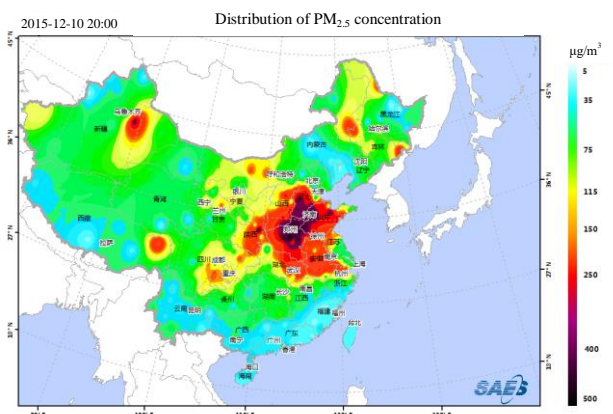


(d)

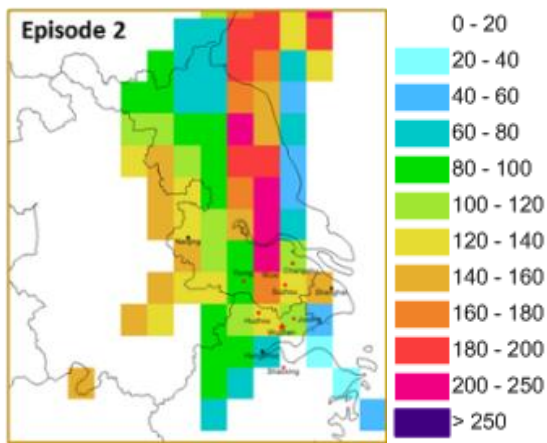
Fig. 4 Analysis of (a) the large-scale weather patterns, (b) distribution of $PM_{2.5}$ concentrations, (c) potential regional sources, (d) Observed $PM_{2.5}$ time series for selected sites during December 6 to December 8, 2015



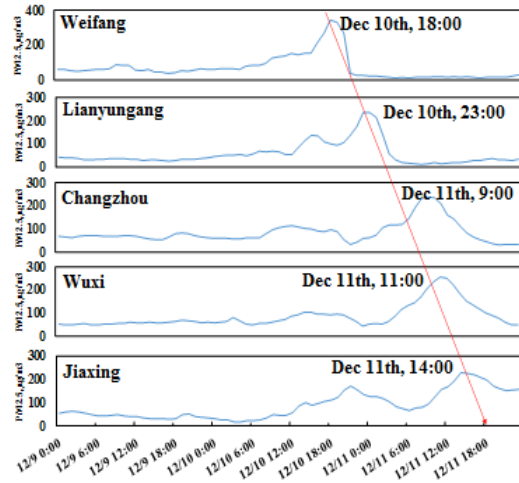
(a)



(b)

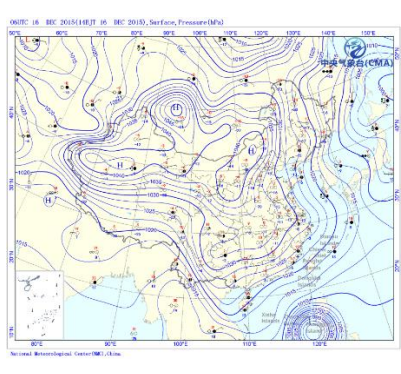
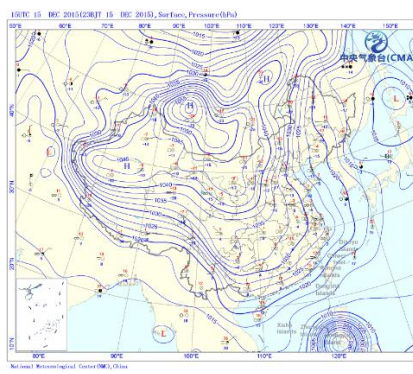
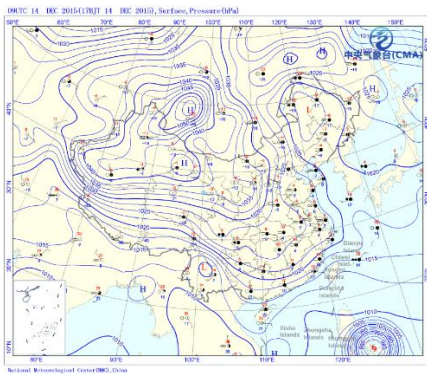


(c)

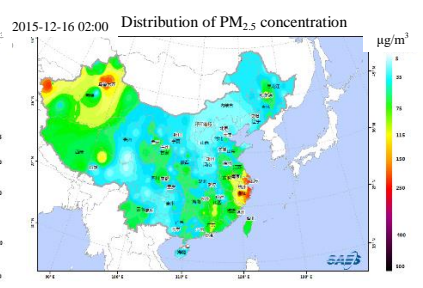
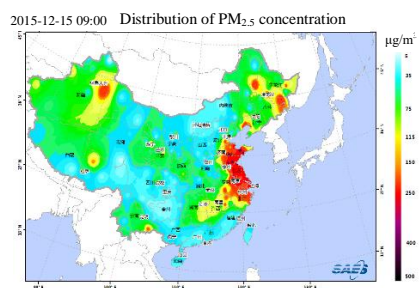
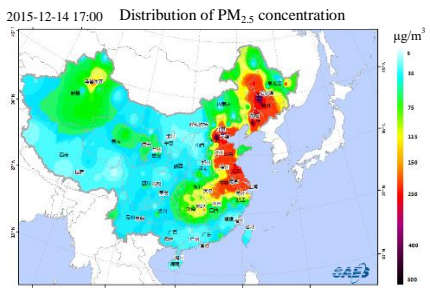


(d)

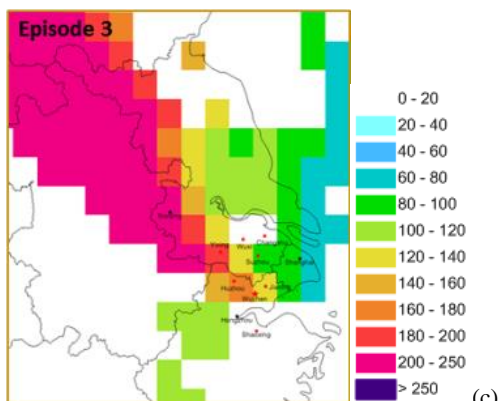
Fig. 5 Analysis of (a) the large-scale weather patterns, (b) distribution of $PM_{2.5}$ concentrations, (c) potential regional sources, (d) Observed $PM_{2.5}$ time series for select sites during December 10 to December 11, 2015



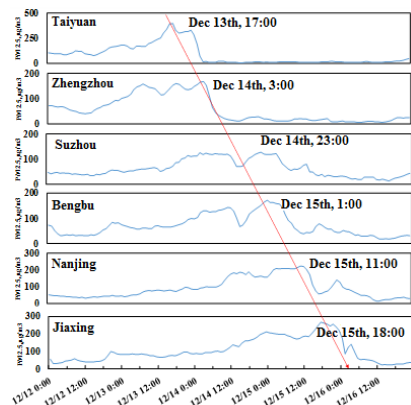
(a)



(b)

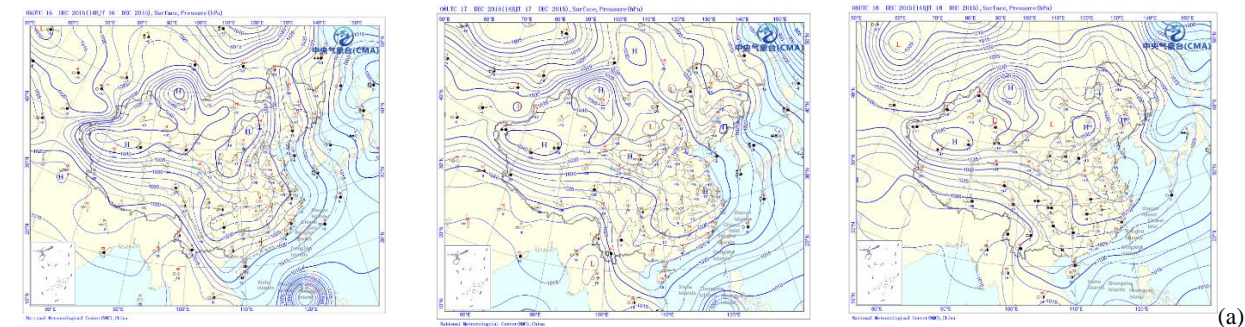


(c)

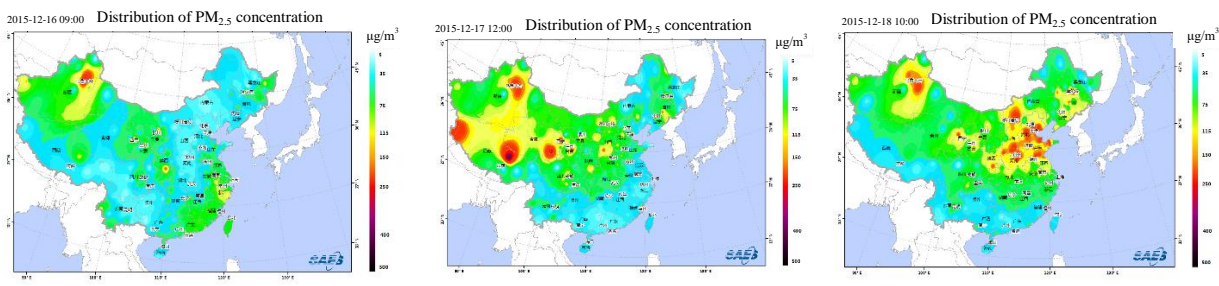


(d)

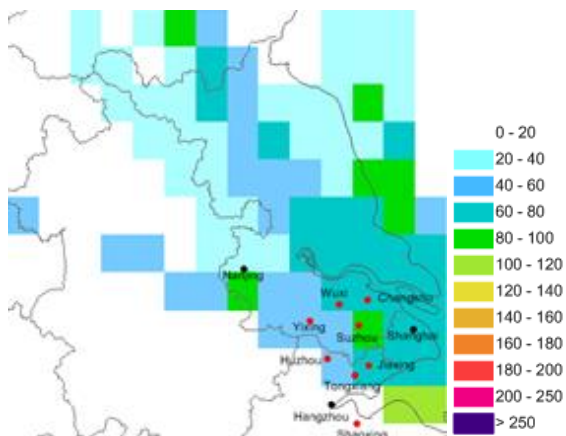
Fig. 6 Analysis of (a) the large-scale weather patterns, (b) distribution of $PM_{2.5}$ concentrations, (c) potential regional sources, (d) Observed $PM_{2.5}$ time series for select sites during December 14 to December 16, 2015



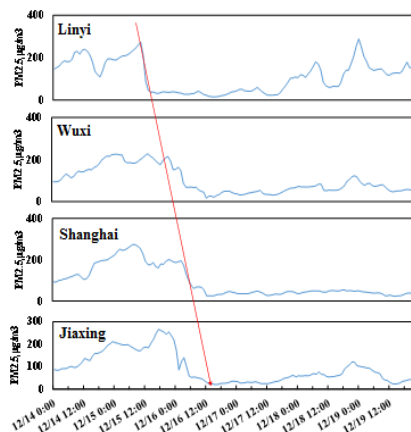
(a)



(b)

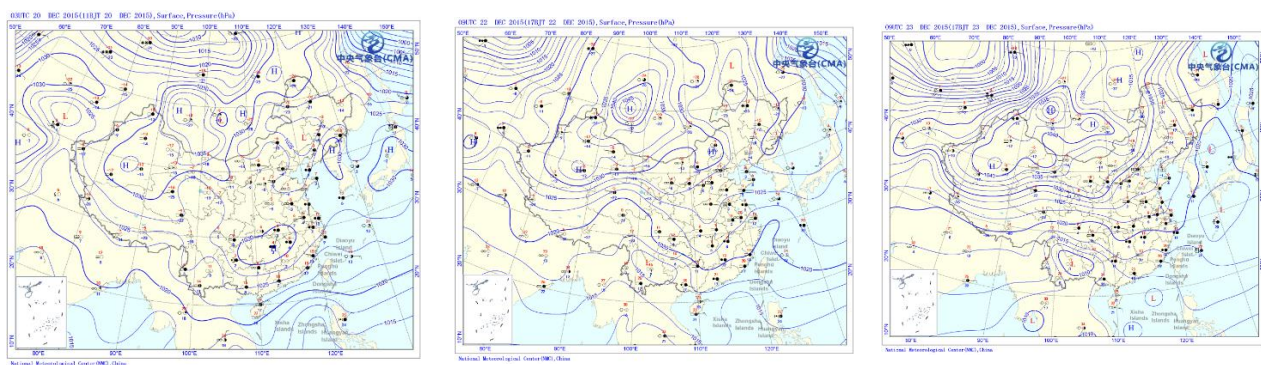


(c)



(d)

Fig. 7 Analysis of (a) the large-scale weather patterns, (b) distribution of $PM_{2.5}$ concentrations, (c) potential regional sources, (d) Observed $PM_{2.5}$ time series for select sites during December 16 to December 18, 2015



(a)

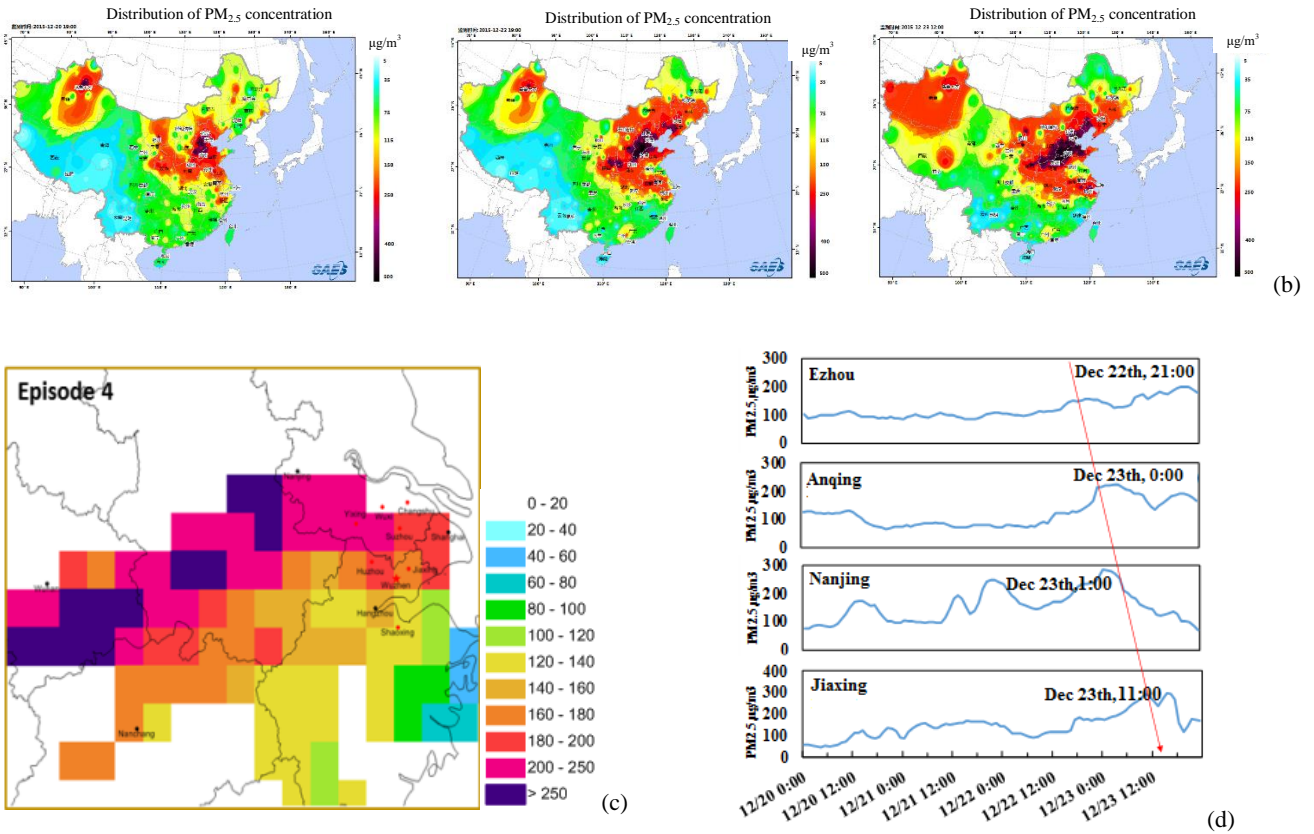


Fig. 8 Analysis of (a) the large-scale weather patterns, (b) distribution of $PM_{2.5}$ concentrations, (c) potential regional sources, (d) Observed $PM_{2.5}$ time series for select sites during December 20 to December 23

3. Line 153: “GDAS” needs to be defined at its first appearance.

“GDAS” has been revised to “Global Data Assimilation System (GDAS)”.

4. Line 201: : : : Index of Agreement (IOA). Same apply to Line 209:and the IOA value of 0.67 to 0.70.

Revised.

5. Line 340: “ under static weather condition”

Revised.

6. Figure 9: what is the unit of the measurement (%)?

The unit is “ $\mu\text{g}/\text{m}^3$ ”. It has been revised in the manuscript.

7. Figure 11: WS/WD panel has similar information as the $PM_{2.5}$ (top panel) regarding the wind direction. I suggest change the WS/WD panel to wind speed only and use contour lines to represent that.

The top panel with different colors indicates the trajectories at 500m height, which can be used to represent long-range transport; the WS/WD panel indicates surface wind, which can give information regarding pollution dispersion or accumulation. Therefore, we believe it is better to keep both.

8. Line 649-652: Please be consistent on the notification, such as SO₂ PM_{2.5}. This occurs in other sections of the manuscript, e.g. line 669-672. 2019.

We have gone through the manuscript and made edits accordingly.

Author Comments: Response to reviewers' comments

Title: Evaluation on the effect of regional joint control measures in changing photochemical transformation: A comprehensive study of the optimization scenario analysis

Reviewer #3:

The emission reduction during the Second World Internet Conference provided a unique scenario to evaluate the chemical/physical processes affecting the air quality in Yangtze River Delta region. This paper estimated the emission reduction and simulated this scenario in a reasonable way. It provides some useful insights in the air quality management in this region. One thing is missing is this paper did not show how the chemistry works during the emission reduction period. Since sulfate and nitrate are both secondary, how they were formed and how they were affected? How did nitrate become more significant than sulfate with and without the control measures? The role of dust emission was not paid enough attention in the discussion. There is also a big room for improvement of overall writing. This paper is not presented consistently. It gives me a feeling that this paper is written by two different people. Later part was better presented than the first half.

Thanks to the reviewer for the comments. We have carefully revised the manuscript accordingly, especially in providing insights into the changes of chemistry and dust impact as well. Follows are detailed discussions and revisions.

- Chemistry

To get insights into the changes of chemistry, we replotted figures 9-10, added SOR/NOR/partition of gas phase vs gas + particle phase, and added more discussions regarding the chemistry changes before, during and after the regulations (we selected static weather conditions to set aside the impact of transport). Figure 9 shows the concentration of criteria pollutants including SO₂, NO, CO, NO₂ and PM_{2.5} before, during and after the

regulation under stagnant weather conditions. It can be seen that pollutant concentrations during the campaign were less than those before the campaign, in which SO₂ had the most significant decline of 40.1%, NO_x, CO, PM_{2.5} and PM₁₀ declined 8.0%, 2.6%, 12.5% and 16.3%, respectively, indicating that control measures have significantly improved the air quality in Jiaxing City, especially in the reduction of primary emissions of SO₂ and PM₁₀.

However, after the campaign, all pollutant concentrations rebounded sharply. SO₂, NO, NO₂, CO, PM_{2.5}, PM₁₀ increased 8.3%, 15.4%, 10.3%, 31.8%, 32.2% and 28.6%, respectively. Concentrations of some pollutants were even higher than those before the campaign, suggesting that the source emission intensity had significantly increased after the campaign; the rebounding ratio of NO_x is higher than SO₂.

The changes of major PM_{2.5} chemical components before, during and after the campaign under static weather conditions, could be utilized to characterize the changes of atmospheric chemistry. The concentrations of major chemical components of PM_{2.5} during the campaign were less than those before the campaign, which is consistent with the observation for criteria pollutant concentrations. On average, SO₄²⁻, NH₄⁺, NO₃⁻, OC, mineral soluble ions (Ca²⁺ and Mg²⁺) and K⁺ declined 11.8%, 5.1%, 32.1%, 9.8%, 56.8% and 5.1%, respectively. During the campaign, NO₃⁻ significantly decreased, indicating that vehicle control measures successfully reduced NO_x emissions and subsequently the formation of inorganic aerosols. Significant decrease in SO₄²⁻ also indicate that restricting and/or suspending the operation of coal-burning boilers in local and neighbouring cities had a positive impact.

The chemistry also changes if we compare during and after the regulation. As is shown from figure 10, the SO₂ concentrations after control is a little bit higher than during control (+5.9%). However, the SO₄²⁻ after control is much higher than during control (25.8%). This is probably due to two reasons: firstly, increase of SO₂ emissions and primary sulfate emissions after the control measures were terminated; secondly, previous studies have reported that increased NO₂ emissions could accelerate the formation of secondary sulfate (Cheng et al., 2016). This can be clearly seen from the SOR and NOR indicators. A different trend is observed for NO₂ and NO₃⁻, with the NO₂ concentrations after control being much higher than during control (+9.4%), while the increase of NO₃⁻ (+9.45%) is about the same. Sulfate

originates from both primary emissions and secondary formation, but nitrate is mostly secondary. The NOR during and after regulation is about the same and most of the N is in the gas phase as indicated by $\text{NO}_x/(\text{NO}_x+\text{NO}_3^-)$ (0.87). Therefore, the increase of NO_3^- is lower than SO_4^{2-} .

From the descriptions above, we can see that the secondary formation of nitrate was greatly slowed down due to the strict emission reduction measures. But after the control measures were terminated, the secondary formation rebounded, with the rebounding ratio of sulfate higher (26%) than nitrate (9%). But in terms of absolute concentrations, the nitrate is higher than sulfate, showing that nitrate has become the most important chemical species within $\text{PM}_{2.5}$ in winter in the YRD region.

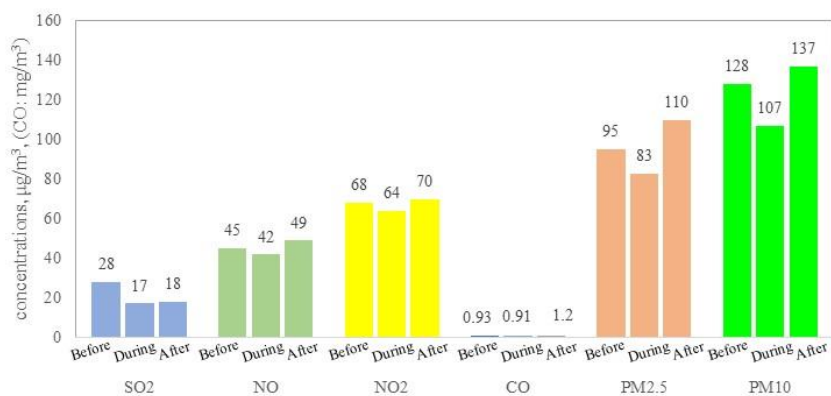
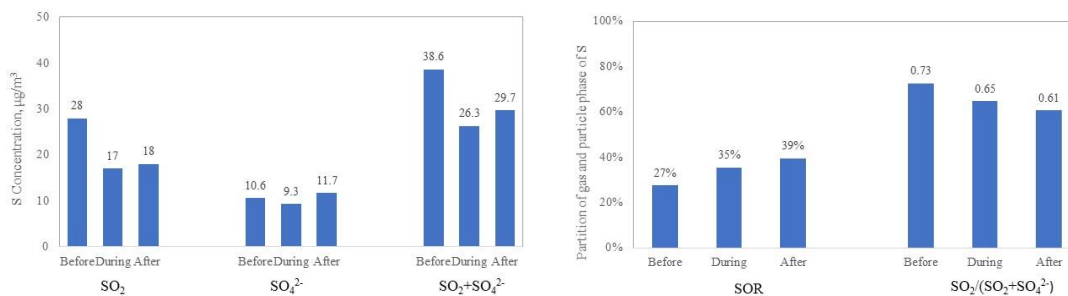


Fig. 9 Comparison between air pollutant concentrations at Shanxi station before, during, and after the campaign under stagnant meteorological conditions



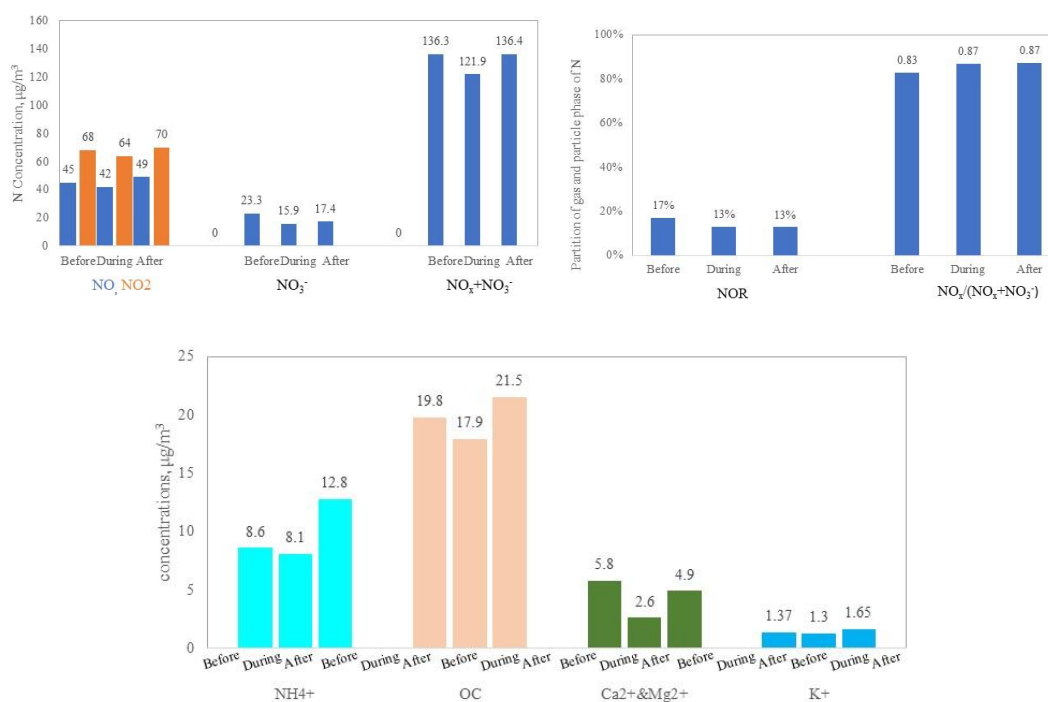


Fig. 10 Comparison between PM_{2.5} chemical components at Shanxi station before and after the campaign under static meteorological conditions

- Dust

We do agree that dust control should be paid enough attention in this study. The dust control is also one of the major control measures during this campaign. Most construction sites were shut down, and cleaning frequencies of the paved roads were increased during the campaign. We added more discussions in the revised manuscript.

Changes in manuscript:

Page 3, Line 82: Specifically, the impact of measures such as management and control of coal-burning power plants, production restriction and suspension of industrial enterprises, motor vehicle limitation and work site suspension, dust control were investigated.

Page 16, Line 331: On average, SO₄²⁻, NH₄⁺, NO₃⁻, OC, mineral soluble irons (Ca²⁺ and Mg²⁺) and K⁺ declined 11.8%, 5.1%, 32.1%, 9.8%, 56.8% and 5.1%, respectively. Comparisons between the distribution of PM_{2.5} chemical components before and during the campaign under static conditions suggest that Ca²⁺ and Mg²⁺ decreased most significantly during the control period, which indicates that the suspension of construction

operations which result in dust emissions and the rising frequency of rinsing and cleaning paved roads, significantly reduced dust emissions.

Page 21, Line 406: Emission reduction of $PM_{2.5}$ caused by dust control was estimated to be 266.0 tons. Dust control contributed 10% to emission reductions of $PM_{2.5}$.

In the conclusion part, (3) The effect of dust control measures is remarkable. During the conference, most of the construction sites in Jiaying were suspended from operation. Increased frequency for road cleaning activities greatly lowered the dust emissions. Speciation of the measured $PM_{2.5}$ suggest that the mass concentration of crust material, decreased by 14% compared to measurements after the conference. Specially, under static conditions, mineral soluble irons (Ca^{2+} and Mg^{2+}) declined 56.8% before and during the campaign. This suggests that the suspension of construction operations and increased frequency of rinsing and cleaning of paved roads significantly reduced dust emissions.

- Writing

We have read through the manuscript and revised the language thoroughly.

Some detail suggestions:

1. Transport vs transportation

Better not to use ‘transportation of air mass’. Transportation is for traffic related business. It’s used for mobile emission. A better way is to say ‘the transport of air mass’ for the movement of air mass/pollutants/plumes.

We have read through the manuscript and revised improper use of “transportation” to “transport” after careful check.

2. Pollution vs pollutant

The used of a lot of ‘pollution’ in this paper is quite confusing. I think you refer it as either ‘plumes’ or ‘polluted air masses’. Pollution is a status, it does not mean any subject and cannot be moved around. While the plumes or pollutants can be moved or transported. I’d strongly suggest the author to check all the wordings in this paper.

We have read through the manuscript and revised improper usage of “pollution” to “plumes”, “polluted air masses” or “emissions”.

3. P3, line 69-70, ‘Many studies: : :’, ‘Some have reported : : :’. Any references?

We have inserted the references.

Changes in manuscript:

Many studies have provided descriptive analysis of changing concentrations of air pollutants during mega events; some have reported the emission reductions and related air quality changes (Wang, et al., 2009; Wang, et al., 2010; Liu, et al., 2013; Tang, et al., 2015; Li, et al., 2016; Wang, et al., 2016; Sun, et al., 2016; Wang, et al., 2015; Chen, et al., 2017; Han, et al., 2016; Qi, et al., 2016).

4. P3, Figure 12 may be better shown here in the introduction.

We agree that putting figure 12 into the introduction part is more suitable, so we moved it forward, and revised the numbers in the figure captions accordingly.

Changes in manuscript:

These areas cover 9 cities including Jiaxing, Huzhou, Hangzhou, Ningbo and Shaoxing in Zhejiang province, Suzhou and Wuxi in Jiangsu province and Xuancheng in Anhui province, as shown in Fig.1.

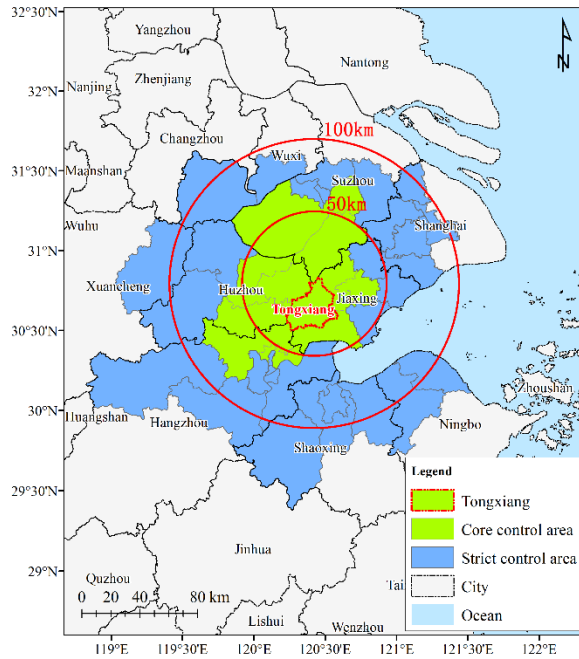


Fig.1 Controlled regions in the Action Plan for Air Quality Control during the World Internet Conference

5. P4, line 101-102, ‘online’ and ‘On-line’?

Revised.

6. P4, line 108, ‘consisting of’ to ‘such as/including’?

Revised.

7. P4, line 110, ‘data conform’ to ‘data quality conform’?

Revised.

8. P5, line 137, ‘with observation data and meteorological data included’. Did you used met observations for TrajStat? How?

Yes. We applied TrajStat to analyze potential source contribution areas of PM_{2.5} in Jiaxing during different pollution episodes. We included observation data and meteorological data as well. For the meteorological data, we combined Global Data Assimilation System (GDAS) meteorological data provided by the NCEP (National Center for Environmental Prediction). For observation data, we included the observed

hourly PM_{2.5} concentrations. The long-term measurement data could be assigned to their corresponding trajectories. The model can be used to identify the trajectories to which a user can distinguish the polluted trajectories with high measurement concentration from a large number of trajectories and then the pollutant pathway could be roughly estimated. The mean pollutant concentration for each cluster can be computed using the cluster statistics function. Pollutant pathways could then be associated with the high concentration clusters. After calculating the PSCF and CWT value, an arbitrary weight function (Polissar et al., 1999) is applied to reduce the uncertainty of cells with few endpoints. Then the potential source regions with high PSCF or CWT value could be identified. (Wang et al., 2009.) We also added color scale to PM_{2.5} concentrations in figures 4-8 (c).

Ref.

Polissar A V, Hopke P K, Paatero P, et al. The aerosol at Barrow, Alaska: long-term trends and source locations. *Atmospheric Environment*, 1999, 33(16): 2441-2458.

Wang Y Q, Zhang X Y, Draxler R R. TrajStat: GIS-based software that uses various trajectory statistical analysis methods to identify potential sources from long-term air pollution measurement data. *Environmental Modelling and Software*, 2009, 24(8): 938-939.

9. P5, line 140, 1x1 degree is quite coarse. Why not just used WRF simulations?

We used GDAS as the meteorological data input. These data are global assimilation data, which can well reflect the meteorological conditions and trajectories. Since we focus on the potential source regions instead of specific sources or each city, we believe 1x1 degree data should suffice for this analysis.

10. P5, line 144, 'increase with the raise of distance' to 'increase with the distance' that's true, dust PM_{2.5} would be the most important equal to or after sulfate. If the dust can be controlled, it's more than what has been achieved due to the control measures.

Any idea what can be done to reduce the dust emissions?

We agree that the dust control is of great importance to improve the air quality. We have highlighted the importance of dust controls, as answered in the following question 33.

The control of dust pollution includes: Construction work sites were suspended in key areas and control areas. Transport of dust materials were forbidden within key neighborhoods. Dust control measures were implemented on renovation operations at ports, docks, railway stations and commercial concrete mixing stations and on materials storage yards. These measures have resulted in the decrease of particle emissions and decrease of mineral ions. Speciation of the measured $PM_{2.5}$ suggest that the mass concentration of crust material, which is greatly affected by dust, decreased by 14% compared to measurements after the conference. Specially, under static conditions, mineral soluble ions (Ca^{2+} and Mg^{2+}) declined 56.8% before and during the campaign.

28. P20, Line 393, One more evidence of other components is 33%

The original sentence “The major chemical components during this cleaner period were organic carbon (26%), nitrate (16%), ammonium (12%) and sulphate (9%)...” has been revised to “The major chemical components during this cleaner period were organic carbon (26%), nitrate (16%), ammonium (12%), sulphate (9%) and other components (37%)...”.

29. P20, section 3.3.1. This section can be more concise. If needed, Details can be moved into supplement materials. The focus here is the Table3.

We agree that the section 3.3.2 and Table 4 is the major focus, so we deleted section 3.3.1, and just add a short description at the beginning of 3.3.2, which has currently been revised to 3.3.

3.3 Emissions reduction estimation during the campaign

The air quality assurance campaign for the 2nd World Internet Conference was from December 8 to December 18. In order to ensure the air quality during the conference,

three provinces and Shanghai municipality in the YRD region carried out joint control measures. Based on the implementation of control measures in all areas during the conference and whether each area had effectively implemented control measures on December 8-18, regional emission reductions have been assessed.....

30. P20, line 394, 'obvious regional pollution characteristics', what is it?

It means regional transport, to avoid misunderstanding, we revised this sentence to:

The major chemical components during this cleaner period were organic carbon (26%), nitrate (16%), ammonium (12%), sulphate (9%) and other components (37%), with some newly formed particles and no obvious regional transport, suggesting that air pollutants were mainly derived from local emissions.

31. P28, line 589, 'percent reduction' to 'percentage reduction', 'conducted' to 'considered/investigated/discussed/etc'

Revised accordingly.

32. P30, section 3.6 seems to be not that relevant here. It may be moved into the introduction or the supplement.

We removed section 3.6, and revised to short descriptions in the introduction part.

Many studies have provided descriptive analysis of the changing concentrations of air pollutants during mega events, some have reported the emission reductions and related air quality changes (Wang, et al., 2009; Wang, et al., 2010; Liu, et al., 2013; Tang, et al., 2015; Li, et al., 2016; Wang, et al., 2016; Sun, et al., 2016; Wang, et al., 2015; Chen, et al., 2017; Han, et al., 2016; Qi, et al., 2016). However, different air pollution control targets, different control measures, and different locations, may cause big different effects among those strategies....

33. P32, line 682. 'The effect of dust control measures is remarkable'. This conclusion comes from nowhere. It has not been discussed or showed in this paper. Better to prove it or remove

it.

We revised the conclusion by adding more proves, as follows:

The effect of dust control measures is remarkable. During the conference, most of the construction sites in Jiaxing were suspended from operation. Increased frequency for road cleaning activities greatly lowered the dust emissions. Speciation of the measured $PM_{2.5}$ suggest that the mass concentration of crust material, which is greatly affected by dust, decreased by 14% compared to measurements after the conference. Specially, under static conditions, mineral soluble irons (Ca^{2+} and Mg^{2+}) declined 56.8% before and during the campaign. This suggests that the suspension of construction operations which result in dust emissions and the increased frequency of rinsing and cleaning of paved roads significantly reduced dust emissions.

1 **Evaluation on the effect of regional joint control measures in**
2 **changing photochemical transformation: A comprehensive study of**
3 **the optimization scenario analysis**

4 Li LI^{1,2#*}, Shuhui ZHU^{2#}, Jingyu AN^{2#}, Min ZHOU², Hongli WANG^{2*}, Rusha YAN², Liping
5 QIAO², Cheng Huang^{2*}, Xudong TIAN³, Lijuan SHEN⁴, Ling Huang¹, Yangjun Wang¹, Cheng
6 Huang^{2*}, Jeremy C AVISE⁵, Joshua S FU⁶

带格式的：上标

- 7 1. School of Environmental and Chemical Engineering, Shanghai University, Shanghai, 200444, China
8 2. State Environmental Protection Key Laboratory of the Cause and Prevention of Urban Air Pollution
9 Complex, Shanghai Academy of Environmental Sciences, Shanghai 200233, China
10 3. Zhejiang Environmental Monitoring Center, Hangzhou, 310014, China
11 4. Jiaxing Environmental Monitoring Station, Jiaxing, 314000, China
12 5. Laboratory for Atmospheric Research, Washington State University, Pullman, Washington, USA.
13 6. Department of Civil & Environmental Engineering, University of Tennessee, Knoxville, TN 37996, USA

14
15 *Correspondence to: C. Huang (huangc@saes.sh.cn) ~~and~~ H. L. WANG (wanghl@saes.sh.cn) and
16 L. Li (Lily@shu.edu.cn)

带格式的：默认段落字体，字体：Calibri

17 #These three people contributed equally to this work.

18
19 **Abstract:** Heavy haze usually occurs in winter in eastern China. To control the severe air
20 pollution during the season, comprehensive regional joint-control strategies were implemented
21 throughout a campaign. To evaluate the effectiveness of these strategies and to provide some
22 insights into strengthening the regional joint-control mechanism, the influence of control measures
23 on levels of air pollution were estimated with an integrated measurement-emission-modeling
24 method. To determine the influence of meteorological conditions, and the control measures on the
25 air quality, in a comprehensive study, the 2nd World Internet Conference was held during
26 December 16-18, 2015 in Jiaxing City, Zhejiang Province in the Yangtze River Delta (YRD)
27 region. We first analyzed the air quality changes during four meteorological regimes; and then
28 compared the air pollutant concentrations before, during and after the regulation under static
29 meteorological conditions. Next, we conducted modeling scenarios to quantify the effects caused
30 due to the air pollution control measures. We found that total emissions of SO₂, NO_x, PM_{2.5} and
31 VOCs in Jiaxing were reduced by 56%, 58%, 64% and 80%, respectively; while total emission
32 reductions of SO₂, NO_x, PM_{2.5} and VOCs over the YRD region are estimated to be 10%, 9%, 10%
33 and 11%, respectively. Modelling results suggest that during the campaign from December 8 to
34 December 18, PM_{2.5} daily average concentrations decreased by 10 μg/m³ with an average decrease
35 of 14.6%. Our implemented optimization analysis compared with previous studies also reveal that
36 local emission reductions play a key role in air quality improvement, although it shall be
37 supplemented by regional linkage. In terms of regional joint control, to implement pollution
38 channel control 48 hours before the event is of most benefit in getting similar results. Therefore, it

带格式的：字体：非加粗

带格式的：字体：非加粗，下标

带格式的：字体：非加粗

带格式的：字体：非加粗，倾斜，下标

带格式的：字体：非加粗

带格式的：字体：非加粗，下标

带格式的：字体：非加粗

带格式的：字体：非加粗，下标

带格式的：字体：非加粗

带格式的：字体：非加粗，倾斜，下标

带格式的：字体：非加粗

带格式的：字体：非加粗，下标

带格式的：字体：非加粗

带格式的：字体：非加粗，下标

带格式的：字体：非加粗

带格式的：字体：非加粗，上标

带格式的：字体：非加粗

39 ~~is recommended that a synergistic emission reduction plan between adjacent areas with local~~
40 ~~pollution emission reductions as the core part should be established and strengthened, and~~
41 ~~emission reduction plans for different types of pollution through a stronger regional linkage~~
42 ~~should be reserved.~~ Heavy haze usually occurs in winter in eastern China. To control the severe air
43 ~~pollution during the season, comprehensive regional joint control strategies were implemented~~
44 ~~throughout a campaign. To evaluate the effectiveness of these strategies and to provide some~~
45 ~~insight into strengthening the joint control mechanism, the influence of control measures on levels~~
46 ~~of air pollution were estimated. To determine the influence of meteorological conditions, and the~~
47 ~~control measures on the air quality, in a comprehensive study, the 2nd World Internet Conference~~
48 ~~was held during December 16–18, 2015 in Jiaxing City, Zhejiang Province in the Yangtze River~~
49 ~~Delta (YRD) region. We first analyzed the air quality changes during four meteorological regimes;~~
50 ~~and then compared the air pollutant concentrations during days with stable meteorological~~
51 ~~conditions. Next, we did modeling scenarios to quantify the effects caused due to the air pollution~~
52 ~~control measures. We found that total emissions of SO₂, NO_x, PM_{2.5} and VOCs in Jiaxing were~~
53 ~~reduced by 56%, 58%, 64% and 80%, respectively; while total emission reductions of SO₂, NO_x,~~
54 ~~PM_{2.5} and VOCs over the YRD region are estimated to be 10%, 9%, 10% and 11%, respectively.~~
55 ~~Modelling results suggest that the regional controls (including Jiaxing and surrounding area)~~
56 ~~reduced PM_{2.5} levels in Jiaxing between 5.5%–16.5% (9.9% on average), while local control~~
57 ~~measures contributed 4.5%–14.4%, with an average of 8.8%. Our implemented optimization~~
58 ~~analysis compared with previous studies also reveal that local emission reductions play a key role~~
59 ~~in air quality improvement, although it shall be supplemented by regional linkage. In terms of~~
60 ~~regional joint control, to implement pollution channel control 48 hours before the event is of most~~
61 ~~benefit in getting similar results. Therefore, it is recommended that a synergistic emission~~
62 ~~reduction plan between adjacent areas with local pollution emission reductions as the core part~~
63 ~~should be established and strengthened, and emission reduction plans for different types of~~
64 ~~pollution through a stronger regional linkage should be reserved.~~

65 **Keywords:** PM_{2.5}; regional joint control; ~~meteorology~~; YRD

66 **1 Introduction**

67 High concentrations of PM_{2.5} has attracted much attention due to its impact on visibility (Pui
68 et al., 2014), human health (West et al., 2016) and global environment. To control air pollution
69 situation in China, the Ministry of Ecology and Environment of the People’s Republic of China
70 has released a lot of policies, which can generally be divided into long-term action plans (such as
71 the Clean Air Action Plan (2013-2017), the Five-year Action Plans) and short-term control
72 measures (such as Clean Air Protection ~~during~~ Mega Events, Air Pollution Warning and
73 Protection Measures). China has successfully implemented some mega event air pollution control

74 plans and ensured good air quality, including the 2008 Beijing Olympics (Kelly and Zhu, 2016);
75 the 2010 World Expo in Shanghai (CAI-Asia, 2010); the 2010 Guangzhou Asian Games (Liu et
76 al., 2013); the 2014 Asia-Pacific Economic Cooperation Forum (APEC) (Liang et al., 2017); 2014
77 Summer Youth Olympics in Nanjing (CAI-Asia, 2014) and the 2015 China Victory Day Parade
78 (Victory Parade 2015) (Liang et al., 2017), etc. After implementation of these control measures, it
79 is important to understand how effective these strategies are.

80 | The 2nd World Internet Conference was held in ~~Tongxiang, Wuzhen~~, Jiaxing, Zhejiang during
81 16-18 December, 2015. To reduce air pollution during the conference, Zhejiang Province and the
82 Regional Air-pollution Joint Control Office of the Yangtze River Delta (YRD) region developed
83 an Action Plan for Air Pollution Control during the Conference (henceforth referred to as the
84 Action Plan), which clarified target goals, time periods for implementing controls, regions in
85 which the controls would be applied, and the control measures to be implemented, as described
86 below. **Targets:** achieve an Air Quality Index (AQI) below 100 in “key areas”, an AQI below 150
87 in “control areas”, and to achieve significant improvement of the air quality in the surrounding (or
88 | buffer) regions outside ~~of~~ the control areas. **Time Periods:** the time periods of interest for
89 implementing various controls include the early stage (3 months before the conference), the
90 advanced stage (2 weeks to 4 days before the conference) and the central stage (3 days before and
91 2 days after the conference). **Regions:** areas within a 50km radius, within a 100km radius and
92 | outside of a 100km radius from the centre of ~~Wuzhen-Tongxiang~~ were classified as key areas,
93 control areas and buffer areas, respectively. These areas cover 9 cities including Jiaxing, Huzhou,
94 Hangzhou, Ningbo and Shaoxing in Zhejiang province, Suzhou and Wuxi in Jiangsu province and
95 | Xuancheng in Anhui province, ~~as shown in Fig.1.~~

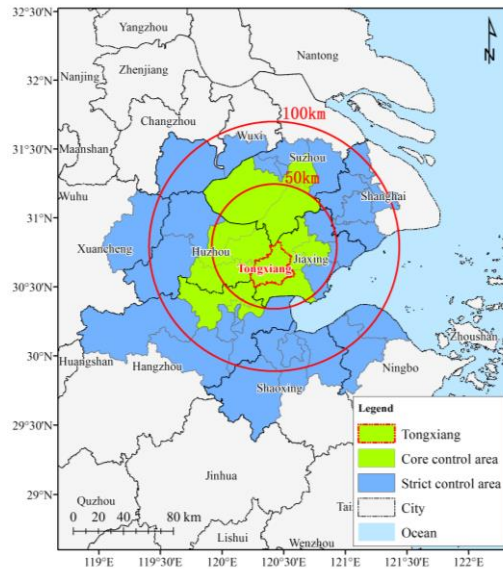


Fig.1 Controlled regions in the Action Plan for Air Quality Control during the World Internet Conference

96
 97
 98
 99 Many studies have provided descriptive analysis of changing concentrations of air pollutants
 100 during mega events; some have reported the emission reductions and related air quality changes
 101 (Wang, et al., 2009; Wang, et al., 2010; Liu, et al., 2013; Tang, et al., 2015; Li, et al., 2016; Wang,
 102 et al.,2016; Sun, et al., 2016; Wang, et al., 2015; Chen, et al., 2017; Han, et al., 2016; Qi, et al.,
 103 2016).Many studies have provided descriptive analysis of the changing concentrations of air
 104 pollutants during mega events. Some have reported the emission reductions and related air quality
 105 changes. However, different air pollution control targets, different control measures, and different
 106 locations, may cause big different effects among those strategies. In this paper, the reduction in
 107 $PM_{2.5}$ achieved through the Action Plan is investigated further to help quantify the level of $PM_{2.5}$
 108 reduction that can be attributed to different aspects of the Action Plan. An integrated
 109 emission-measurement-modelling method described in the next section including analysis of
 110 multi-pollutant observations, backward trajectory and potential source contribution analyses,
 111 estimates of pollutant emission reductions, and photochemical model simulations were adopted to
 112 conduct a comprehensive assessment of the impact of control measures on air quality
 113 improvement based on three aspects: meteorological conditions, pollutant emission reductions of
 114 local sources, and regional contributions.

115

116 2 Methodology

117 In order to strengthen the regional air pollution joint-control mechanism in the YRD region,
118 various measures and their implementation were systematically reviewed, and the qualitative and
119 quantitative relationships ~~between~~among the implementation of measures, changes in emissions
120 of air pollution sources and air quality improvement were studied. Specifically, the impact of
121 measures such as management and control of coal-burning power plants, production restriction
122 and suspension of industrial enterprises, motor vehicle limitation and work site suspension, dust
123 control were investigated. In addition, the role of meteorology (in particular, transport) was
124 assessed in terms of its influence on the relevance and effectiveness of various measures, and
125 ways of optimising air quality control measures and emergency emission reductions under heavy
126 pollution during major events were evaluated.

127 To assess the effectiveness of the various controls outlined in the Action Plan, emission
128 reductions associated with those controls were calculated, and photochemical modelling was
129 conducted to determine the change in PM_{2.5} attributed to specific controls. On this basis, an
130 assessment of how to optimise control measures was carried out with respect to both the area in
131 which the emission reduction took place, as well as the start time for implementing the controls
132 (i.e., how far in advance do the controls need to be implemented). Analysis of the numerical
133 modelling results is focused on the effectiveness of the control measures with respect to regional
134 transport of pollutants in the YRD region.

135

136 2.1 Measurements

137 The ~~On-en~~line observational station was set up at the Shanxi supersite of Zhejiang Province
138 (30.82 °-N, 120.87 °-E), which was located at the core area for pollution-control measures.
139 On-line hourly PM_{2.5} mass concentration, carbonaceous aerosols, elements, and ionic species were
140 measured by the Synchronized Hybrid Ambient Real-time Particulate Monitor (SHARP, model
141 5030, Thermo Fisher Scientific Corporation, USA), the OC/EC carbon aerosol analyzer (Model-4,
142 Sunset Laboratory Corporation, USA), the Xact multi-metals monitor (XactTM 625, PALL
143 Corporation, USA), and the Ambient Ion Monitor-Ion Chromatograph (AIM IC, model URG 9000,

144 | URG Corporation, USA), respectively. Meteorological parameters, ~~consisting of~~including wind
145 | speed, wind direction, temperature, pressure, and relative humidity, were measured as well.

146 | PM_{2.5} concentration data quality conform to the standards of data quality control published
147 | by Ministry of Ecology and Environment of the People's Republic of China.

148 | A semi-continuous Sunset OC/EC analyser was used to measure OC and EC mass loadings at
149 | the observation site by adopting NIOSH-5040 protocol based on thermal-optical transmittance
150 | (TOT). The ambient air was first sampled into a PM_{2.5} cyclone inlet with a flow rate of 8 L min⁻¹.
151 | The OC and EC were collected on a quartz fiber filter with an effective collection area of 1.13 cm².
152 | The analyzer was programmed to collect aerosol for 45 min at the start of each hour, followed by
153 | the analysis of carbonaceous species during the remainder of the hour. The analysis procedure is
154 | described in detail by Huang et al. (2018)

155 | The ionic concentrations of nitrate, sulphate, chloride, sodium, ammonium, potassium,
156 | calcium and magnesium (Na⁺, K⁺, Ca²⁺, NH₄⁺, Mg²⁺, NO₃⁻, SO₄²⁻, Cl⁻) in the fine fraction (PM_{2.5})
157 | were measured with a 1-hour time resolution using the AIM IC. The sample analysis unit is
158 | composed by an anion and a cation ion chromatographs (Dionex ICS-1100), which was using
159 | guard columns with potassium hydroxide eluent (KOH) for the anion system and methane sulfonic
160 | acid (MSA) eluent for the cation system. The limit of the detection reported by the manufacturer is
161 | 0.1 ug/m³ for all species. The operation principle of AIM-IC is described in detail by Markovic et
162 | al. (2012)

163 | Hourly ambient mass concentrations of sixteen elements (K, Ca, V, Mn, Fe, As, Se, Cd, Au,
164 | Pb, Cr, Ni, Cu, Zn, Ag, Ba) in PM_{2.5} were determined by the Xact multi-metals monitor. In brief,
165 | the Xact instrument samples the air through a section of filter tape at a flow rate of 16.7 lpm using
166 | a PM_{2.5} sharp cut cyclone. The exposed filter tape spot then advances into an analysis area where
167 | the collected PM_{2.5} is analyzed by energy-dispersive X-ray fluorescence (XRF) to determine metal
168 | mass concentrations. The sequence of sampling and analysis were performed continuously and
169 | simultaneously on an hourly basis.

170 | **2.2 Potential Source Contribution Analysis**

171 | TrajStat is a HYSPLIT model developed by Chinese Academy of Meteorological Sciences
172 | and NOAA Air Resources Laboratory based on geographic information system (GIS). It uses

173 statistical methods to analyze air mass back trajectories to cluster trajectories and compute
174 potential source contribution function (PSCF) with observation data and meteorological data
175 included (Wang et al., 2009).

176 PSCF analysis is a conditional probability function using air mass trajectories to locate
177 pollution sources. It can be calculated for each 1° longitude by 1° latitude cell by dividing the
178 number of trajectory endpoints that correspond to samples with factor scores or pollutant
179 concentrations greater than specified values by the number of total endpoints in the cell (Zeng et
180 al., 1989). Therefore, pollution source areas are indicated by high PSCF values. Since the
181 deviation of PSCF results could increase with the raise of distance between cell and receptor,

182 therefore a weight factor (W_{ij}) was adopted in this study to lower the uncertainty of PSCF results.
183 PSCF and W_{ij} calculations are described in Eq. (1) and Eq. (2), where m_{ij} is the number of
184 trajectory endpoints greater than specified values in cell (i, j), n_{ij} is the number of total endpoints
185 in this cell (Zeng et al., 1989; Polissar et al., 1999).

$$186 \quad P = \frac{m_{ij}}{n_{ij}} \cdot W(n_{ij}) \quad (1)$$

$$187 \quad W(n_{ij}) = \begin{cases} 1.00, & 80 < n_{ij} \\ 0.70, & 20 < n_{ij} \leq 80 \\ 0.42, & 10 < n_{ij} \leq 20 \\ 0.05, & n_{ij} \leq 10 \end{cases} \quad (2)$$

188 In this study, the TrajStat modelling system was used to analyze potential source contribution
189 areas of $PM_{2.5}$ in Jiaxing during different pollution episodes with the combination of [Global Data](#)
190 [Assimilation System \(GDAS\)](#) meteorological data provided by the NCEP (National Center for
191 Environmental Prediction). ~~Pollution~~-Polluted air mass trajectories corresponded to those
192 trajectories with $PM_{2.5}$ hourly concentration higher than $75 \mu g/m^3$.

193 **2.3 Model setup ~~for separating meteorological influence and control measures~~**

194 **2.3.1 Model selection and parameter settings**

195 In this study, the WRF-CMAQ/CAMx air quality numerical modelling system was used to
196 evaluate the improvement in air quality resulting from the control measures outlined in the Action
197 Plan. It takes into account of modeling variations from different air quality models. For the
198 mesoscale meteorological field, we adopted the WRF model Version 3.4
199 (<https://www.mmm.ucar.edu/wrf-model-general>), the CAMx model Version 6.1

带格式的：下标

带格式的：下标

带格式的：下标

带格式的：下标

带格式的：下标

带格式的：下标

200 (http://www.camx.com/) and the CMAQ model Version 5.0 (Nolte et al., 2015;
 201 http://www.cmascenter.org/cmaq/). The chemical mechanism utilized in CMAQ was the CB05
 202 gas phase chemical mechanism (Yarwood, et al., 2005) and AERO5 aerosol mechanism, which
 203 includes the inorganic aerosol thermodynamic model ISORROPIA (Nenes, et al., 1998) and
 204 updated SOA yield parameterizations. The gaseous and aerosol modules used in CAMx are the
 205 CB05 chemical mechanism and CF module, respectively. The aqueous-phase chemistry for both
 206 models is based on the updated mechanism of the Regional Acid Deposition Model (RADM)
 207 (Chang et al., 1987). Particulate Source Apportionment Technology (PSAT) coupled in the CAMx
 208 is applied to quantify the regional contributions to PM_{2.5} as well. The WRF meteorological
 209 modeling domain consists of three nested Lambert projection grids of 36km-12km-4km, with 3
 210 grids larger than the CMAQ/CAMx modeling domain at each boundary. WRF was run
 211 simultaneously for the three nested domains with two-way feedback between the parent and the
 212 nest grids. Both the three domains utilized 27 vertical sigma layers with the top layer at 100hpa,
 213 and the major physics options for each domain listed in Table 1. For the CMAQ/CAMx modelling
 214 domain shown in Figure 2, we adopted a 36-12-4km nested domain structure with 14 vertical
 215 layers, which were derived from the WRF 27 layers. The two outer domains cover much of
 216 eastern Asia and eastern China, respectively, while the innermost domain covers the YRD region.
 217 The simulation period was from 1-18 December, 2015, during which 1-7 December was utilized
 218 for model spin-up and 8-18 December was the key period for analysis of the modelling results
 219 with control measures.

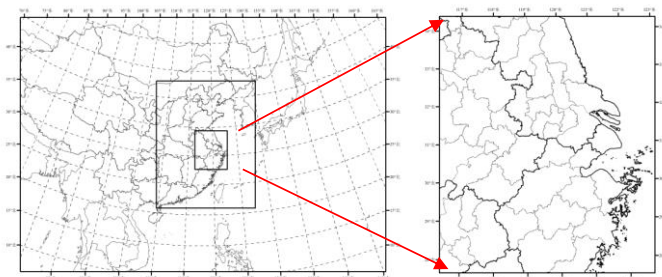


Fig 2. Modeling domain

Table 1 Parameterization scheme of the physical processes in the WRF model

Physical Processes	Parameterization Scheme	Reference
Microphysical Process	Purdue Lin Scheme	(Lin, 1983)

带格式的：行距：最小值 12 磅
 带格式表格
 带格式的：行距：最小值 12 磅

Cumulus Convective Scheme	Grell-3 Scheme	(Grell and Dévényi, 2002)
Road Process Scheme	Noah Scheme	(Ek, 2003)
Boundary Layer Scheme	Yonsei University (YSU) Scheme	(Hong, 2006)
Long-wave Radiation	RRTM Long-wave Radiation Scheme	(Mlawer et al., 1997)
Short-wave Radiation Scheme	Goddard Short-wave Radiation Scheme	(Chou and Suarez, 1999)

- 带格式的：行距：最小值 12 磅
- 带格式的：行距：最小值 12 磅
- 带格式的：行距：最小值 12 磅
- 带格式的：行距：最小值 12 磅
- 带格式的：行距：最小值 12 磅

224 Initial and boundary conditions (IC/BCs) for the WRF modeling were based on 1-degree by
 225 1-degree grids FNL Operational Global Analysis data that are archived at the Global Data
 226 Assimilation System (GDAS). Boundary conditions to WRF were updated at 6-hour intervals for
 227 D01.

228 Anthropogenic source emission inventory in YRD is based on a most recent inventory
 229 developed by our group (Huang et al., 2011; Li et al., 2011; Liu et al., 2018). The emission
 230 inventory for areas outside YRD in China is derived from the MEIC model (Multi-resolution
 231 Emission Inventory of China, latest data for 2012(<http://www.meicmodel.org>) and anthropogenic
 232 emissions over other Asian region are from the MIX emission inventory for 2010 (Li et al., 2017).
 233 Biogenic emissions are calculated by the MEGAN v2.1 (Guenther et al., 2012). The Sparse Matrix
 234 Operator Kernel Emissions (SMOKE, <https://www.cmascenter.org/smoke>) model is applied to
 235 process these emissions for modeling inputs that is more detailed emission processes and not
 236 usually used in China.

237 2.3.2 Model performance

238 Prior to evaluating the effectiveness of the control measures and reactions, the performance
 239 of the modelling system was evaluated to ensure it was able to reasonably reproduce the observed
 240 meteorological conditions and PM_{2.5} levels. Statistical indexes used for model evaluation include
 241 Normalised Mean Bias (NMB), Normalised Mean Error (NME) and Index of Agreement (IOA).

242 The equations to calculate these statistical indexes are as follows:

$$NMB = \frac{\sum(P_j - O_j)}{\sum O_j} \times 100\%$$

(3)

$$NME = \frac{\sum |P_j - O_j|}{\sum O_j} \times 100\%$$

(4)

$$IOA = 1 - \frac{\sum(P_j - O_j)^2}{\sum(|P_j - \bar{O}| + |O_j - \bar{O}|)^2}$$

(5)

243 where P_i and O_j are predicted and observed hourly concentrations, respectively. \bar{O} is the
 244 average value of observations. IOA ranges from 0 to 1, with 1 indicating perfect agreement
 245 between model and observation.

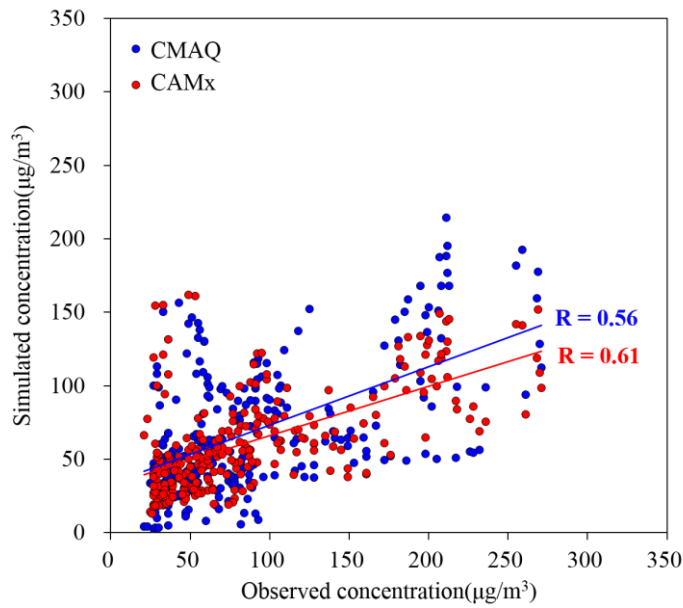
- 带格式的：字体：Times New Roman
- 带格式的：字体：Times New Roman
- 带格式的：字体：Times New Roman
- 带格式的：字体：(默认) Times New Roman, (中文) 宋体, 英语(英国)
- 带格式的：字体：(中文) 宋体, 英语(英国)
- 带格式的：字体：(默认) Times New Roman, (中文) 宋体, 英语(英国)
- 带格式的：字体：(默认) Times New Roman, (中文) 宋体, 英语(英国)
- 带格式的：字体：(中文) 宋体, 英语(英国), 到齐到网格

246 Observational data from the Shanxi supersite in Jiaxing City were compared with model
 247 results for model evaluation verification. Table 2 shows the summary statistics for the main
 248 meteorological parameters simulated with the WRF model and hourly PM_{2.5} concentrations
 249 simulated by CMAQ. Among the meteorological parameters, wind speed is slightly over predicted
 250 with the ~~IOA-NMB~~ value of 28%, while temperature, relative humidity and pressure all have
 251 ~~NMBIOA~~ values greater than 0.9. Figure 2–3 compares the simulated and observed PM_{2.5}
 252 concentrations at the Shanxi supersite. In general, model predicted data are lower than the
 253 observed data with the NMB value of -22% to -30%, the NME value of 45% to 47% and the IOA
 254 value of 0.67 to 0.70 (Table 2). These underestimations may be due to three reasons: Firstly,
 255 winter underestimation of PM_{2.5} (especially SOA) is a common issue with CMAQ or CAMx
 256 simulations over China (Hu et al., 2017; Li et al., 2016), which can be explained by a lack of
 257 model calculated oxidants or missing reactions (Kasibhatla et al., 1997) of SOA formation
 258 pathways (Appel et al., 2008; Foley et al., 2010). Secondly, uncertainty still exists in the regional
 259 emission inventory, including the basic emissions inventory and the control scenarios. Thirdly, the
 260 wind speed is slightly overestimated over the region, with NMB and NME of 28% and 33%,
 261 causing fast dispersion of air pollutants. Overall, these statistics for both the meteorological
 262 parameters and simulated PM_{2.5} are generally consistent with the results in other published
 263 modelling studies(Zheng et al., 2015;Wang et al., 2014;Zhang et al., 2011;Fu et al., 2016;Li et al.,
 264 2015b;Li et al., 2015a), which suggests that the simulation performance is acceptable.

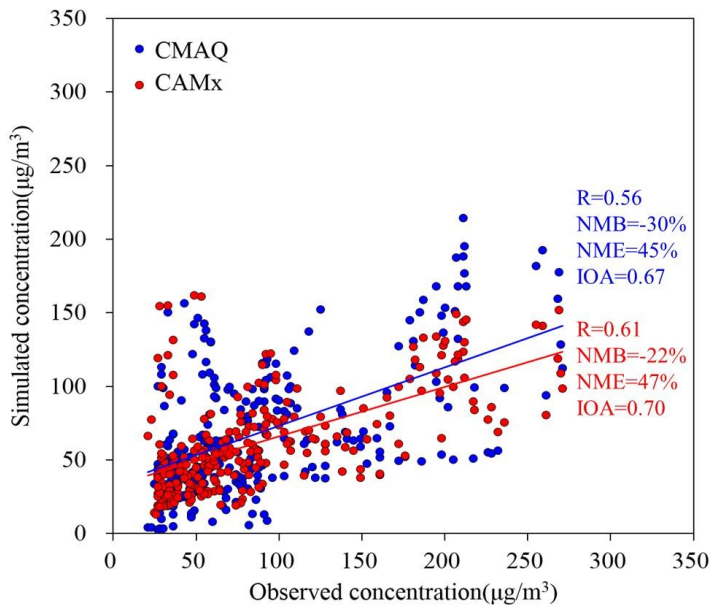
265 Table 2 Statistics of simulation verification for meteorological parameters and hourly PM_{2.5} concentration

Statistical indexes	Wind speed	Temperature	Relative humidity	Air pressure	CAMx-P M _{2.5}	CMAQ-P M _{2.5}
NMB	28%	3%	-9%	0%	-30%	-22%
NME	33%	14%	12%	0%	45%	47%
IOA	0.81	0.97	0.93	1.00	0.67	0.70

266



267



268

Fig. 2-3 Scatter plot of the simulated and observed PM_{2.5} at the Shanxi supersite

269

2.3.3 Method for quantifying the effectiveness of a control

270

Quantifying the PM_{2.5} reduction in response to emission reductions was done using the so called Brute Force Method (BFM) (Burr and Zhang, 2011), where a baseline scenario was simulated using unadjusted emissions (i.e., those emissions that would have occurred in absence of the Action Plan) and a campaign scenario was modelled based on the emission controls outlined in the Action Plan. In both cases, the same meteorology and chemical boundary

271

272

273

274

275 conditions were utilized to drive the photochemical model simulations. Through a comparative
276 analysis of the scenarios, a relative improvement factor (RF) for a given atmospheric pollutant,
277 resulting from emission controls, can be calculated and combined with ground based observations
278 to assess the improvement in air quality associated with those emission controls.

$$279 \quad RF = (C_b - C_s) / C_b \quad (63)$$

$$280 \quad C_d = C_o - RF \cdot C_o \quad (74)$$

281 where C_b is the simulated pollutant concentration in the baseline scenario ($\mu\text{g}/\text{m}^3$), C_s is the
282 pollutant concentration in the campaign scenario ($\mu\text{g}/\text{m}^3$), C_o denotes the actual observed
283 concentration at the site ($\mu\text{g}/\text{m}^3$) and C_d is the concentration improvement caused by the control
284 measures ($\mu\text{g}/\text{m}^3$). Utilizing models in a relative sense to assess the ~~effieacy~~ efficiency of emission
285 controls on air quality is common practice in regulatory modelling, with the assumption that there
286 may be biases in the absolute concentrations simulated by a modelling system, but that the relative
287 response of that system will reflect the response observed in the atmosphere (US EPA, 2014).

288 3 Results and discussion

289 3.1 Photochemical transformation changes of air pollutants during the campaign

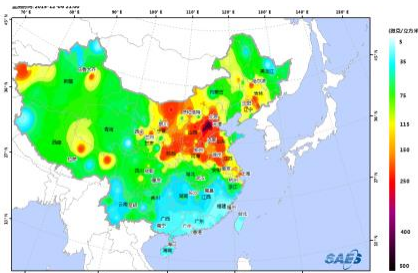
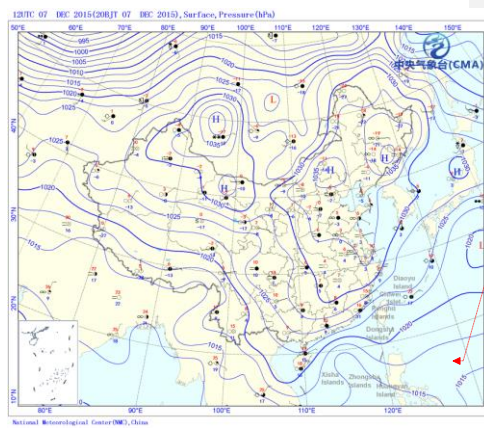
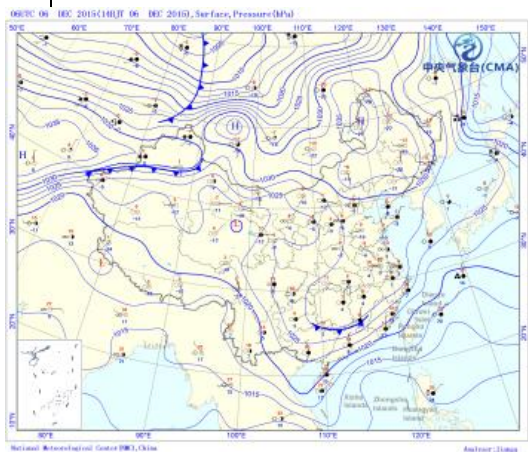
290 Ground observation^{al} data show that from December 1 to December 23, Jiaying City
291 experienced four distinct physical and chemical processes that contributed to the observed
292 pollution levels at different periods. ~~For each of these processes, this study has~~
293 ~~comprehensively in the integrated emission measurement modeling method considered the~~
294 ~~backward air flow trajectory, potential contribution source areas, meteorological conditions and~~
295 ~~the variation of PM_{2.5} concentration to analyse the evolution of the observed air quality. For each~~
296 ~~of these processes, this study utilized the integrated emission-measurement-modeling method to~~
297 ~~analyze the evolution of air quality from several aspects, including the backward air flow~~
298 ~~trajectory, potential contribution source areas, meteorological conditions and the variation of~~
299 ~~PM_{2.5} concentration.~~

带格式的：下标

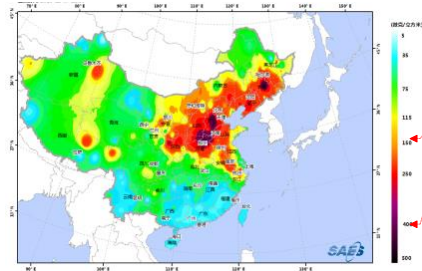
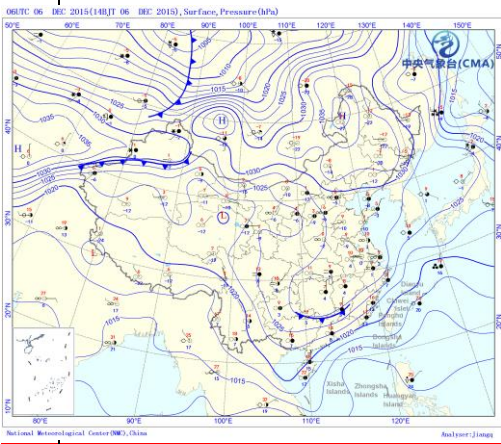
300 3.1.1 Pollution process before the campaign with local emission accumulation as the main 301 contributor

302 The first time period of interest was from December 6 to December 8. Analysis about the
303 potential source contribution areas resulting from PSCF modelling suggests that the polluted air
304 mass primarily originated from the northwest and northerly airstreams, passing Shandong, the

305 | eastern coastal areas of Jiangsu and Shanghai and into northern Zhejiang, as is shown in Fig. 34.
 306 | Analysis of the large-scale weather patterns showed that ~~pollution~~ the polluted air mass occurred
 307 | in Beijing, Tianjin, Shandong peninsula and northern Jiangsu as a result of cold air with polluted
 308 | air mass transported into the region on the morning of December 5. In the southern part of
 309 | Shandong province, the PM_{2.5} concentration peak appeared on the morning of December 6, while
 310 | the PM_{2.5} concentration peak appeared around midnight on December 7 at the coastal area of
 311 | Jiangsu. On December 6, the development of warm and humid air flow, resulted in increasing
 312 | ground humidity, which contributed to the growth of secondary fine particles and the gradual
 313 | accumulation of ~~pollution~~ polluted air mass in northern Zhejiang and the surrounding areas of
 314 | Shanghai. On December 7, affected by the surface high-pressure system, the spread of ~~pollution~~
 315 | plume was slow, and the spatial extent of the ~~pollution~~ plumes in northern Zhejiang expanded.
 316 | Therefore, during this time period, the pollution was primarily affected by regional transport and
 317 | worsened by stagnant local conditions in Jiaying.



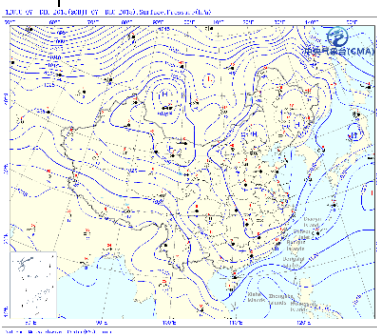
带格式表格



带格式的：两端对齐，段落间距段前：0 磅

带格式的：段落间距段前：0 磅

(+)



带格式的：段落间距段前：0 磅

带格式的：居中，段落间距段前：0 磅

带格式的：段落间距段前：0 磅

带格式的：字体：6 磅

带格式的：字体：Times New Roman, 6 磅, 字体颜色：文字 1

带格式的：居中，行距：固定值 10 磅

带格式的：字体：7 磅

带格式的：字体：7 磅, 字体颜色：文字 1

带格式的：字体：7 磅, 字体颜色：文字 1, 下标

带格式的：字体：7 磅

带格式的：字体：Times New Roman, 7 磅, 字体颜色：文字 1

带格式的：居中，行距：固定值 10 磅

带格式的：字体：7 磅

带格式的：居中，行距：固定值 10 磅

带格式的：字体：7 磅, 字体颜色：文字 1

带格式的：字体：7 磅, 字体颜色：文字 1, 下标

带格式的：字体：7 磅

带格式的：字体：Times New Roman, 7 磅, 字体颜色：文字 1

带格式的：居中，行距：固定值 6 磅

带格式的：字体：Times New Roman, 八号, 字体颜色：文字 1

带格式的：上标

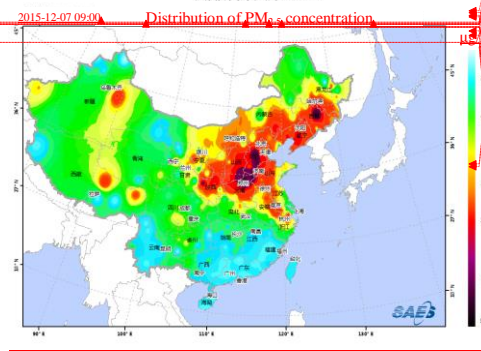
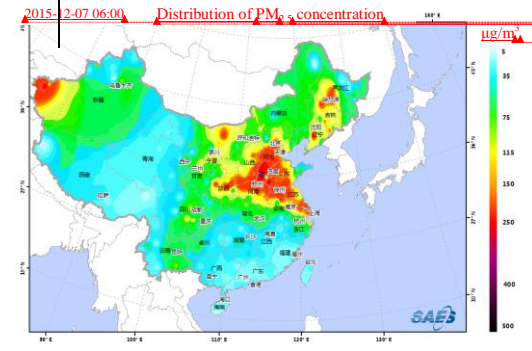
带格式的：字体：Times New Roman, 7 磅, 字体颜色：文字 1

带格式的：居中，行距：固定值 10 磅

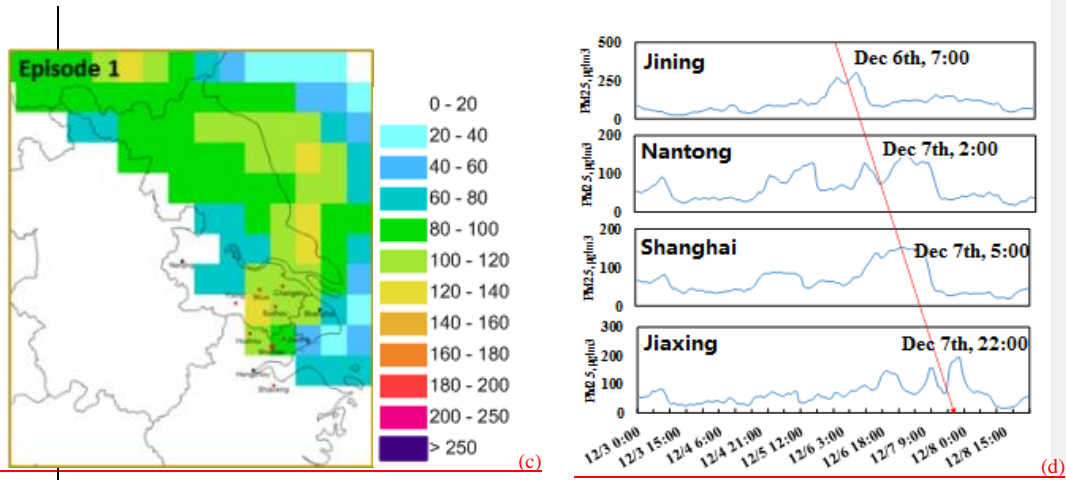
带格式的：居中，行距：固定值 10 磅

带格式的：上标

带格式的：字体：Times New Roman, 7 磅, 字体颜色：文字 1



(b)



318
319
320

Fig. 3-4 Analysis of (a) the large-scale weather patterns, (b) distribution of PM_{2.5} concentrations, (c) potential source regions, (d) Observed PM_{2.5} time series for selected sites during December 6 to December 8, 2015

带格式的：居中，右 0.12 字符，段落间距段前：0 磅，行距：单倍行距，不对齐到网格

带格式的：边框:底端: (无框线)

3.1.2 Pollution process during the campaign with the southward motion of the weak cold air

The second time period of interest was from December 10 to December 11. Analysis about potential source contribution areas suggests that the polluted air mass mainly came from northern regions, passing from south-eastern Shandong peninsula and central-eastern Jiangsu to northern Zhejiang. From the large-scale weather pattern, the diffusion of weak cold air on December 10 gradually transported the pollution-polluted air mass in the upper reaches of the region to the YRD region. The pollution peaked in areas such as Lianyungang in northern Jiangsu on the evening of December 10. On December 11, the PM_{2.5} concentration peak appeared in central and southern Jiangsu as a result of northern weak air flow. The pollution-plume was further transported into Zhejiang province with the expansion in influenced areas as is shown in Figure 5. Therefore, the pollution process was mainly affected by the transportation of polluted air mass caused by the southward motion of cold air.

带格式表格

带格式的：居中

带格式的：字体：6 磅

带格式的：字体：6 磅，字体颜色：文字 1

带格式的：字体：6 磅，字体颜色：文字 1，下标

带格式的：字体：6 磅

带格式的：字体：Times New Roman, 6 磅，字体颜色：文字 1

带格式的：居中，行距：固定值 8 磅

带格式的：字体：6 磅

带格式的：居中，行距：固定值 8 磅

带格式的：字体：6 磅，字体颜色：文字 1

带格式的：字体：6 磅，字体颜色：文字 1，下标

带格式的：字体：6 磅

带格式的：字体：Times New Roman, 6 磅，字体颜色：文字 1

带格式的：居中，行距：固定值 6 磅

带格式的：字体：Times New Roman, 八号，字体颜色：文字 1

带格式的：居中，行距：固定值 6 磅

带格式的：字体：Times New Roman, 八号，字体颜色：文字 1

带格式的：字体：八号

带格式的：居中，行距：固定值 6 磅

带格式的：字体：八号，上标

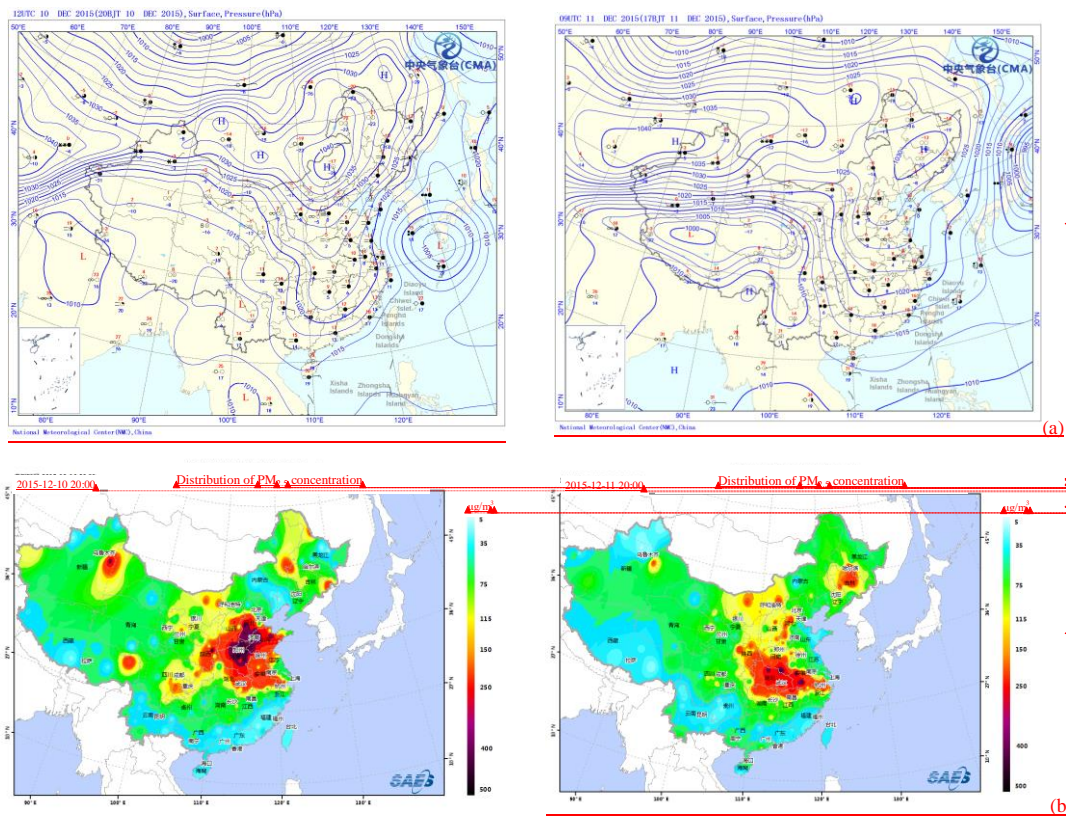
带格式的：字体：Times New Roman, 八号，字体颜色：文字 1

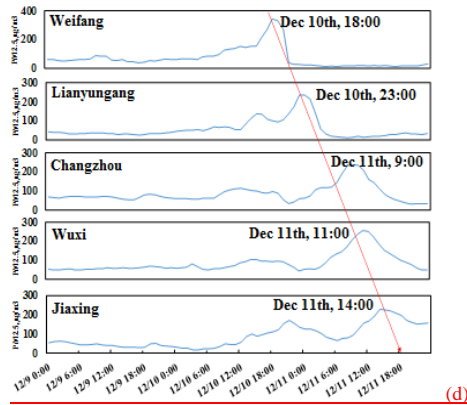
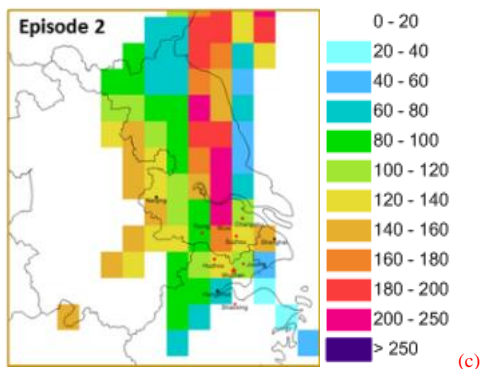
带格式的：字体：八号

带格式的：居中，行距：固定值 6 磅

带格式的：字体：八号，上标

带格式的：字体：Times New Roman, 八号，字体颜色：文字 1





带格式的：边框:底端：(无框线)

带格式的：居中

带格式的：缩进:首行缩进: 0 厘米

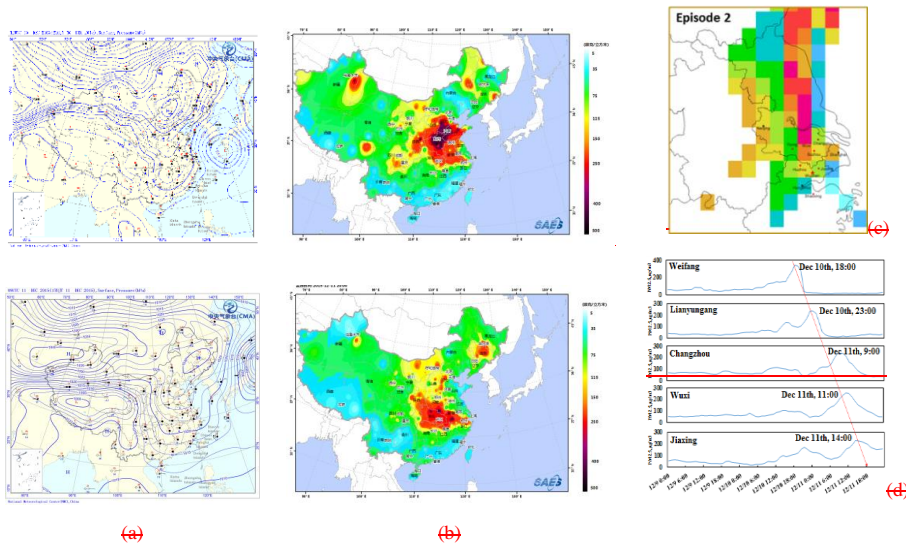


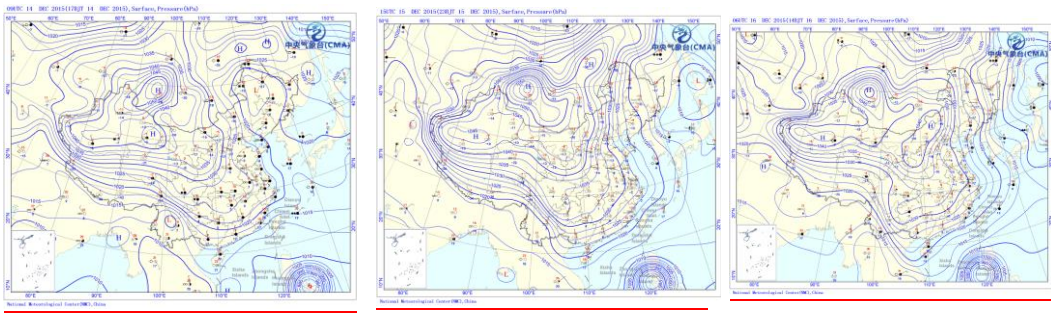
Fig. 4-5 Analysis of (a) the large-scale weather patterns, (b) distribution of $PM_{2.5}$ concentrations, (c) potential regional sources, (d) Observed $PM_{2.5}$ time series for select sites during December 10 to December 11, 2015

3.1.2 Heavy pollution process during the campaign with the transit and transportation of strong cold air

The third period of interest was from December 13 to the early hours of December 16. Analysis of the potential source contribution areas suggests that the polluted air mass mainly came from the northwest direction, passing through south-eastern Shanxi, western Shandong, eastern Anhui and western Jiangsu to Zhejiang province. On December 14, affected by the cold air transportation in the north, northern pollution plumes hit Hebei, Henan and Anhui provinces, with the highest degree of pollution on the 14th. On December 15, the further spread of cold air caused the transport of pollution plumes into Jiangsu and Zhejiang. The northern part of Zhejiang province was in the centre of pollution on the 15th, which worsened the pollution and expanded the scope of pollution, as is shown in Figure 3-126. On December 16, under the control of the high-pressure system in northern Zhejiang, the air mass gradually moved eastward and the air quality improved in the morning. Therefore, for this time period,

344 large-scale transportation was the main factor leading to the increase in pollutant levels.

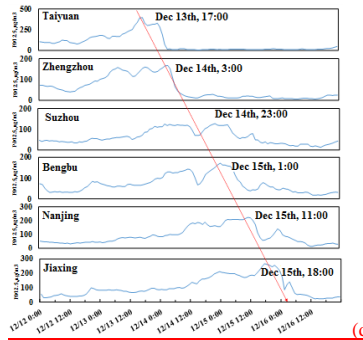
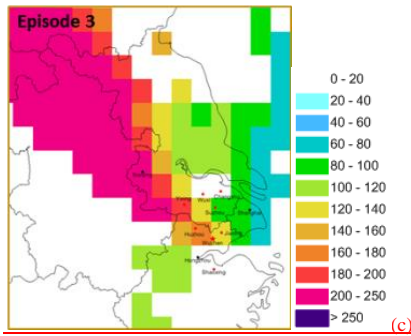
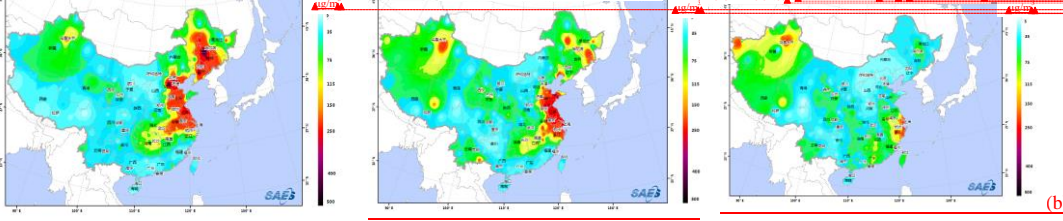
345
346
347
348
349



2015-12-14 17:00 Distribution of PM_{2.5} concentration

2015-12-15 09:00 Distribution of PM_{2.5} concentration

2015-12-16 09:00 Distribution of PM_{2.5} concentration



350

带格式的: 边框:底端: (无框线)

带格式表格

带格式的: 居中

带格式的: 字体: 6 磅

带格式的: 居中, 行距: 固定值 10 磅

带格式的: 字体: 6 磅, 字体颜色: 文字 1

带格式的: 字体: 6 磅, 字体颜色: 文字 1, 下标

带格式的: 字体: 6 磅

带格式的: 字体: Times New Roman, 6 磅, 字体颜色: 文字 1

带格式的: 字体: 6 磅

带格式的: 字体: 6 磅, 字体颜色: 文字 1

带格式的: 字体: 6 磅, 字体颜色: 文字 1, 下标

带格式的: 字体: 6 磅

带格式的: 字体: Times New Roman, 6 磅, 字体颜色: 文字 1

带格式的: 居中, 行距: 固定值 10 磅

带格式的: 字体: 6 磅

带格式的: 字体: 6 磅, 字体颜色: 文字 1

带格式的: 居中, 行距: 固定值 10 磅

带格式的: 字体: 6 磅, 字体颜色: 文字 1, 下标

带格式的: 字体: 6 磅

带格式的: 字体: Times New Roman, 6 磅, 字体颜色: 文字 1

带格式的: 居中, 行距: 固定值 6 磅

带格式的: 字体: Times New Roman, 八号, 字体颜色: 文字 1

带格式的: 居中, 行距: 固定值 6 磅

带格式的: 字体: Times New Roman, 八号, 字体颜色: 文字 1

带格式的

带格式的

带格式的: 字体: 八号

带格式的

带格式的: 字体: 八号, 上标

带格式的

带格式的: 字体: 八号

带格式的

带格式的: 字体: 八号, 上标

带格式的

带格式的: 字体: 八号

带格式的

带格式的: 字体: 八号, 上标

带格式的

带格式的: 居中

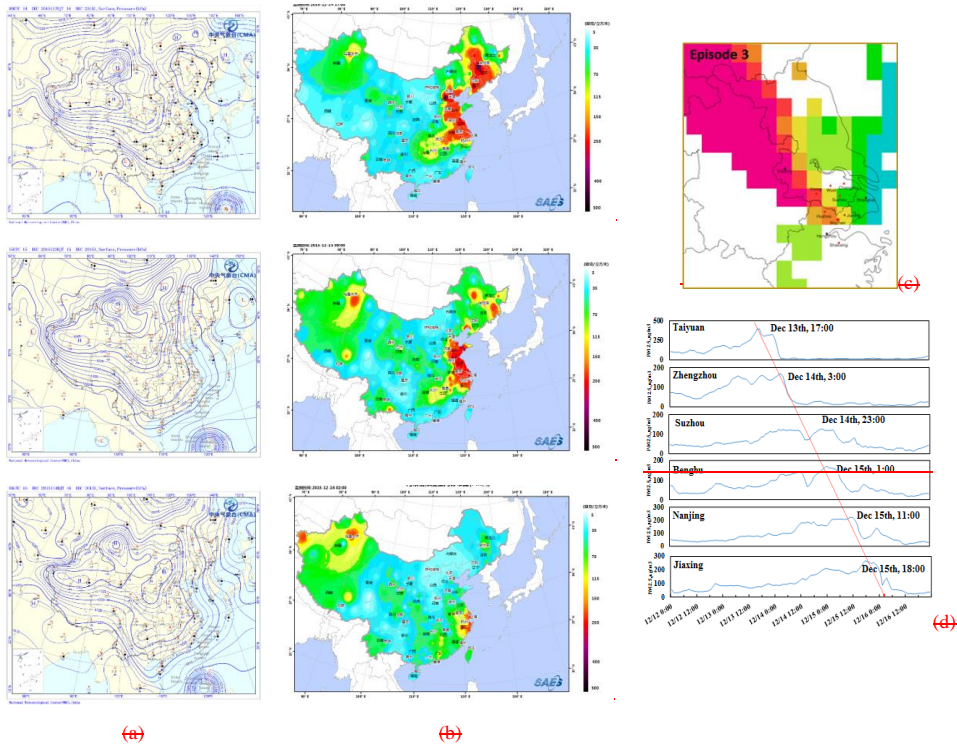
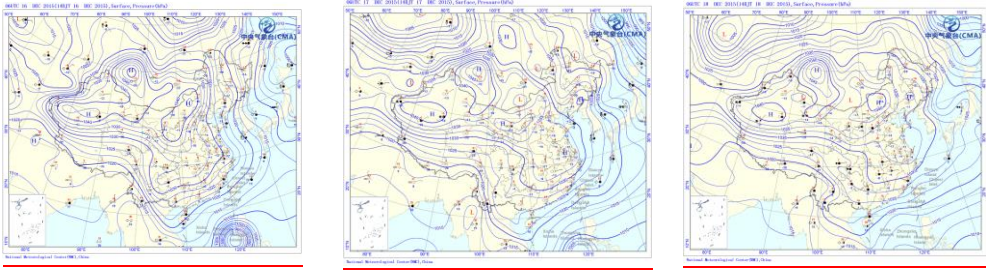


Fig. 5-6 Analysis of (a) the large-scale weather patterns, (b) distribution of $PM_{2.5}$ concentrations, (c) potential regional sources, (d) Observed $PM_{2.5}$ time series for select sites during December 14 to December 16, 2015

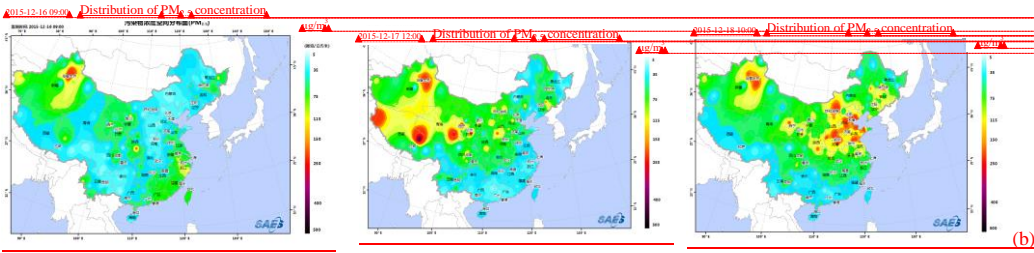
3.1.3 Pollution removal process caused by clean cold air during the conference

During the conference from December 16 to December 18, weather was affected by the large-scale southward transport of cold dry air in northern Zhejiang, resulting in lower temperature and relative humidity, as well as a significant improvement in the air quality. On the 17th and the 18th, under the control of a high pressure system in northern Zhejiang, the sea level pressure increased, the humidity was lower and the wind speed was reduced. Because of the emission reduction effect of the control measures, the pollutant accumulation rate was likely slowed down and the air quality in northern Zhejiang was good overall. From the analysis of potential sources, $PM_{2.5}$ concentrations in Shandong, Jiangsu and Shanghai were significantly reduced. The $PM_{2.5}$ concentration during the conference was mainly controlled by local emissions, as is shown in Figure 67.

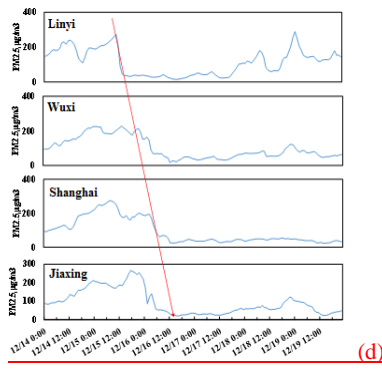
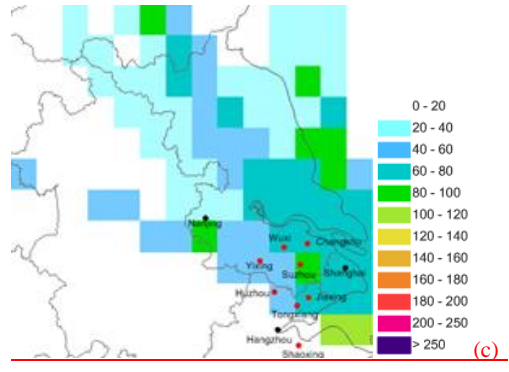


带格式的：边框:底端：(无框线)
带格式表格

带格式的：两端对齐
带格式的：字体：6 磅
带格式的：字体：6 磅，字体颜色：文字 1
带格式的：居中，行距：固定值 8 磅
带格式的：字体：6 磅，字体颜色：文字 1，下标

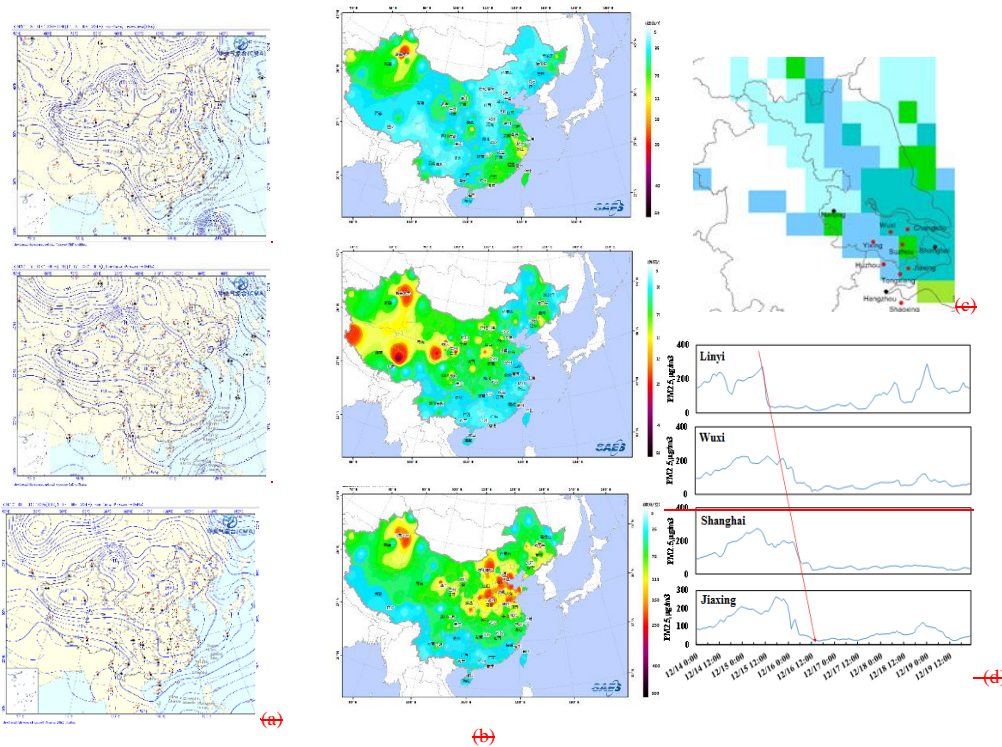


带格式的：字体：6 磅
带格式的：字体：Times New Roman, 6 磅，字体颜色：文字 1
带格式的：字体：4 磅
带格式的：居中，行距：固定值 6 磅
带格式的：字体：Times New Roman, 4 磅，字体颜色：文字 1
带格式的：字体：八号



带格式的：字体：八号，上标
带格式的：字体：Times New Roman, 八号，字体颜色：文字 1
带格式的：居中，行距：固定值 6 磅
带格式的：字体：6 磅
带格式的：居中，行距：固定值 8 磅
带格式的：字体：6 磅，字体颜色：文字 1
带格式的：字体：6 磅，字体颜色：文字 1，下标
带格式的：字体：6 磅

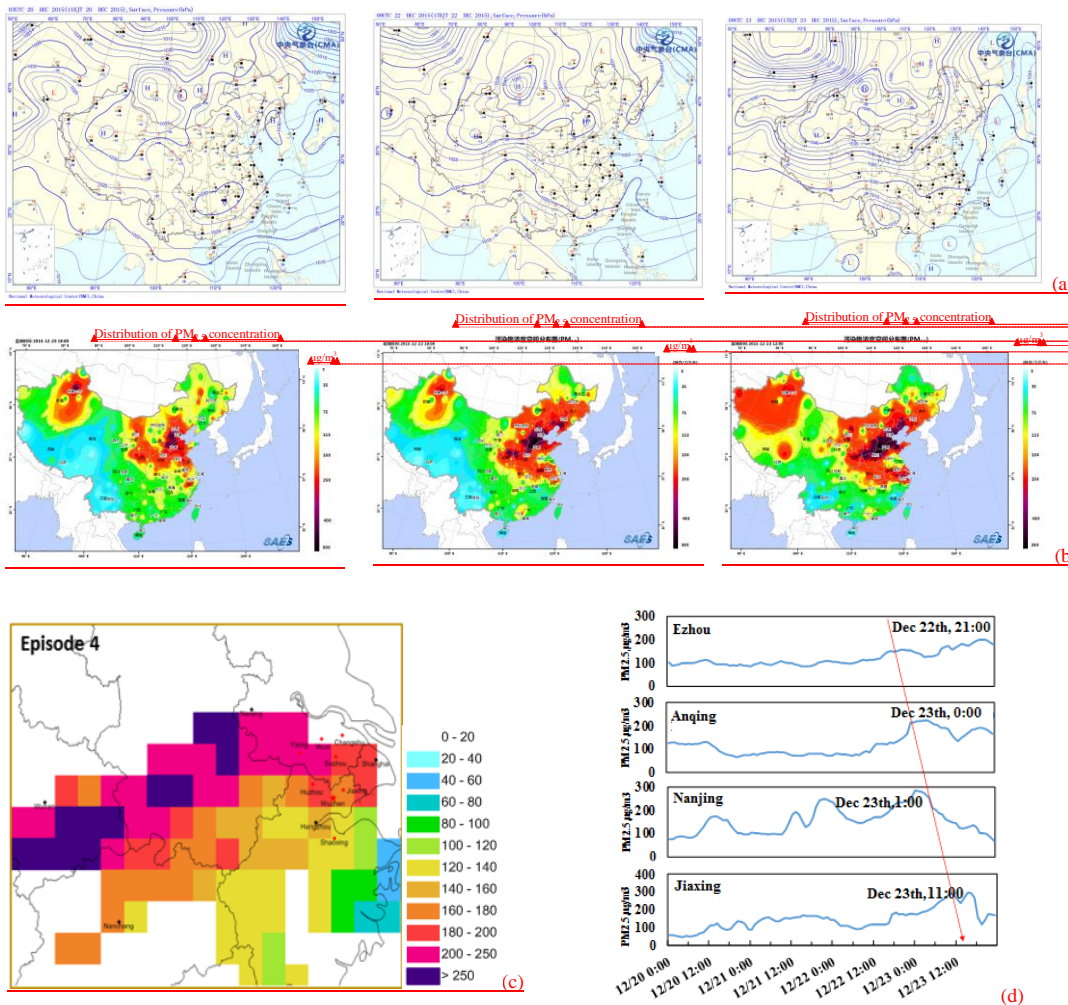
带格式的：字体：Times New Roman, 6 磅，字体颜色：文字 1
带格式的：字体：4 磅
带格式的：字体：Times New Roman, 4 磅，字体颜色：文字 1
带格式的
带格式的：字体：6 磅
带格式的
带格式的
带格式的
带格式的：字体：6 磅
带格式的
带格式的
带格式的
带格式的：字体：八号
带格式的
带格式的：字体：八号，上标
带格式的
带格式的：字体：八号
带格式的
带格式的：字体：八号，上标
带格式的



364 Fig. 6-7 Analysis of (a) the large-scale weather patterns, (b) distribution of PM_{2.5} concentrations, (c) potential regional sources, (d)
 365 Observed PM_{2.5} time series for select sites during December 16 to December 18, 2015

366 **3.1.4 Pollution process after the campaign with local emission accumulation as the main contributor**

367 The fourth period of interest was from December 20 to December 23. Analysis of the potential source
 368 contribution areas suggests that the polluted air mass mainly came from the southwest direction, passing through
 369 southern Hubei, southern Anhui and south-western Jiangsu to northern Zhejiang. On December 20, controlled by
 370 a stagnant air mass, Zhejiang province has a relatively low near-surface wind speed and little dispersion, resulting
 371 in the accumulation of local pollutants. On December 21, northern Zhejiang was located in the centre of a high
 372 pressure system with conditions conducive to little mixing, and therefore pollution-polluted air mass occurred in
 373 some areas in northern Zhejiang. On December 22, affected by the warm and humid southwest air flow, Zhejiang
 374 had experienced some precipitation but the pollution in northern Zhejiang was not improved due to deep polluted
 375 air masses. In Hubei and Anhui located in the southwest of Jiaxing City, high pollution levels appeared from the
 376 evening of December 22 to the early hours of December 23, as is shown in Figure 78. On December 23, the
 377 further expansion of polluted air masses resulted in serious pollution in Jiangsu and northern Zhejiang. In general,
 378 under these heavily polluted conditions, the local accumulation of pollutants was mainly caused by stagnant
 379 conditions with little dispersion and transport within southwest air stream.



380 Fig. 7-8 Analysis of (a) the large-scale weather patterns, (b) distribution of PM_{2.5} concentrations, (c) potential regional sources, (d)
 381 Observed PM_{2.5} time series for select sites during December 20 to December 23
 382

383 **3.2 Air quality changes under the same meteorological conditions before and after the campaign**

384 **3.2.1 Air quality changes under static meteorological conditions before and during the campaign**

385 During the air pollution control campaign for the conference, air quality in Jiaxing City fluctuated greatly
 386 due to the frequent southward motion of cold air from the north. Under static weather conditions, sources of
 387 atmospheric pollution mainly came from the accumulation of ~~pollution-polluted air masses~~ from local sources and
 388 sources in neighbouring areas. Therefore, in order to eliminate the influence of the ~~transportation~~ process of the
 389 air mass, this study compared the air quality status before, during and after the campaign in Jiaxing City under
 390 stagnant weather conditions (wind speed less than 1m/s) and assessed the impact of control measures on ambient
 391 air quality in Jiaxing based on air quality observation data.

带格式的：边框:底端：(无框线)

带格式的：字体：6 磅

带格式的：居中，行距：固定值 8 磅

带格式的：字体：6 磅，字体颜色：文字 1

带格式的：字体：6 磅，字体颜色：文字 1，下标

带格式的：字体：6 磅

带格式的：字体：Times New Roman, 6 磅，字体颜色：文字 1

带格式的：字体：6 磅

带格式的：居中，行距：固定值 8 磅

带格式的：字体：6 磅，字体颜色：文字 1

带格式的：字体：6 磅，字体颜色：文字 1，下标

带格式的：字体：6 磅，字体颜色：文字 1

带格式的：居中

带格式的：字体：6 磅

带格式的：居中，行距：固定值 8 磅

带格式的：字体：6 磅，字体颜色：文字 1

带格式的：字体：6 磅，字体颜色：文字 1，下标

带格式的：字体：6 磅

带格式的：字体：Times New Roman, 6 磅，字体颜色：文字 1

带格式的：字体：八号

带格式的：字体：八号，上标

带格式的：字体：Times New Roman, 八号，字体颜色：文字 1

带格式的：居中，行距：固定值 6 磅

带格式的：字体：八号

带格式的：字体：八号，上标

带格式的：字体：Times New Roman, 八号，字体颜色：文字 1

带格式的：居中，行距：固定值 6 磅

带格式的：字体：八号

带格式的：居中，行距：固定值 6 磅

带格式的：字体：八号，上标

带格式的：字体：Times New Roman, 八号，字体颜色：文字 1

带格式的：缩进：首行缩进：0 厘米

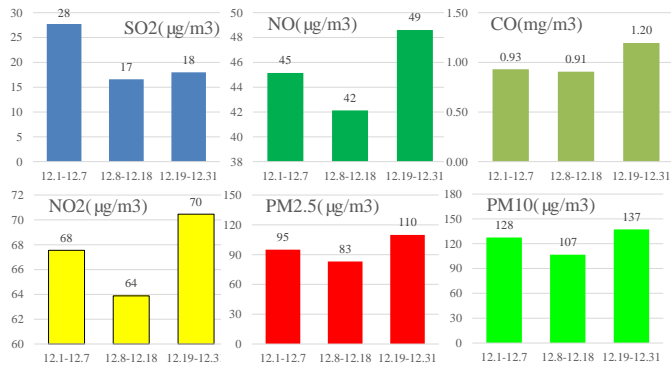
带格式的：边框:底端: (无框线)

392 Figure 8-9 shows the concentration levels of normal criteria pollutants including SO₂, NO, CO, NO₂ and
 393 PM_{2.5} in Jiaxing City before (December 1-7), during (December 8-19) and after the campaign
 394 (December 19-31) under stagnant weather conditions. It can be seen that pollutant concentrations during the
 395 campaign were less than those before the campaign, in which SO₂ had the most significant decline of 40.1%, NO_x,
 396 CO, PM_{2.5} and PM₁₀ declined 8.0%, 2.6%, 12.5% and 16.3%, respectively, indicating that control measures have
 397 significantly improved the air quality in Jiaxing City, especially with respect to SO₂ and PM₁₀.

398 After the campaign, all the pollutant concentrations rebounded sharply. SO₂, NO, NO₂, CO, PM_{2.5}, PM₁₀
 399 increased 8.3%, 15.4%, 10.3%, 31.8%, 32.2% and 28.6%, respectively. Concentrations of some pollutants were
 400 even higher than those before the campaign, which suggests that the emission intensity of the sources had
 401 significantly increased after the campaign.

带格式的：两端对齐

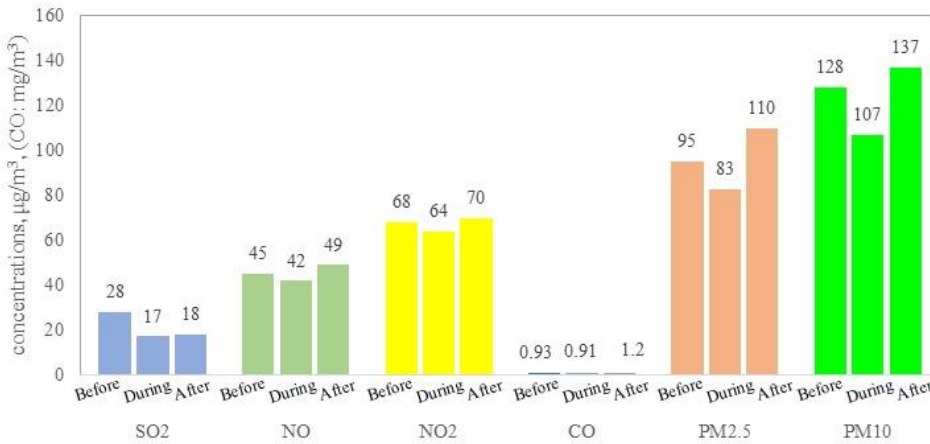
402



403

404 Fig. 8-9 Comparison between air pollutant concentrations at Shanxi station before, during, and after the campaign under stagnant
 405 meteorological conditions

406 There are also some differences in concentrations of major chemical components of PM_{2.5} in Jiaxing City
 407 before (December 1-7), during (December 8-19) and after the campaign (December 19-31) under stagnant static



408 weather conditions, as shown in Figure 9. The concentrations of major chemical components of PM_{2.5} during the
409 campaign were less than those before the campaign, which is consistent with the conclusion about changes in
410 ~~normal-criteria~~ pollutant concentrations. On average, SO₄²⁻, NH₄⁺, NO₃⁻, OC, mineral soluble ions (Ca²⁺ and
411 Mg²⁺) and K⁺ declined 11.8%, 5.1%, 32.1%, 9.8%, 56.8% and 5.1%, respectively. Comparisons between the
412 distribution of PM_{2.5} chemical components before and during the campaign under static conditions suggest that
413 Ca²⁺ and Mg²⁺ decreased most significantly during the control period, which indicates that the suspension of
414 construction operations which result in dust emissions and the rising frequency of rinsing and cleaning paved
415 roads, significantly reduced dust emissions. Comparisons between the distribution of PM_{2.5} chemical components
416 before and during the campaign suggest that Ca²⁺ and Mg²⁺ decreased most significantly during the control period,
417 which indicates that the suspension of construction operations which result in dust emissions and the rising
418 frequency of rinsing and cleaning paved roads, significantly reduced dust emissions. During the campaign, NO₃⁻
419 significantly decreased, indicating that vehicle control measures successfully reduced NO_x emissions and
420 subsequently the formation of inorganic aerosols. The significant decrease in SO₄²⁻ also shows that restricting
421 ~~and~~ or suspending the operation of coal-burning power plants and industries in local and neighbouring cities
422 played a very positive role.

423 The chemistry also changes if we compare observed data during and after the regulation. As is shown from
424 figure 10, the SO₂ concentrations after control is a little bit higher than during control (+5.9%). However, the
425 SO₄²⁻ after control is much higher than during control (25.8%). This is probably due to two reasons: firstly, SO₂
426 emissions and primary sulfate emissions increased after the control measures were terminated; secondly, previous
427 studies have reported that increased NO_x emissions could accelerate the formation of secondary sulfate (Cheng et
428 al., 2016). This can be clearly seen from the SOR. A different trend is observed for NO₂ and NO₃⁻, with the NO₂
429 concentrations after control being much higher than during control (+9.4%), while the increase of NO₃⁻ (+9.45%)
430 is about the same. Sulfate originates from both primary emissions and secondary formation, but nitrate is mostly
431 secondary. The NOR during and after regulation is about the same and most of the N is in the gas phase as
432 indicated by NO_x/(NO_x+NO₃⁻) (0.87). Therefore, the increase of NO₃⁻ is smaller than SO₄²⁻. The PM_{2.5}
433 concentration after control sharply rebounded by 31.8%, indicating that both primary emissions and secondary
434 formation are activated.

带格式的：边框:底端：(无框线)

带格式的：下标

带格式的：上标

带格式的：上标

带格式的：字体：Times New Roman, 五号, 字体颜色：自动设置, 英语(英国)

带格式的：字体：Times New Roman, 五号, 字体颜色：自动设置, 英语(英国)

带格式的：字体：Times New Roman, 五号, 字体颜色：自动设置, 英语(英国)

带格式的：字体：Times New Roman, 五号, 字体颜色：自动设置, 英语(英国)

带格式的：上标

带格式的：字体：Times New Roman, 五号, 字体颜色：自动设置, 英语(英国)

带格式的：字体：Times New Roman, 五号, 字体颜色：自动设置, 英语(英国)

带格式的：下标

带格式的：下标

带格式的：下标

带格式的：上标

带格式的：下标

带格式的：下标

带格式的：上标

带格式的：下标

带格式的：上标

带格式的：下标

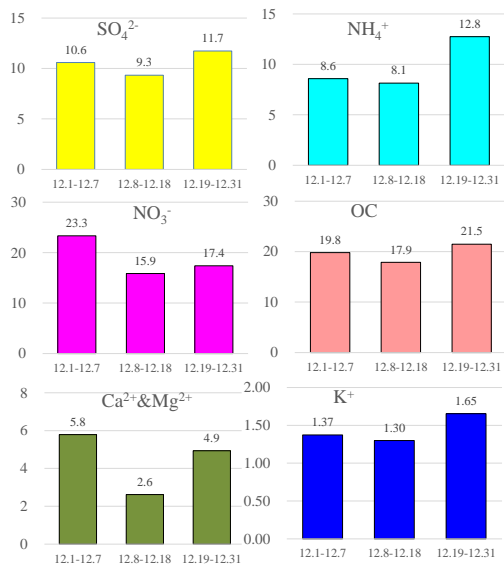
带格式的：上标

带格式的：下标

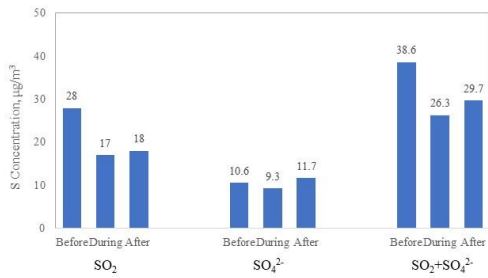
带格式的：上标

带格式的：下标

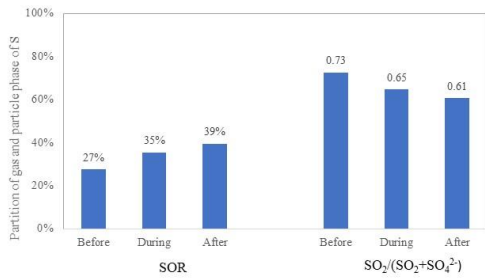
435



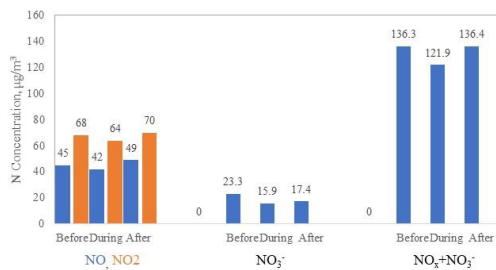
436



437



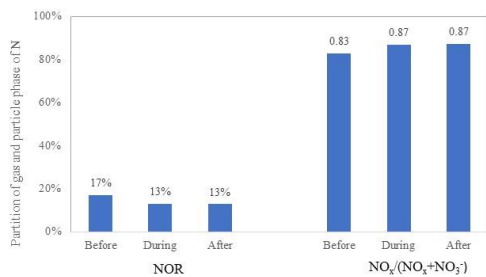
438



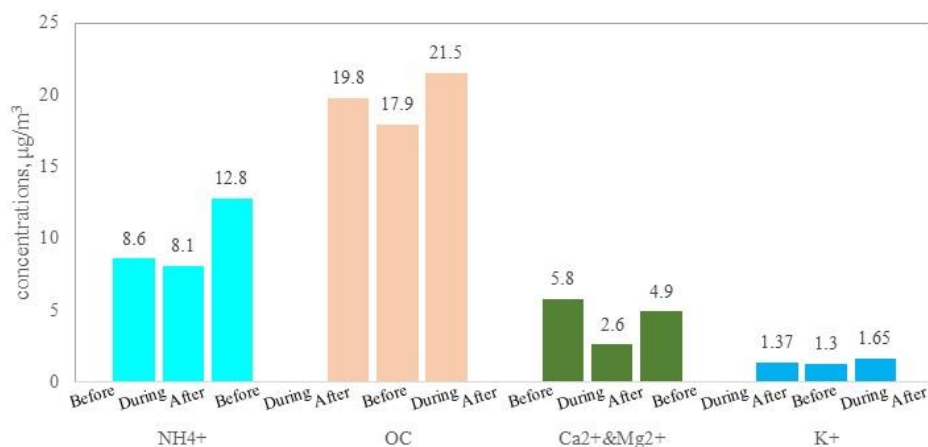
带格式的：边框:底端: (无框线)

带格式的：两端对齐, 缩进: 左 0 字符, 首行缩进: 0 字符, 右 0 字符, 定义网格后不调整右缩进, 段落间距段前: 2.5 磅, 行距: 1.5 倍行距, 不调整西文与中文之间的空格, 不调整中文和数字之间的空格

带格式的：边框:底端: (无框线)



439



440

441

442

443

Fig. 9-10 Comparison between PM_{2.5} chemical components at Shanxi station before and after the campaign under static meteorological conditions

带格式的：两端对齐，缩进：首行缩进： 0 字符

444

3.2.2 Air quality changes under the same air mass trajectory before and during the campaign

445

446

447

448

449

450

451

452

453

454

455

456

In order to distinguish the impact of meteorological conditions on air quality in Jiaxing City and better analyze the effects of control measures on air quality during the conference, this study has combined meteorological conditions with backward air flow trajectory analysis and carried out a comparative study by selecting a relatively similar pollution period before and during the campaign. The first period occurred before the campaign from 12:00 December 2 to 20:00 December 4, while the second period occurred during the campaign from 9:00 December 16 to 5:00 December 18. Both of these periods were relatively unaffected by long-range transport of ~~pollution plumes~~ into the study area, and have similar backward airflow trajectories and meteorological conditions. Table 3 and Figure 10-11 compare average mass concentrations of pollutants (SO₂, NO_x, PM_{2.5} and PM₁₀) during these two periods. As can be seen from the figure, SO₂, PM_{2.5} and PM₁₀ decreased during the campaign by roughly 46%, 13% and 27%, respectively, while NO_x exhibited only a small decrease. This shows that without the impact of long-range transport, emission reduction measures carried out by local and surrounding cities play a significant role in defining the air quality in Jiaxing.

带格式的：字体：倾斜，下标

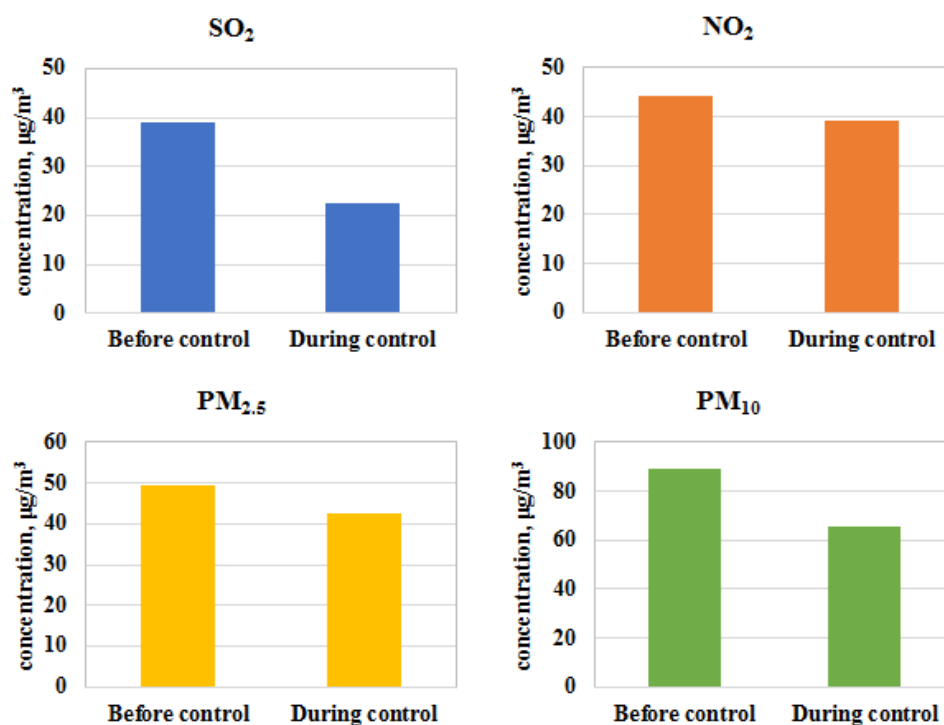
457
458

Table 3 Concentrations of major pollutants under similar meteorological conditions before and during the campaign

Period	Time	Wind speed m/s	Wind direction °	Relative humidity %	Temperature °C	Pressure hPa	Visibility km	SO ₂ μg/m ³	NO ₂ μg/m ³	PM ₁₀ μg/m ³	PM _{2.5} μg/m ³
Before the campaign	12.2 12:00-12.4 20:00	3.1	268.0	59.2	8.2	102.6	22.8	39.1	44.4	89.5	49.4
During the campaign	12.16 9:00-12.18 5:00	3.4	247.5	53.0	2.6	103.2	32.1	22.4	39.3	65.3	42.8

带格式的: 边框:底端: (无框线)

带格式表格



459
460
461
462

Fig. 10-11 Comparison between concentrations of major air pollutants in Jiaxing before and after the campaign under same meteorological conditions

463
464
465
466
467
468

There were two regional pollution episodes that occurred during the campaign. The first was on December 10-12 caused by the southward motion of northern weak cold air. Polluted air masses from south-eastern Shandong peninsula passed through central eastern Jiangsu and into northern Zhejiang, affecting the air quality in Jiaxing. During this period, the average daily PM_{2.5} concentration in Jiaxing was 145.7 μg/m³, higher than the regional average, and its major chemical components were nitrate (31%), sulphate (18%), ammonium (13%) and organic carbon (13%), with obvious regional secondary pollution characteristics.

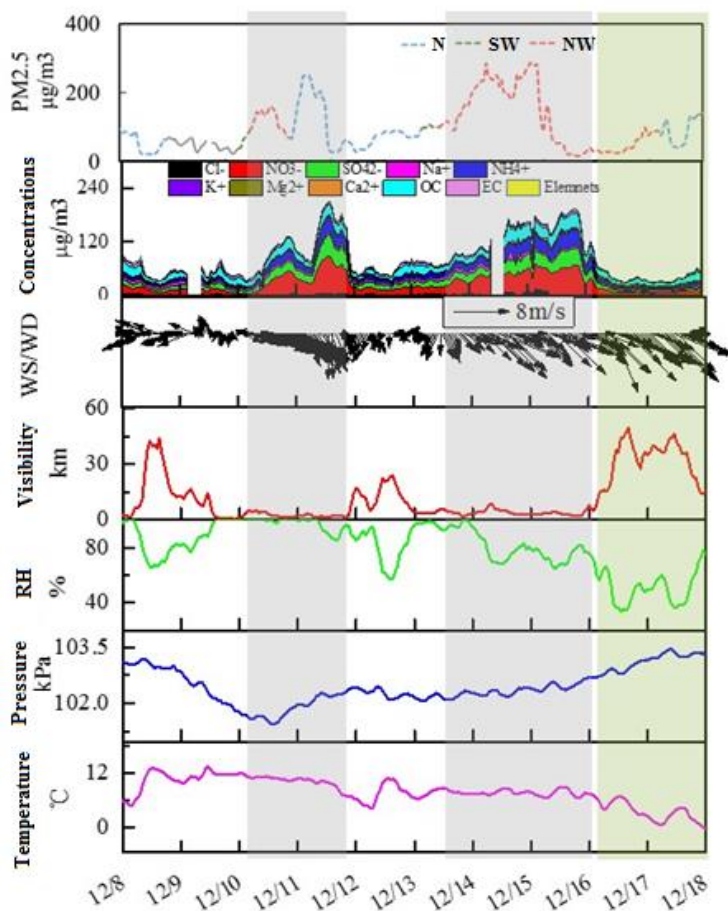


Fig.44-12 Changes in air quality and meteorological parameters in Jiaxing City during the campaign

469
470

471 The second episode occurred from December 14-15, and was caused by the transit of northwesterly strong cold
472 air. Polluted air masses came from the northwest direction, moved rapidly to the southeast, passed through Shanxi,
473 Hebei, west Shandong, east Anhui and west Jiangsu and ultimately into Zhejiang province. The air masses left
474 China through south-eastern Zhejiang on the early morning of the 16th. The YRD region was strongly affected by
475 the transport of the polluted air mass, with heavy ~~pollution~~ polluted air masses appearing and lasting for about one
476 day over the YRD region from north to south. PM_{2.5} peaked in Jiaxing on the 15th with a daily average of 201.6
477 µg/m³. The main chemical components of PM_{2.5} during the episode were nitrate (25%), sulphate (14%),
478 ammonium (12%) and organic carbon (13%)-, which is consistent with an aged air mass as well as regional
479 secondary pollution characteristics.

480 The regional linkage was initiated from December 16 to December 18, combined with favourable mixing
481 conditions brought by the cold front. The overall air quality in the YRD region during this time period was good,
482 with an average daily PM_{2.5} concentration in Jiaxing of 45 µg/m³. The major chemical components during this

带格式的：边框:底端：(无框线)

483 cleaner period were organic carbon (26%), nitrate (16%), ammonium (12%), sulphate (9%) and other components
484 (37%), with some newly formed particles and no obvious regional transport, suggesting that air pollutants were
485 mainly derived from local emissions. The major chemical components during this cleaner period were organic
486 carbon (26%), nitrate (16%), ammonium (12%) and sulphate (9%), with some newly formed particles and no
487 obvious regional pollution characteristics, suggesting that air pollutants were mainly derived from local emissions.

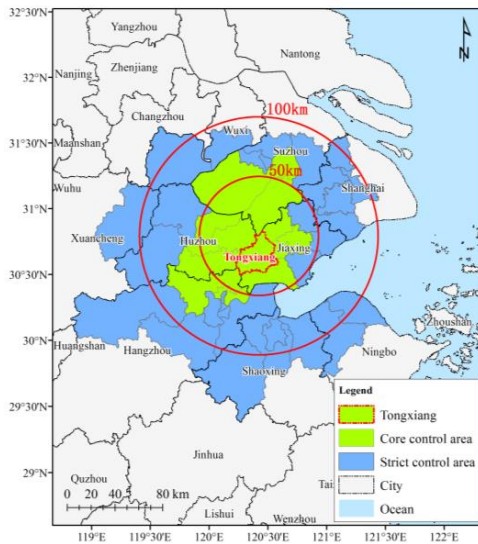
488 3.3 Emissions reductions estimation during the campaign

489 3.3.1 Control Measures adopted to reduce air pollutant emissions

带格式的：上标

490 The air quality assurance campaign for the 2nd World Internet Conference was from December 8 to
491 December 18. In order to ensure the air quality during the conference, three provinces and Shanghai municipality
492 in the YRD region carried out joint control measures. The air quality assurance campaign for the 2nd World
493 Internet Conference was from December 8 to December 18. In order to ensure the air quality during the
494 conference, three provinces and Shanghai municipality in the YRD region carried out joint control measures and
495 established key areas, strict control areas, control areas and extension areas, respectively, according to the degree
496 of pollution impact from each region on the air quality in Jiaxing. Among them, key areas and strict control areas
497 included Zhejiang province (including Hangzhou, Ningbo, Huzhou, Jiaxing and Shaoxing), Shanghai (including
498 Jinshan and Fengxian), Jiangsu province (including Suzhou and Wuxi) and Anhui province (including Xuancheng,
499 Ma'anshan and Wuhu), as shown in figure 12.

带格式的：两端对齐，缩进：首行缩进：0.74 厘米，定义网格后不调整右缩进，段落间距段前：2.5 磅，行距：1.5 倍行距，无孤行控制，不调整西文与中文之间的空格，不调整中文和数字之间的空格，到齐到网格



500
501 Fig.12 Controlled regions in the Action Plan for Air Quality Control during the World Internet Conference

502 The following measures were taken in key areas and control areas: (1) Strictly control emissions from

~~coal burning power plants: reduce emissions from power plants which have not completed ultra-low emission transmission processes by 50% in key areas and by 30% in control areas. (2) Reduce emissions from key enterprises: production restriction or suspension would be imposed on industries including cement, steel, construction materials, petrochemicals, chemicals, casting, leather, non-ferrous metals, plate glass, pharmaceuticals, surface spraying and printing. All key enterprises in key areas were discontinued (maximum production limits will be imposed on steel and petrochemical industries), while key enterprises in control areas cut emissions by 30%. Enterprises which could not meet the emission standards in a stable way, do not have facilities for exhaust gas treatment or cannot operate facilities normally were to be discontinued. Petrochemical and chemical enterprises were forbidden to turn on/off for operation or maintenance. (3) Strictly control motor vehicle pollution: in the core areas in Zhejiang province, motor vehicle restrictions were implemented, which means that low-speed trucks were forbidden to pass except for people's livelihood-related activities. Vehicles which had not obtained valid qualifications for environmental inspection were prohibited on the road. (4) Control dust pollution: Controlled work sites were suspended in key areas and control areas. Dust materials were forbidden to be transported within key neighbourhoods. Dust control measures were implemented on renovation operations at ports, docks, railway stations and commercial concrete mixing stations and on materials storage yards. (5) Control other sources of pollution: in key areas and control areas, oil storage facilities, gas stations or tank trucks which were not equipped with facilities for recovery of oil and gas or facilities that could not operate normally were forbidden to sell or transport oil products. Open air barbecue, garbage burning or straw burning in the open air were prohibited. All the primary schools, secondary schools, kindergartens, institutions and public institutions in Jiaxing were given a three-day vacation.~~

~~Zhejiang province initiated control measures on December 8, which included: First, strictly control emissions from coal-burning power plants through the use of low sulphur coal and production restrictions; Second, cut emissions from key enterprises through measures such as production restriction and suspension; Third, all enterprises that cannot meet the emission standards in a stable way shall be discontinued; Fourth, rubbish and straw burning shall be strictly supervised. During the period, 109 coal-burning power plants in total had imposed production restrictions in Hangzhou, Ningbo, Huzhou, Jiaxing, Shaoxing and Jinhua. A total of 1331 key enterprises reduced their operations among which 720 were restricted from production. Similarly, 3950 key controlled construction sites were suspended from operation, 83 concrete enterprises were restricted from production, 444 sites of straw burning were regulated, and 296 "black chimneys" were inspected.~~

~~As a neighbouring city, the Shanghai municipality released their Action Plan for Air Quality Control at the World Internet Conference in 2015, focusing on key areas such as Jinshan district, Fengxian district, Shanghai~~

534 ~~chemical industry and Shanghai petrochemical industry, and implemented emissions controls on petrochemical,~~
535 ~~steel, chemical, coating and printing industries. On the morning of December 14, temporary control measures~~
536 ~~were initiated. In total, 313 key enterprises and over 1000 key buildings and municipal sites were under the~~
537 ~~control of the city, more than 320 construction sites were suspended from operation, and over 600 yard terminals~~
538 ~~strengthened dust control measures. The ban on Yellow Label cars and the restriction on diesel vehicles within the~~
539 ~~middle ring in Shanghai were implemented. On the morning of December 15, the Yellow Alert emergency plan~~
540 ~~was launched. On that day, 643 key enterprises were controlled, among which 178 were restricted from~~
541 ~~production. In total, 174 construction sites, 310 demolition sites, 66 municipal road sites and 44 dock yards were~~
542 ~~suspended from operation, along with an increase in rinsing and cleaning frequency for 2060 roads to reduce~~
543 ~~fugitive dust emissions.~~

544 ~~Jiangsu province expanded key areas for air quality control from two districts in Suzhou (Wujiang and~~
545 ~~Wuzhong) to three cities (Suzhou, Wuxi and Changzhou). In total, 8 power plants adopted high quality coals in~~
546 ~~Suzhou, another 8 power plants limited their production by 30%, and over 60 key enterprises took measures such~~
547 ~~as restricting the production and shutting down of coal fired boilers. Construction work sites in control areas were~~
548 ~~suspended from operation. In Wuxi, thermal power enterprises adopted high quality low sulphur coals, electricity~~
549 ~~power enterprises and 82 key enterprises were restricted or suspended from production.~~

550 ~~In Anhui province, three control areas (Ma'anshan, Xuancheng and Wuhu) and 6 extension areas including~~
551 ~~Anhui all developed and implemented control programs. During the campaign, 23 coal fired power plants were~~
552 ~~controlled for low emission, 126 enterprises were restricted from production and 287 construction work sites were~~
553 ~~controlled. Among which, 3 cement enterprises in Xuancheng limited their production by 30%, another 3 cement~~
554 ~~enterprises and 2 chemical enterprises limited their production by 50%, 9 construction sites were suspended from~~
555 ~~operation, lime production and process enterprises were discontinued, quarrying and stone transportation were~~
556 ~~prohibited, and other non coal mines were discontinued.~~

557 ~~During the campaign, the YRD region was frequently affected by unfavourable weather conditions such as~~
558 ~~pollution transportation from the north. There were four distinct meteorological regimes, which occurred in~~
559 ~~Jiaxing and its surrounding cities. Therefore, some cities further took stricter pollution reduction measures.~~
560 ~~Shanghai municipality started temporary control of heavy pollution on December 14 and initiated the yellow~~
561 ~~warning for heavily polluted weather on December 15. On that day, 643 key enterprises were controlled, 178~~
562 ~~enterprises were restricted from production, over 1000 dusty construction sites were discontinued and the rinsing~~
563 ~~and cleaning frequency increased for over 2000 roads. Starting from December 11 in Jiangsu province, 1260~~

564 ~~enterprises were restricted from production, 1429 enterprises were discontinued, and all construction sites in~~
565 ~~control areas were suspended from operation. Emergency control measures were initiated on December 15,~~
566 ~~strengthening control efforts for industries, work sites and motor vehicles.~~

带格式的: 边框:底端: (无框线)

567 3.3.2 Emissions reduction estimation

568 Based on the implementation of control measures in all areas during the conference and whether each area
569 had effectively implemented control measures ~~on~~ during December 8-18, regional emission reductions have been
570 assessed. It is estimated that emission reductions of SO₂, NO_x, PM_{2.5} and VOCs caused by production restriction
571 in regional industrial enterprises are 2867.8 tons, 3064.7 tons, 2165.5 tons and 5055.4 tons, respectively. Emission
572 reductions of various pollutants caused by the restrictions on motor vehicle traffic are estimated ~~as to be~~ 4.7 tons
573 of SO₂, 326.9 tons of NO_x, 36.1 tons of PM_{2.5} and 452.5 tons of VOCs. Emission reduction of PM_{2.5} caused by
574 dust control was estimated ~~to be~~ 266.0 tons. Therefore, it can be seen that emission reductions mainly come
575 from industrial sources, while motor vehicle restrictions contributed greatly to emission reductions of NO_x and
576 VOCs, and dust control contributed 10% to emission reductions of PM_{2.5}.

带格式的: 字体颜色: 文字 1

带格式的: 字体: 倾斜, 下标

577 When looking at specific industries, the ~~electricity~~ power ~~plants~~ industry contributed most to the emission
578 reductions of SO₂ and NO_x at 49.7% and 46.9%, respectively, followed by the chemical industry, building
579 materials industry, steel industry and petrochemical industry with a total contribution from all four sectors to
580 emission reductions of SO₂ and NO_x of 42.0% and 47.2%, respectively. For PM_{2.5}, the building materials industry
581 contributed the most at 62.0%, followed by steel and processing industry, power industry and non-ferrous
582 smelting and process industry with a contribution of 14.3%, 13.1% and 8.1%, respectively. For VOCs, the
583 emission reduction sectors are mainly chemical, petrochemical and machinery manufacturing sectors with a total
584 contribution of 65.7% and individual contributions of 25.1%, 23.2% and 17.4%, respectively. In addition, metal
585 products processing, building materials and steel and processing sectors also contributed significantly to emission
586 reductions of 13.4%, 8.0% and 6.5%, respectively.

带格式的: 字体: 倾斜, 下标

带格式的: 字体: 倾斜, 下标

587 In terms of the regional distribution of emission reductions, Jiaxing, Hangzhou, Suzhou and Shaoxing have
588 the largest contribution of around 80%. These four cities contribute 87% to the total emission reduction of PM_{2.5}.

589 Combing all control measures, total emission reductions of SO₂, NO_x, PM_{2.5} and VOCs are estimated ~~as to be~~
590 2872.5 tons, 3391.6 tons, 2467.6 tons and 5507.9 tons, respectively, which accounts for 10%, 9%, 10% and 11%,
591 respectively, of the total urban emissions. It is worth mentioning that if we consider the emergency emission
592 reduction measures for heavy pollution during the campaign, the amount of emission reduction for all pollutants
593 and the proportion of their emission reductions would be even larger. Table 4 shows the percentage and the

594 amount of emission reductions for pollutants under various control measures.

595
596

Table 4 Emission reduction estimations for various control measures

Province	City	Sector	Amount of emission reduction (tons)				Percentage of reduction			
			SO ₂	NO _x	PM _{2.5}	VOCs	SO ₂	NO _x	PM _{2.5}	VOCs
Zhejiang	Jiaxing		925.6	709.5	462.3	1872.7	56%	58%	64%	80%
	Huzhou		414.8	585.6	602.5	514.0	46%	37%	47%	53%
	Hangzhou		657.2	654.1	476.2	1043.2	36%	42%	59%	33%
	Ningbo	Industries	59.1	65.3	107.5	84.0	32%	30%	37%	33%
	Shaoxing	and enterprises	365.9	414.8	403.9	678.7	34%	38%	62%	31%
Shanghai	Shanghai		253.6	368.7	83.6	796.1	9%	7%	6%	8%
Jiangsu	Suzhou		89.4	34.9	10.2	11.4	3%	1%	1%	1%
	Wuxi		94.4	163.0	10.2	55.3	12%	10%	1%	5%
Anhui	Xuancheng		7.8	68.8	9.1	0.0	15%	42%	28%	0%
	Sub-total		2867.8	3064.7	2165.5	5055.4	23%	19%	27%	19%
Zhejiang	Jiaxing	Motor vehicles	2.3	157.7	16.4	211.3	46%	53%	38%	25%
	Huzhou		0.7	48.4	6.2	81.0	23%	24%	19%	12%
	Hangzhou		1.7	120.8	13.5	160.2	8%	15%	20%	20%
	Sub-total		4.7	326.9	36.1	452.5	15%	25%	25%	19%
Zhejiang	Jiaxing	Dust control	/	/	119.5	/	/	/	100%	/
	Huzhou		/	/	11.1	/	/	/	10%	/
	Hangzhou		/	/	26.6	/	/	/	10%	/
	Ningbo		/	/	28.8	/	/	/	5%	/
	Shaoxing		/	/	5.8	/	/	/	5%	/
Shanghai	Shanghai		/	/	69.3	/	/	/	6%	/
Jiangsu	Suzhou		/	/	2.7	/	/	/	1%	/
	Wuxi		/	/	1.8	/	/	/	1%	/
Anhui	Xuancheng		/	/	0.4	/	/	/	1%	/
	Sub-total		/	/	266.0	/	/	/	9%	/
	In total		2872.5	3391.6	2467.6	5507.9	10%	9%	10%	11%

597

598 **3.4 Quantitative estimates of the contribution of ~~meteorological and~~ control measures to air quality**
599 **improvement**

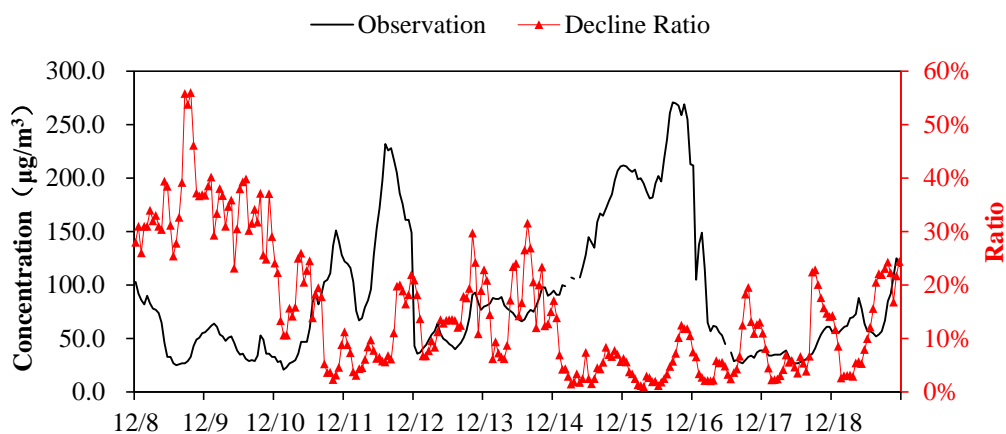
600 3.4.1 PM_{2.5} concentration improvement in Jiaxing

601 The WRF-CMAQ air quality model, combined with observations, was used to evaluate the ~~reduction~~
602 ~~improvement in of~~ PM_{2.5} ~~concentration~~ in Jiaxing due to the emission reductions achieved through the campaign.

603 This analysis utilized two model simulations to assess the impact of the emission reductions: 1) a baseline
604 scenario, which utilized an uncontrolled emission inventory (i.e., the emissions that would have occurred without
605 the campaign), and 2) an emission inventory, which reflects the emission reductions achieved by the campaign.

606 Figure 13 shows the time series of PM_{2.5} observed concentrations and the percent change in PM_{2.5} after the air
607 quality control measures were implemented. It can be seen that the ~~reduction in~~ PM_{2.5} ~~concentrations decline ratio~~

608 in Jiaxing varies with time. The ~~reduction in~~ PM_{2.5} ~~decline ratio~~ was ~~the~~ most significant ~~during~~ December 8-9
 609 with a maximum reduction of 56%. ~~The percent reduction in hourly PM_{2.5} during the conference (December~~
 610 ~~16-18) ranged between 2% -24%, while the average decrease in PM_{2.5} concentration was 5.8 μg/m³ with an average~~
 611 ~~improvement of about 12.9%.~~ During the campaign from December 8 to December 18, average PM_{2.5}
 612 concentrations decreased by 10.5 μg/m³ with an average decrease of 14.4%. However, Although there are many
 613 control strategies implemented, the effects during 12/14-12/16 are low. As described in section 3.1.2, the
 614 prevailing wind direction during this period is NW, and Jiaxing experienced a heavy pollution process with the
 615 transit and ~~transportation~~ of strong cold air. Therefore, we can not see obvious effect without strong upwind
 616 precursor emissions reductions.



617 Fig. 13 Time series of observed PM_{2.5} and the percent~~age~~ reduction resulting from the implementa~~tion~~ of air quality control measures

619 Figure 14 shows the reduction in daily average PM_{2.5} concentrations in Jiaxing resulting from the emission
 620 reductions associated with the Action Plan for Air Quality Control ~~during~~at the World Internet Conference. As
 621 can be seen from the figure, the improvement in PM_{2.5} before the conference (December 8 and 9) was relatively
 622 significant, with a daily average decline of roughly 31% and 35%, respectively, which corresponds to a decrease
 623 of around 17 μg/m³. The reduction in PM_{2.5} ~~on~~ ~~during~~ December 14-15, two of the days with some of the highest
 624 observed PM_{2.5}, was relatively low at around 6%, while daily average PM_{2.5} concentrations on those days
 625 decreased by around 10.0 μg/m³. The magnitude of emission reductions during those two time periods was
 626 basically the same, so it's likely that the observed difference in PM_{2.5} levels was the result of meteorological
 627 differences, and in particular, enhanced transport of polluted air into Jiaxing from December 14 to 15. Overall,
 628 under the influence of regional control measures for emission reductions from December 8 to December 18, PM_{2.5}
 629 daily average concentration decreased by 5.5%-34.8% with an average of 14.6% or 10 μg/m³.

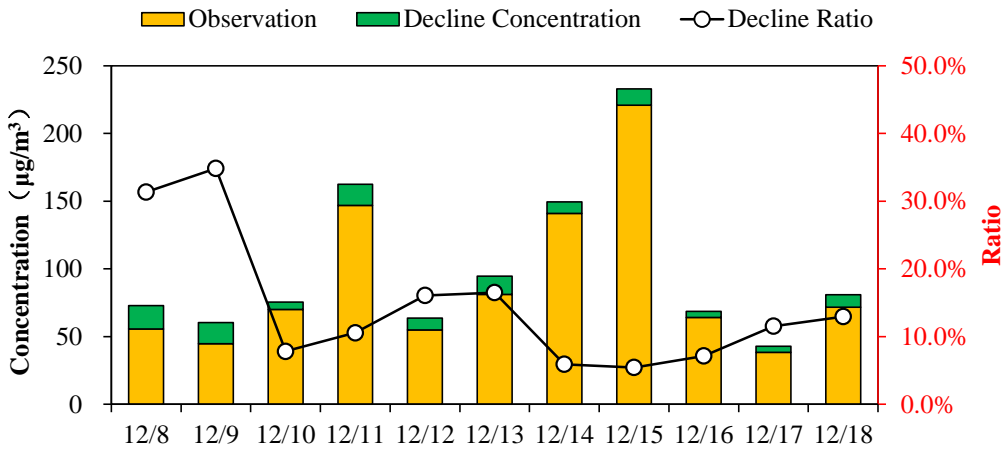


Fig.14 Percentage reduction in PM_{2.5} resulting from the control measures

带格式的：边框:底端：(无框线)

带格式的：正文，缩进：首行缩进：0.74 厘米，定义网格后不调整右缩进，段落间距段前：2.5 磅，不调整西文与中文之间的空格，不调整中文和数字之间的空格，到齐到网格

带格式的：字体：加粗，下标

带格式的：字体：加粗，下标

带格式的

带格式的：字体：加粗，下标

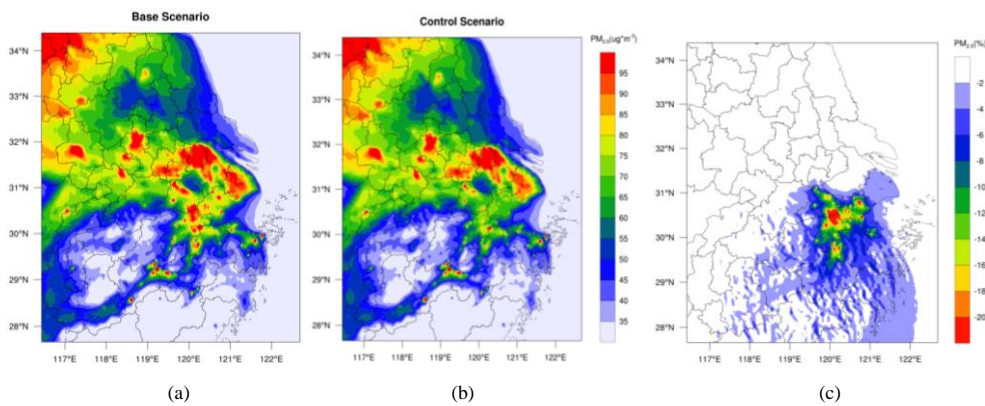
带格式的：字体：(默认) Calibri, (中文) 宋体, 五号, 英语(英国)

The decline ratio changes with meteorological conditions even under the same emissions reduction situation, because meteorological conditions influence dispersion from primary emissions, regional transport and secondary formation. The magnitude of emission reductions during those two time periods was basically the same, so it is possible that the observed difference in PM_{2.5} levels was the result of meteorological differences. Overall, the residual PM_{2.5} may come from three aspects: (1) although stringent control measures have been implemented, there are still some precursor emissions in the city, which accumulated and formed secondary particles under favorable meteorological conditions; (2) enhanced transport under specific meteorological conditions, especially upwind emissions; (3) in view of the uncertainties of model performance (underestimation of PM_{2.5}, especially underestimation of SOA) described in previous sections, it should be noted that the secondary formation may probably be underestimated, causing modeled decline ratio lower than observed.

3.4.2 PM_{2.5} concentration improvement across regions

Figure 15 shows the spatial distribution of PM_{2.5} concentrations in the Yangtze River Delta region from December 8 to December 18 in the baseline scenario and the campaign scenario. As can be seen from the figure, southern Jiangsu, Shanghai and northern Zhejiang in the central YRD region had relatively high PM_{2.5} concentrations, which is consistent with the typically more serious pollution levels in autumn and winter in the YRD region. Under the influence of regional control measures, PM_{2.5} average concentrations declined significantly in Jiaxing, Hangzhou and Huzhou, especially at the junction of these three cities, with a slight improvement in central southern Zhejiang as well. The average percentage reduction in PM_{2.5} concentrations decline ratio in Jiaxing, Hangzhou and Huzhou was about 6%-20%. Meanwhile, given that the prevailing winds are north-westerly in winter, there was also some improvement in central and southern Zhejiang.

带格式的：边框:底端: (无框线)



653

654

655 Fig. 15 Spatial distribution of $PM_{2.5}$ concentrations in the Yangtze River Delta region under the baseline scenario (a) and the
656 campaign scenario (b), and the percentage reduction in $PM_{2.5}$ throughout the YRD region (c)

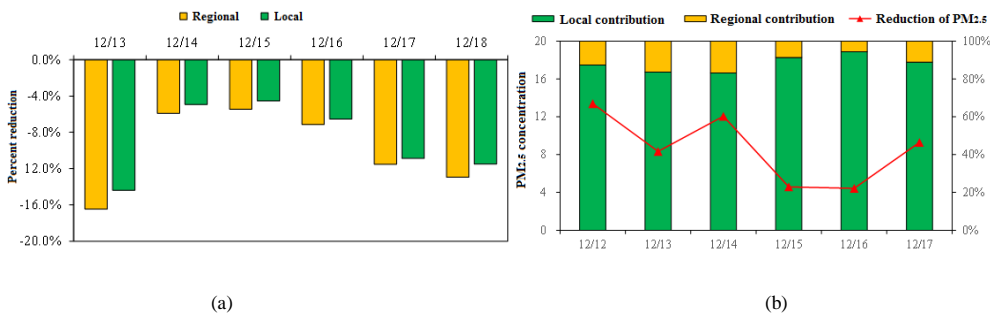
657 3.4.3 Regional contributions of $PM_{2.5}$ concentration improvement in Jiaxing

658 Figure 16(a) shows the percentage reduction in $PM_{2.5}$ daily average concentrations from December 13 to
659 December 18 after control measures were implemented in Jiaxing and regionally. The reduction in $PM_{2.5}$ was the
660 results of both local controls, as well as regional controls which reduced pollution in the air masses transported
661 into Jiaxing. Overall, modelling suggests that the regional controls reduced $PM_{2.5}$ levels in Jiaxing between
662 5.5%-16.5% (9.9% average), while local control measures contributed 4.5%-14.4%, with an average of 8.8%.

663 Figure 16(b) shows the average contribution of local emissions reductions in Jiaxing and in the YRD region
664 over the entire campaign (Dec.13-18), as well as the corresponding improvement in $PM_{2.5}$ levels in Jiaxing.
665 During this period, $PM_{2.5}$ daily average concentration declined by 4-13 $\mu g/m^3$, while there were differences in the
666 contribution of regional remission reductions and local emission reductions in Jiaxing during different periods.
667 Overall, local control measure in Jiaxing had the largest impact on $PM_{2.5}$ levels and accounted for 89% of the
668 decline in $PM_{2.5}$, while regional control measures contributed the remaining 11%.

669

670



671 Fig. 16 Percentage reduction in daily average $PM_{2.5}$ concentrations from December 13 to December 18 after implementation of the
672 control measures across the region and in Jiaxing (a) and Contribution of local and regional emissions reductions in Jiaxing, and the
673 resulting improvement of daily average $PM_{2.5}$ concentrations in Jiaxing (b)

带格式的：下标

带格式的：下标

674 3.5 Optimisation scenario analysis of regional linkage control measures

675 3.5.1 Optimization scenario settings

676 In order to further analyse the optimisation potential of air quality control measures for major events and
 677 enhance the effectiveness of the control measure scheme design, three control measure optimisation scenarios
 678 have been set on the basis of the evaluation scenario (Base) after the implementation of air quality control
 679 measures during the conference. These scenarios include local emission reductions in Jiaxing under stagnant
 680 meteorological conditions, where local emission accumulation is the main contributor to the pollution process
 681 (Sce.1), and the emission reduction scenario where transport of polluted air masses into Jiaxing is a major
 682 contributor to the PM_{2.5} levels in Jiaxing. In order to investigate the transport processes further, the latter scenario
 683 was further divided into a scenario 24 hours in advance (Sce.2) and a scenario 48 hours in advance (Sce.3). Table
 684 5 describes the details of each scenario.

685 Table 5 Control measure optimization scenario settings

Scenario name	Scenario settings	Emission reduction regions	Emission reduction measures	Starting time
Base	Regional emission reduction	All the cities and areas involved in the campaign scheme	All control measures mentioned in the campaign scheme	December 8
Sce.1	Local emission reduction in Jiaxing	Jiaxing	Control measures in Jiaxing mentioned in the campaign scheme	December 8
Sce.2	Emission reduction through transportation channels 24 hours in advance	Cities located in the northwest transportation channel of Jiaxing	Cut down industrial sources by 30%	December 13
Sce.3	Emission reduction through transportation channels 48 hours in advance	Cities located in the northwest transportation channel of Jiaxing	Cut down industrial sources by 30%	December 12

687 Figure 17 shows the cities that primarily influence the polluted air masses transported into Jiaxing, where the
 688 transport channels were determined through backward trajectory analysis. These cities include Huzhou in
 689 Zhejiang province, Suzhou, Wuxi, Changzhou, Nanjing, Zhenjiang, Huai'an, Suqian and Suzhou in Jiangsu
 690 province and Suzhou, Huaibei, Bozhou, Bengbu, Chuzhou and Ma'anshan in Anhui province. Each of these cities
 691 took measures to reduce emissions by limiting production from industry industries by 30%.

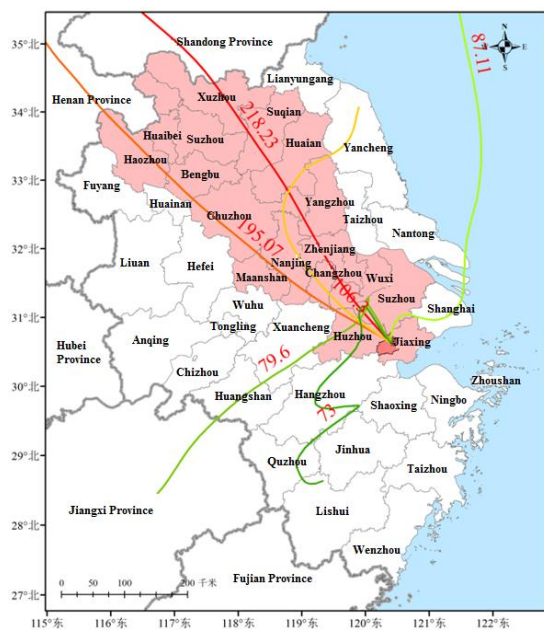


Fig. 17 Cities involved in the transportation channel and the emission reduction channel

692

693

694 The WRF-CMAQ modelling system was used to analyse and compare the air quality improvement effect
 695 under different pollution process in four scenarios.

696 **3.5.2 Analysis of optimization scenario effects**

697 In order to evaluate the effect of the different starting time for the same control measures, and the same
 698 starting time for local and regional control measures, we conducted-investigated four scenarios. Figure 18 shows
 699 the percentage reduction in daily average $PM_{2.5}$ concentrations in Jiaxing City from December 13 to December 18
 700 under the regional emission reduction scenario, the Jiaxing local emission reduction scenario and the
 701 transportation channel emission reduction scenario. Overall, there are differences in the distribution of $PM_{2.5}$
 702 under the different scenarios. The air quality improvement due to the regional emission reductions was higher
 703 than that of local emission reductions in Jiaxing, and lower than that of channel emission reductions.

704

705

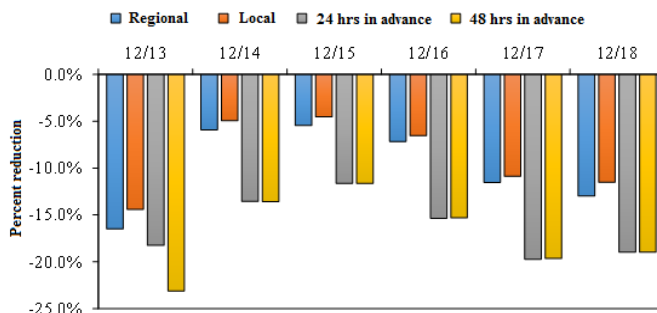


Fig. 18 Decline rates of $PM_{2.5}$ daily average concentrations in Jiaxing under different scenarios

(1) Effect of local emission reductions in Jiaxing

By comparing the effect of local emission reductions in Jiaxing (Sc.1) and the effect of regional emission reductions (Base), we can see that PM_{2.5} daily average concentrations in Jiaxing declined by around 5.5%-16.5% under the regional emission reduction plan (regional emission plan including the local emissions control) from December 13 to December 18 and by around 4.5%-14.4% under the local emission reduction plan. Local emission reductions in Jiaxing contributed 83%-94% to the emission reduction effect. Therefore, local emission reduction in Jiaxing is the key factor in improving the local air quality.

Compared with the channel emission reduction scenario 24 hours in advance (11.6%-18.2%), local emission reductions also contributed more than 50% to the improvement effect on December 13, 17 and 18. Therefore, local emission reductions contributed most to the air quality improvement effect in Jiaxing, indicating that local areas are still the most important control areas during the campaign.

(2) Effect of emission reductions through transportation channels

As mentioned above, during the large-scale transport of heavily polluted air masses into the Yangtze River Delta region from December 14 to December 15, the PM_{2.5} pollution in Jiaxing was significantly affected. Under the local emission reduction scenario (Sc.1) and the regional linkage emission reduction scenario (Base), PM_{2.5} daily average concentrations in Jiaxing decline by only 4.5%-5.9%. If a 30% reduction in emissions from industrial sources in the upwind transportation channel is implemented, PM_{2.5} daily average concentrations in Jiaxing declined by 11.6%-13.6%, while local emission reductions contributed less than 40% to the improvement of PM_{2.5}. Therefore, to reduce PM_{2.5} under these large-scale transport conditions, in addition to intensifying local emission reduction efforts, it is more effective to prevent and control such pollution by adopting emission reductions of industrial sources over key transportation channels, especially for elevated sources.

In this study, the main transportation channel involved is the northwest transportation channel in control areas, which basically represents the typical winter transportation channel in the region. In this study, the main transport channel involved is the northwest transport channel in control areas, which basically represents the typical winter transport channel in the region. Air quality improvement due to regional emission reductions was slightly larger than that of local emission reductions in Jiaxing, and smaller than that of channel emission reductions. This suggests that emissions reduction in the downwind cities does not have much effect on Jiaxing's air quality. In contrast, emissions reduction based on predicted transport pathway in advance are much more effective than local emissions reduction as well as regional emission reductions. Therefore, a well-designed management plan for the main transport channel is necessary to ensure optimized air quality improvement in

带格式的：边框:底端：(无框线)

带格式的：字体：(中文)宋体，英语(英国)，到齐到网格

~~autumn and winter, in addition to reducing local emissions. A well-designed management plan for the main transportation channel is necessary to ensure the air quality in autumn and winter is improved, in addition to reducing local emissions.~~

(3) Effect of the starting time for channel emission reductions

According to the comparisons between the emission reduction scenario 24 hours in advance (Sce.2) and the emission reduction scenario 48 hours in advance (Sce.3) during the large-scale PM_{2.5} transport, we can see that if we take December 13 as the target and adopt channel emission reductions 48 hours in advance, PM_{2.5} daily average concentrations will decline by 23.1% when compared to the baseline scenario, which is significantly better than the improvement achieved by the emission reduction scenario 24 hours in advance (18.2%). Therefore, early measures to reduce emissions will lead to the improvement of air quality.

If we focus on the conference period (December 16-18), PM_{2.5} daily average concentrations will both decline by 15.3%-19.7% under the two channel emission reduction scenarios, indicating a close improvement effect. Therefore, during the pollution process when local emissions are the main contributor, local emission reductions should be the top priority with no difference between channel reductions 24 hours in advance and 48 hours in advance. If transportation emissions are the main contributor to the pollution, adopting channel reductions 48 hours in advance can bring about more improvement effect than 24 hours in advance.

~~3.6 Comparisons with other air quality guarantee events~~

~~Besides the 2nd World Internet Conference, China has hosted many other mega-events in recent years, like 2008 Beijing Olympics, 2010 Guangzhou Asian Games, 2014 Beijing APEC, 2014 Nanjing Youth Olympics and 2015 Victory Parade. To guarantee the better air quality and protect people's health, local government had implemented numerous short-term stringent strategies to guarantee air quality during these events, which significantly reduced the emissions and concentrations of air pollutants in these cities and surrounding area. Through banning yellow label vehicles from driving, stopping all construction activities and requiring heavily polluting factories to reduce their operating capacities or completely shut down during the 2008 Olympics, the mean concentrations of SO₂, PM_{2.5} and NO₂ in Beijing and its surrounding area were reduced by 51.0%, 43.7% and 13% compared to the period before Olympics, and concentrations of O₃, SO₂, CO and NO_x decreased 23%, 61%, 25% and 21% compared to previous years (Wang, et al., 2009; Wang, et al., 2010). During the 2010 Asian Games, the Guangzhou government made great efforts to improve the air quality, such as controlling emissions from industries and transportation restrictions, requiring vehicles to drive only on alternate days depending on license plate numbers, and prohibiting all construction activities. The emissions of SO₂, NO_x, PM₁₀, PM_{2.5} and~~

766 VOCs were reduced by 41.1%, 41.9%, 26.5%, 25.8% and 39.7%, respectively, leading to a dramatic decrease on
 767 concentrations of SO₂, NO₂, PM₁₀ and PM_{2.5} in Guangzhou (Liu, et al., 2013). During the 2014 Asia Pacific
 768 Economic Cooperation (APEC) period, the average concentrations of PM_{2.5}, PM₁₀, SO₂ and NO₂ decreased by
 769 47%, 36%, 62% and 41% respectively by controlling emissions from traffic, industry, construction sites and so on
 770 (Tang, et al., 2015; Li, et al., 2016; Wang, et al., 2016; Sun, et al., 2016; Wang, et al., 2015). During 2014 Nanjing
 771 Youth Olympics and 2015 Victory Parade, the local governments also successfully improved air quality by
 772 carrying out many air pollution control measures including relocating some heavily polluting enterprises,
 773 encouraging natural gas instead of coal-fired boilers and domestic stoves, limiting the use of cars and so on (Chen,
 774 et al., 2017; Han, et al., 2016). Also, 22 surrounding cities in the YRD region were asked to cooperate with
 775 Nanjing to close industries with high pollution emissions. Some research papers demonstrate that, the mean
 776 concentrations of PM_{2.5}, PM₁₀, SO₂, NO₂, CO and O₃ in Nanjing during the Youth Olympics decreased by 35.92%,
 777 36.75%, 20.40%, 15.05%, 8.54% and 47.15%, respectively, compared with the average levels in July 2014 (Qi, et
 778 al., 2016). The emission reductions for SO₂, NO₂, PM₁₀, PM_{2.5}, VOCs during the Victory Parade were 36.5%,
 779 49.9%, 50.3%, 49.0% and 32.4%, respectively. These results show that stringent emission reduction strategies had
 780 greatly relief the air pollution of these cities including their surrounding area, and further improve their air quality
 781 through regional joint control measures.

782 Table 6 Summary of control strategies taken during different periods

Periods	Control area	Control policies	Main achievements or targets
Beijing- Olympics, 2008	Jing jin ji- area Inner- Mongolia, Shanxi, Shandong	Yellow label vehicles were banned from driving; personal vehicles were taken off the roads through the alternative day driving scheme; all construction activities were halted; power plants were asked to use cleaner fuels and reduce their emissions by 30% from their levels; heavily polluting factories were ordered to reduce operating capacities or completely shut downs.	The emissions of SO ₂ , NO _x , CO, VOCs, and PM ₁₀ were reduced by 14%, 38%, 47%, 30% and 20% respectively; the concentrations of fine and coarse particulate matter were reduced by 35-43%.
Beijing- APEC, 2014	Jing jin ji- area Shanxi, Inner- Mongolia, Shandong	Reducing or stopping production in factories; halting production on construction sites; imposing the odd-even traffic rule for vehicles; and strengthening road cleaning measures.	Average concentrations of SO ₂ , NO ₂ , PM ₁₀ and PM _{2.5} decreased by 62%, 41%, 36%, and 47%, respectively.
Nanjing- Youth Olympics, 2014	Nanjing	2630 construction sites were halted; heavy industry factories were required to reduce manufacturing by 20%; high emission vehicles were not allowed to	The mean concentrations of PM _{2.5} , PM ₁₀ , SO ₂ , NO ₂ , CO and O ₃ decreased by 35.92%, 36.75%, 20.40%, 15.05%, 8.54% and 47.15%.

带格式的：边框:底端: (无框线)

带格式的：下标
 带格式的：下标
 带格式的：下标
 带格式的：下标
 带格式的：下标
 带格式的：下标

带格式的：下标
 带格式的：字体: 倾斜, 下标
 带格式的：下标
 带格式的：下标

		drive on the road; open space barbecue restaurants were closed; over 900 electric buses and 500 electric taxis have been put into operation.	
Beijing-Victory Parade, 2015	Jing-jin-ji area, Shanxi, Shandong, Inner Mongolia, Henan	Over 111 businesses with high emissions were required to stop or limit their production; the odd-even rule was implemented to restrict traffic emissions; 80% of government vehicles were prohibited on roads; trucks transporting mud and stone as well as heavy emission vehicles were prohibited from roads; over 10000 enterprises were closed or ordered to limit production, and about 9000 construction sites were shut down.	The emission reductions were 36.5% for SO₂, 49.9% for NO_x, 50.3% for PM₁₀, 49.0% for PM_{2.5} and 32.4% for VOCs in Beijing.

带格式的: 边框:底端: (无框线)

783

784 **4 Conclusions**

785 **(1) The effect of restricting production in industrial enterprises is remarkable.** The power industry and
786 related industrial enterprises in Jiaxing cut down SO₂ and NO_x emissions by over 50%, while the building
787 materials industry, smelting industry and other industrial enterprises cut down PM_{2.5} emissions by 63%,
788 contributing greatly to the reduction of primary PM_{2.5} concentrations. The petrochemical industry, chemical
789 industry and other related industrial enterprises cut down VOCs emission by 66% in total, contributing greatly to
790 the reduction of PM_{2.5} formed through the conversion of precursor species. The observation data of PM_{2.5}
791 components suggest that the relative contribution of secondary components dropped significantly during the
792 conference. Production restriction or suspension for industrial enterprises is the main contributor to emission
793 reductions for various pollutants during the campaign, which resulted in the largest improvement in air quality.

带格式的: 下标
带格式的: 字体: 倾斜, 下标
带格式的: 下标
带格式的: 下标

794 **(2) Motor vehicle pollutant emissions declined significantly.** In Jiaxing, motor vehicle restrictions were
795 fully implemented during heavy pollution days, temporary traffic control was implemented during certain periods,
796 and enterprises and institutions had a three-day vacation during the conference. Emission reduction rates for
797 various pollutants from motor vehicle emissions were around 40%-50%. Motor vehicle emission reduction
798 measures contributed to the total emission reductions of nitrogen oxides by 18.2%, fine particles by 3.4% and
799 volatile organic compounds by 10.1%.

带格式的: 下标
带格式的: 下标

800 **(3) The effect of dust control measures is remarkable.** During the conference, most of the construction
801 sites in Jiaxing were suspended from operation. Increased frequency for road cleaning activities greatly lowered
802 the dust emissions. Speciation of the measured PM_{2.5} suggest that the mass concentration of crust material,
803 decreased by 14% compared to measurements after the conference. Specially, under static conditions, mineral

带格式的: 下标

804 soluble irons (Ca²⁺ and Mg²⁺) declined 56.8% before and during the campaign. This suggests that the suspension
805 of construction operations and increased frequency of rinsing and cleaning of paved roads significantly reduced
806 dust emissions~~During the conference, all the work sites in Jiaxing and 3950 work sites in total in Zhejiang~~
807 ~~province were suspended from operation. Measures of increasing frequency for road cleaning activities greatly~~
808 ~~lowered the dust emissions. Speciation of the measured PM_{2.5} suggest that the mass concentration of crust~~
809 ~~material, which is greatly affected by dust, decreased by 14% compared to measurements after the conference,~~
810 ~~indicating the effectiveness of dust control measures.~~

811 **(4) Regional linkage between surrounding areas played an important role.** PM_{2.5} is a typical regional air
812 pollutant, with obvious regional transport~~ation~~ characteristics. In accordance with the requirements of the
813 campaign scheme, eight cities around Jiaxing have actively implemented emissions reduction measures. During
814 the campaign, PM_{2.5} concentrations in eight surrounding cities and south-eastern Zhejiang also declined with
815 obvious regional synergies.

816 It is worth noting that the implementation of control measures has also had a negative impact on the economy
817 and the society in the short term while improving the air quality. For example, production restriction or
818 suspension on a large number industrial enterprises were taken at great economic costs, and motor vehicle
819 restriction had a large impact on the society.

820 **(5) Suggestions on emission reduction plans:** Local emission reductions shall be supplemented by regional
821 linkage. Assessment results show that local emission reductions play a key role in ensuring air quality. Therefore,
822 it is recommended that a synergistic emission reduction plan between adjacent areas with local pollution emission
823 reductions as the core part should be established and strengthened, and emission reduction plans for different
824 types of pollution through a stronger regional linkage should be reserved. Strengthen the pollution reduction in the
825 upper reaches along the transport~~ation~~ channel. It is especially crucial to enhance pollution emission reductions in
826 the upper reaches of the channel since long-distance transport of pollution plumes is a problem. This is especially
827 true for key industrial sources and elevated sources. Considering that polluted air mass transport~~ation~~ is more
828 frequent in winter, it is necessary to develop emission reduction plans for different pollution-plume transport~~ation~~
829 channels, combined with forecasting and warning mechanisms which could be initiated on time.

830 Author contribution

832 L. Li designed this study and wrote the paper, H. L. Wang co-designed the study and provided valuable advice on
833 the data analysis, C. Huang developed the regional emissions inventory, S. H. Zhu performed observational data
834 analysis and J. Y. An carried out the CMAQ and CAMx modelling work. R. S. Yan performed the WRF

带格式的：边框:底端：(无框线)

带格式的：上标

带格式的：上标

带格式的：下标

带格式的：字体：Times New Roman, 五号, 字体颜色：自动设置

带格式的：字体：非加粗, 英语(英国)

带格式的：字体：非加粗, 英语(英国)

带格式的：字体：非加粗, 英语(英国)

带格式的：字体：非加粗, 英语(英国)

带格式的：字体：非加粗, 英语(英国)

带格式的：字体：非加粗, 英语(英国)

835 [modelling. M. Zhou and L. P. Qiao helped observation and data quality control. X. D. Tian and L. J. Shen carried](#)
836 [out the measurements and provided the observed data. L. Huang and Y. J Wang helped to revise the paper.](#)
837 [Jeremy C Avise and Joshua S Fu helped revise and polish the manuscript and gave advices on paper writing.](#)

带格式的: 边框: 底端: (无框线)
带格式的: 字体: 非加粗, 英语(英国)
带格式的: 字体: 非加粗, 英语(英国)

838 **Competing interests**

839 [The authors declare that they have no conflict of interest.](#)

带格式的: 字体: 非加粗, 英语(英国)
带格式的: 字体: 非加粗, 英语(英国)
带格式的: 字体: 非加粗, 英语(英国)
带格式的: 字体: 非加粗, 英语(英国)
带格式的: 字体: 非加粗, 英语(英国)
带格式的: 字体: 非加粗, 英语(英国)
带格式的: 字体: 非加粗, 英语(英国)

840 **Acknowledgements.**

841 This study was financially supported by the “Chinese National Key Technology R&D Program” via grant No.
842 2014BAC22B03 and the National Natural Science Foundation of China (NO. 41875161). We also thank the Joint
843 pollution control office over the Yangtze River Delta region for co-ordinating the data share.

844 **References**

845 [Appel, K.W., Bhave, P.V., Gilliland, A.B., Sarwar, G., Roselle, S.J.: Evaluation of the community multiscale air quality \(CMAQ\)](#)
846 [model version 4.5: sensitivities impacting model performance: part II particulate matter. Atmos. Environ. 42, 6057-6066, 2008.](#)

847 Borge, R., Lumberras, J., Vardoulakis, S., et al.: Analysis of long-range transport influences on urban PM10 using two-stage
848 atmospheric trajectory clusters, Atmos. Environ., 41, 4434-4405, 2007.

849 Burr, M. J., and Zhang, Y.: Source apportionment of fine particulate matter over the Eastern U.S. Part I: source sensitivity
850 simulations using CMAQ with the Brute Force method, Atmos. Pollut. Res., 2, 300-317, 2011.

851 Chen, P. L., Wang, T. J., Lu, X. B., et al.: Source apportionment of size-fractionated particles during the 2013 Asian Youth Games
852 and the 2014 Youth Olympic Games in Nanjing, China, Sci. Total Environ., 579,860-870, 2017.

带格式的: 缩进: 左侧: 0 厘米, 悬挂缩进: 1 字符, 首行缩进: -1 字符

853 [Chen, O., Fu, T. M., Hu, J., Ying, O., & Zhang, L.: Modelling secondary organic aerosols in China. National Science Review, 4\(6\),](#)
854 [806-809, 2017.](#)

855 Chang, J. S., Brost, R. A., Isaksen, I. S. A., Madronich, S., Middleton, P., Stockwell, W. R., and Walcek, C. J.: A
856 3-DIMENSIONAL EULERIAN ACID DEPOSITION MODEL - PHYSICAL CONCEPTS AND FORMULATION, J.
857 Geophys. Res., 92, 14681-14700, 1987.

858 [Cheng, Y., Zheng, G., Wei, C., Mu, O., Zheng, B., Wang, Z., Gao, M., Zhang, O., He, K., Carmichael, G., Pöschl, U., and Su, H.:](#)
859 [Reactive nitrogen chemistry in aerosol water as a source of sulfate during haze events in China. Science Advances., 2,](#)
860 [1601530-1601530, doi:10.1126/sciadv.1601530, 2016.](#)

带格式的: 字体: (默认) Times New Roman, (中文) Calibri, 小五, , 图案: 清除
带格式的: 缩进: 左侧: 0 厘米, 悬挂缩进: 1 字符, 首行缩进: -1 字符, 行距: 1.5 倍行距

861 Chou, M. D., and Suarez, M. J.: A solar radiation parameterization (CLIR-AD-SW) for atmospheric studies, 1999.

862 CAI-Asia: “Blue Skies at Shanghai EXPO 2010 and Beyond: Analysis of Air Quality Management in Cities with Past and
863 Planned Mega-Events: A Survey Report.” Pasig City, Philippines, 2010.

864 CAI-Asia: “Nanjing YOG 2014 Home” Pasig City, Philippines, 2014.

865 Ek, M. B.: Implementation of Noah land surface model advances in the National Centers for Environmental Prediction operational

mesoscale Eta model, *J. Geophys. Res.*, 108(D22), 2003.

[Foley, K.M., Roselle, S.J., Appel, K.W., Bhawe, P.V., Pleim, J.E., Otte, T.L., Mathur, R., Sarwar, G., Young, J.O., Gilliam, R.C., Nolte, C.G., Kelly, J.T., Gilliland, A.B., Bash, J.O.: Incremental testing of the community multiscale air quality \(CMAQ\) modeling system version 4.7. *Geosci. Model Dev.* 3, 205-226, 2010.](#)

Fu, X., Cheng, Z., Wang, S., Hua, Y., Xing, J., and Hao, J.: Local and Regional Contributions to Fine Particle Pollution in Winter of the Yangtze River Delta, China, *Aerosol Air. Qual. Res.*, 16, 1067-1080, 2016.

Guenther, A. B., Jiang, X., Heald, C. L., Sakulyanontvittaya, T., Duhl, T., Emmons, L. K., and Wang, X.: The Model of Emissions of Gases and Aerosols from Nature version 2.1 (MEGAN2.1): an extended and updated framework for modeling biogenic emissions, *Geosci. Model Dev.*, 5, 1471-1492, 2012.

Grell, G. A., and Déry, D.: A generalized approach to parameterizing convection combining ensemble and data assimilation techniques, *Geophys. Res. Lett.*, 29(14), 587-590, 2002.

Han, X. K., Guo, Q. J., Liu, C.Q., et al.: Effect of the pollution control measures on PM_{2.5} during the 2015 China Victory Day Parade: Implication from water-soluble ions and sulfur isotope, *Environ. Pollut.*, 218, 230-241, 2016.

[Hu, J., Wang, P., Ying, Q., Zhang, H., Chen, J., Ge, X., et al.: Modeling biogenic and anthropogenic secondary organic aerosol in China. *Atmospheric Chemistry and Physics*, 17\(1\), 77-92, 2017.](#)

Hu, J. L., Wang, Y. G., Ying, Q., et al.: Spatial and temporal variability of PM_{2.5} and PM₁₀ over the North China Plain and the Yangtze River Delta, China, *Atmos. Environ.*, 95, 598-609, 2014.

Hu, J. L., Wu, Li., Zheng, B., et al.: Source contributions and regional transport of primary particulate matter in China, *Environ. Pollut.*, 207, 31-42, 2015.

Hsu, Y. K., Holsen, T. M., and Hopke, P. K.: Comparison of hybrid receptor models to locate PCB sources in Chicago, *Atmos. Environ.*, 37, 545-562, 2003.

Hong, S. Y.: A new vertical diffusion package with an explicit treatment of entrainment processes, *Mon. Weather Rev.*, 134, 2318, 2006.

Huang, C., Chen, C. H., Li, L., Cheng, Z., Wang, H. L., Huang, H. Y., Streets, D. G., Wang, Y. J., Zhang, G. F., and Chen, Y. R.: Emission inventory of anthropogenic air pollutants and VOC species in the Yangtze River Delta region, China, *Atmos. Chem. Phys.*, 11, 4105-4120, 2011.

Huang, Y. M., Liu, Y., Zhang, L. Y., et al.: Characteristics of Carbonaceous Aerosol in PM_{2.5} at Wanzhou in the Southwest of China, *Atmosphere*, 9, 37, 2018,.

Jiang, C., Wang, H., Zhao, T., et al.: Modeling study of PM_{2.5} pollutant transport across cities in China's Jing-Jin-Ji region during a severe haze episode in December 2013, *Atmos. Chem. Phys.*, 15, 5803-5814, 2015.

Kang, H. Q., Zhu, B., Su, J. F., et al.: Analysis of a long-lasting haze episode in Nanjing, China, *Atmos. Res.*, 120-121, 78-87,

带格式的：边框:底端：(无框线)

带格式的：下标

带格式的：下标

897 2013.

898 [Kasibhatla, P., Chameides, W.L., Jonn, J.S.: A three dimensional global model investigation of seasonal variations in the](#)

899 [atmospheric burden of anthropogenic sulphate aerosols. *J. Geophys. Res.* 102, 3737-3759, 1997.](#)

900 Kelly, F. J., and Zhu, T.: Transport solutions for cleaner air, *Science*, 352, 934–936, 2016.

901 [Li, J. L., ZHANG, M. G., GAO, Y., and CHEN, L.: Model analysis of secondary organic aerosol over China with a regional air](#)

902 [quality modeling system \(RAMS-CMAQ\). *Atmospheric and Oceanic Science Letters*, 9\(6\), 443-450, 2016.](#)

903 Li, L., An, J. Y., Zhou, M., Yan, R. S., Huang, C., Lu, Q., and Chen, C. H.: Source apportionment of fine particles and its chemical

904 components over the Yangtze River Delta, China during a heavy haze pollution episode, *Atmos. Environ.*, 123, 415–429, 2015.

905 Li, R. P., Mao, H. J., Wu, L., et al.: The evaluation of emission control to PM concentration during Beijing APEC in 2014, *Atmos.*

906 *Pollut. Res.*, 7 (2), 363-369, 2016.

907 Liu, H., Wang, X. M., Zhang, J. P., et al.: Emission controls and changes in air quality in Guangzhou during the Asian Games,

908 *Atmos. Environ.*, 76, 81-93, 2013.

909 [Lv, B. L., Liu, Y., Yu, P., et al.: Characterizations of PM_{2.5} Pollution Pathways and Sources Analysis in Four Large Cities in China,](#)

910 [*Aerosol Air Qual. Res.*, 15, 1836–1843, 2015.](#)

911 Li, L., Chen, C. H., Fu, J. S., Huang, C., Streets, D. G., Huang, H. Y., and Fu, J. M.: Air quality and emissions in the Yangtze

912 River Delta, China, *Atmos. Chem. Phys.*, 11(4), 1621-1639, 2011.

913 Liu, Y., Li, L., An, J. Y., Zhang, W., Yan, R. S., L, H., and M, W.: Emissions, chemical composition, and spatial and temporal

914 allocation of the BVOCs in the Yangtze River Delta Region in 2014, *Environ. Sci.*, 39(2), 2018.

915 Li, M., Zhang, Q., Kurokawa, J.-i., Woo, J.-H., He, K., Lu, Z., and Zheng, B.: MIX: a mosaic Asian anthropogenic emission

916 inventory under the international collaboration framework of the MICS-Asia and HTAP, *Atmos. Chem. Phys.*, 17(2), 935-963,

917 2017.

918 Lin, Y. L.: Bulk parameterization of the snow field in a cloud model, *J. Appl. Meteorol.*, 22(6), 1065-1092, 1983.

919 Li, L., Chen, C. H., Fu, J. S., Huang, C., Streets, D. G., Huang, H. Y., Zhang, G. F., Wang, Y. J., Jang, C. J., Wang, H. L., Chen, Y.

920 R., and Fu, J. M.: Air quality and emissions in the Yangtze River Delta, China, *Atmos. Chem. Phys.*, 11, 1621-1639, 2011.

921 Li, L., An, J. Y., Zhou, M., Yan, R. S., Huang, C., Lu, Q., Lin, L., Wang, Y. J., Tao, S. K., Qiao, L. P., Zhu, S. H., and Chen, C. H.:

922 Source apportionment of fine particles and its chemical components over the Yangtze River Delta, China during a heavy haze

923 pollution episode, *Atmos. Environ.*, 123, 415-429, 2015.

924 Li, M., Zhang, Q., Kurokawa, J.-i., Woo, J.-H., He, K., Lu, Z., Ohara, T., Song, Y., Streets, D. G., Carmichael, G. R., Cheng, Y.,

925 Hong, C., Huo, H., Jiang, X., Kang, S., Liu, F., Su, H., and Zheng, B.: MIX: a mosaic Asian anthropogenic emission inventory

926 under the international collaboration framework of the MICS-Asia and HTAP, China, *Atmos. Chem. Phys.*, 17, 935-963, 2017.

927 Li, X., Zhang, Q., Zhang, Y., Zheng, B., Wang, K., Chen, Y., Wallington, T. J., Han, W., Shen, W., Zhang, X., and He, K.: Sou rce

带格式的：边框:底端：(无框线)

带格式的：下标

- 928 contributions of urban PM 2.5 in the Beijing–Tianjin–Hebei region: Changes between 2006 and 2013 and relative impacts of
929 emissions and meteorology, *Atmos. Environ.*, 123, 229-239, 2015.
- 930 Lin, Y. L.: Bulk parameterization of the snow field in a cloud model, *J. Appl. Meteorol.*, 22, 1065-1092, 1983.
- 931 Liu, Y., Li, L., An, J. Y., Zhang, W., Yan, R. S., L, H., Huang, C., Wang, H. L., Q, W., and M, W.: Emissions, chemical
932 composition, and spatial and temporal allocation of the BVOCs in the Yangtze River Delta Region in 2014, *Environ. Sci.*, 39,
933 608-617, 2018.
- 934 Liang, P. F., Zhu, T., Fang, Y. H., Li, Y. R., Han, Y. Q., Wu, Y. S., Hu, M., and Wang, J. X.: The role of meteorological
935 conditions and pollution control strategies in reducing air pollution in Beijing during APEC 2014 and Victory Para de 2015,
936 *Atmos. Chem. Phys.*, 17, 13921–13940, 2017.
- 937 Liu, J., and Zhu, T.: NOx in Chinese Megacities, *Nato. Sci. Peace. Secur.*, 120, 249–263, 2013.
- 938 Markovic, M. Z., VandenBoer, T.C., and Murphy, J. G.: Characterization and Optimization of an Online System for the
939 Simultaneous Measurement of Atmospheric Water-soluble Constituents in the Gas and Particle Phases, *J. Environ. Monit.*, 14,
940 1872–1874, 2012.
- 941 Mlawer, E. J., Taubman, S. J., Brown, P. D., Iacono, M. J., and Clough, S. A.: Radiative transfer for inhomogeneous atmospheres:
942 RRTM, a validated correlated-k model for the longwave, *J. Geophys. Res.*, 102(D14), 16663-16682, 1997.
- 943 Nolte, C. G., Appel, K. W., Kelly, J. T., Bhave, P. V., Fahey, K. M., Collet Jr., J. L., Zhang, L., and Young, J. O.: Evaluation of
944 the Community Multiscale Air Quality (CMAQ) model v5.0 against size-resolved measurements of inorganic particle
945 composition across sites in North America, *Geosci. Model Dev.*, 8, 2877-2892, 2015.
- 946 Nenes, A., Pilinis, C., and Pandis, S. N.: ISORROPIA: A New Thermodynamic Model for Multiphase Multicomponent Inorganic
947 Aerosols, *Aquat. Geochem.*, 4, 123-152, 1998.
- 948 Pui, D. Y. H., Chen, S. C., and Zuo, Z. L.: PM2.5 in China: Measurements, sources, visibility and health effects, and mitigation,
949 *Particuology*, 13, 1-26, 2014.
- 950 Polissar, A. V., Hopke, P. K., Kaufmann, P. P., Kaufmann, Y., Hall, D., Bodhaine, B., Dutton, E., and Harris J.: The aerosol at
951 Barrow, Alaska: long-term trends and source location, *Atmos. Environ.*, 33(16), 2441-2458, 1999.
- 952 Qi, L., Zhang, Y. F., Ma, Y. H., et al.: Source identification of trace elements in the atmosphere during the second Asian Youth
953 Games in Nanjing, China: Influence of control measures on air quality, *Atmos. Pollut. Res.*, 7 (3), 547-556, 2016.
- 954 Swagata, P., Pramod, K., Sunita, V., et al.: Potential source identification for aerosol concentrations over a site in Northwestern
955 India, *Atmos. Res.*, 169, 65-72, 2016.
- 956 Sun, Y. L., Wang, Z. F., Wild, O., et al.: “APEC Blue”: Secondary Aerosol Reductions from Emission Controls in Beijing, *Sci.*
957 *Rep-UK.*, 6, 20668, 2016.
- 958 Tang, L., Haeger-Eugensson, M., Sjoberg, K., et al.: Estimation of the long-range transport contribution from secondary

959 inorganic components to urban background PM10 concentrations in south-western Sweden during 1986-2010, Atmos. Environ.,
960 89, 93-101, 2014.

961 Tang, G., Zhu, X., Hu, B.m et al.: Impact of emission controls on air quality in Beijing during APEC 2014: lidar ceilometer
962 observations, Atmos. Chem. Phys., 15, 12667–12680, 2015.

963 Tian, Mi., Wang, H. B., Chen, Y., et al.: Characteristics of aerosol pollution during heavy haze events in Suzhou, China, Atmos.
964 Chem. Phys., 16, 7357–7371, 2016.

965 US EPA.: Draft Modeling Guidance for Demonstrating Attainment of Air Quality Goals for Ozone, PM_{2.5}, and Regional Haze,
966 2014.

967 Wang, L. T., Wei, Z., Yang, J., Zhang, Y., Zhang, F. F., Su, J., Meng, C. C., and Zhang, Q.: The 2013 severe haze over southern
968 Hebei, China: model evaluation, source apportionment, and policy implications, Atmos. Chem. Phys., 14, 3151-3173, 2014.

969 Wang, Y. Q., Zhang, X. Y., and Draxler, R. R.: TrajStat: GIS-based software that uses various trajectory statistical analysis
970 methods to identify potential sources from long-term air pollution measurement data, Environ. Modell. Softw., 24(8), 938-939,
971 2009.

972 West, J. J., Cohen, A., Dentener, F., Brunekreef, B., Zhu, T., Armstrong, B., Bell, M. L., Brauer, M., Carmichael, G., Costa, D. L.,
973 Dockery, D. W., Kleeman, M., Krzyzanowski, M., Künzli, N., Liousse, C., Lung, S. C., Martin, R. V., Pöschl, U., Pope, C. A.,
974 Roberts, J. M., Russell, A. G., and Wiedinmyer, C.: “What We Breathe Impacts Our Health: Improving Understanding of the
975 Link between Air Pollution and Health”, Environ. Sci. Technol., 50 (10), 4895–4904, 2016.

976 Wang, T., Nie, W., Gao, J., et al.: Air quality during the 2008 Beijing Olympics: secondary pollutants and regional impact, Atmos.
977 Chem. Phys., 10, 7603–7615, 2010.

978 Wang, Y., Hao, J., McElroy, M. B., et al.: Ozone air quality during the 2008 Beijing Olympics: effectiveness of emission
979 restrictions, Atmos. Chem. Phys., 9, 5237–5251, 2009.

980 [Wang Y Q, Zhang X Y, Draxler R R. TrajStat: GIS-based software that uses various trajectory statistical analysis methods to](#)
981 [identify potential sources from long-term air pollution measurement data. Environmental Modelling and Software. 24\(8\):](#)
982 [938-939, 2009.](#)

983 Wang, Y. Q., Zhang, Y., Schauer, J. J., et al.: Relative impact of emissions controls and meteorology on air pollution mitigation
984 associated with the Asia-Pacific Economic Cooperation (APEC) conference in Beijing, China, Sci. Total Environ., 571,
985 1467-1476, 2016.

986 Wang, Z. S., Li, Y. T., Chen, T., et al.: Changes in atmospheric composition during the 2014 APEC conference in Beijing, J.
987 Geophys. Res., 120 (24), 2015.

988 Wang, Q. Z., Zhuang, G. S., Huang, Kan., et al.: Probing the severe haze pollution in three typical regions of China:
989 Characteristics, sources and regional impacts, Atmos. Environ., 120, 76-88, 2015.

带格式的：边框:底端：(无框线)

带格式的：下标

- 990 Xu, W., Song, Wei., Zhang, Y. Y., et al.: Air quality improvement in a megacity: implications from 2015 Beijing Parade Blue
991 pollution control actions, *Atmos. Chem. Phys.*, 17, 31–46, 2017.
- 992 Xiao, Z. M., Zhang, Y. F., Hong, S. M., et al.: Estimation of the Main Factors Influencing Haze, Based on a Long-term Monitoring
993 Campaign in Hangzhou, China, *Aerosol Air Qual. Res.*, 11, 873–882, 2011.
- 994 Yang, H. N., Chen, J., Wen, J. J., et al.: Composition and sources of $PM_{2.5}$ around the heating periods of 2013 and 2014 in Beijing:
995 Implications for efficient mitigation measures, *Atmos. Environ.*, 124, 378-386, 2016.
- 996 Yu, S. C., Saxena, V. K., Zhao, Z.: A comparison of signals of regional aerosol-induced forcing in eastern China and the
997 southeastern United States, *Geophys. Res. Lett.*, 28, 713-716, 2001.
- 998 Yu, S. C., Zhang, Q. Y., Yan, R. C., et al.: Origin of air pollution during a weekly heavy haze episode in Hangzhou, China,
999 *Environ. Chem. Lett.*, 12, 543-550, 2014.
- 1000 Yarwood, G., Rao, S., Yocke, M., et al.: Updates to the Carbon Bond chemical mechanism: CB05, Final Report prepared for US
1001 EPA, 2005.
- 1002 Zhang, Y., Cheng, S. H., Chen, Y. S., and Wang, W. X.: Application of MM5 in China: Model evaluation, seasonal variations, and
1003 sensitivity to horizontal grid resolutions, *Atmos. Environ.*, 45, 3454-3465, 2011.
- 1004 Zheng, B., Zhang, Q., Zhang, Y., He, K. B., Wang, K., Zheng, G. J., Duan, F. K., Ma, Y. L., and Kimoto, T.: Heterogeneous
1005 chemistry: a mechanism missing in current models to explain secondary inorganic aerosol formation during the January 2013
1006 haze episode in North China, *Atmos. Chem. Phys.*, 15, 2031-2049, 2015.
- 1007 Zeng, Y., and Hopke, P. K.: A study of the sources of acid precipitation in Ontario, Canada, *Atmos. Environ.*, 23(7), 1499-1509,
1008 1989.
- 1009 Zhang, X. Y., Wang, Y. Q., Niu, T., et al.: Atmospheric aerosol compositions in China: spatial/temporal variability, chemical
1010 signature, regional haze distribution and comparisons with global aerosols, *Atmos. Chem. Phys.*, 12, 779–799, 2012.
- 1011 Zhang, Y. J., Tang, L. L., Wang, Z., et al.: Insights into characteristics, sources, and evolution of submicron aerosols during
1012 harvest seasons in the Yangtze River delta region, China, *Atmos. Chem. Phys.*, 15, 1331–1349, 2015.

带格式的：边框:底端: (无框线)

带格式的：下标